THE UNIVERSITY OF ALBERTA

UNSTEADY FLOWS AT HIGH MACH NUMBERS OVER

SLENDER WEDGE WINGS

BY

(C) TAPAN KUMAR CHATTOPADHYAY

A THESIS

SUBMITTED TO THE FACULTY OF GRADUATE STUDIES AND RESEARCH

IN PARTIAL FULFILMENT OF THE REQUIREMENTS FOR THE DEGREE

OF DOCTOR OF PHILOSOPHY

DEPARTMENT OF MECHANICAL ENGINEERING

EDMONTON, ALBERTA

FALL, 1972

ABSTRACT

A slender two-dimensional wedge wing at a high Mach number is subjected to an impulsive change in the angle of attack. The time history of the flow, till the final steady state is reached, is analysed and the unsteady flow solutions determining the temporal variations in the lift, drag, and rate of heat transfer are numerically obtained.

The used parameters defining the problem are the free stream Mach number M_∞, Reynolds number $Re_{\infty,L*}$ based on the free stream conditions and the length of the wedge $L*$, the semi-wedge angle θ_w and the initial and final angles of attack α_i and α_f. In the problem considered M_∞ and $Re_{\infty,L*} \gg 1$ and the angles involved θ_w, α_i, $\alpha_f \ll 1$. However, their relative magnitudes are such that the combination $M_\infty^3/(Re_{\infty,L*})^{1/2}$ remains finite and the product $M_\infty|\theta| \leq O(1)$, where θ is the maximum deflection of the wedge surfaces.

Two types of thermal conditions on the wedge surface are used: insulated wedge surface and the wedge surface maintained at a constant temperature. The fluid is assumed to be a perfect gas with constant specific heat at constant pressure c_p^*, constant ratio of the specific heats γ, and constant Prandtl number Pr.

iii

ABSTRACT

A slender two-dimensional wedge wing at a high Mach number is subjected to an impulsive change in the angle of attack. The time history of the flow, till the final steady state is reached, is analysed and the unsteady flow solutions determining the temporal variations in the lift, drag, and rate of heat transfer are numerically obtained. The used parameters defining the problem are the free stream Mach number M_∞, Reynolds number Re_{∞,L^*} based on the free stream conditions and the length of the wedge L^*, the semi-wedge angle θ_w and the initial and final angles of attack α_i and α_f. In the problem considered M_∞ and $\sqrt{Re}_{\infty,L^*} \gg 1$ and the angles involved $\theta_w, \alpha_i, \alpha_f \ll 1$. However, their relative magnitudes are such that the combination $M_\infty^3/(Re_{\infty,L^*})^{1/2}$ remains finite and the product $M_\infty|\theta| \leq O(1)$, where θ is the maximum deflection of the wedge surfaces.

Two types of thermal conditions on the wedge surface are used: insulated wedge surface and the wedge surface maintained at a constant temperature. The fluid is assumed to be a perfect gas with constant specific heat at constant pressure c_p^*, constant ratio of the specific heats γ, and constant Prandtl number Pr.

ACKNOWLEDGEMENT

TABLE OF CONTENTS

TABLE OF CONTENTS (continued)

LIST OF TABLES

LIST OF FIGURES

LIST OF SYMBOLS

All dimensional quantities are represented with a superscript *. The corresponding non dimensional quantity is represented without the superscript. Symbols having only local significance are defined in the text where they appear.

a^*	velocity of sound
c_p^*	specific heat at constant pressure
C	coefficient of the linear viscosity-temperature relation
C_L	lift coefficient of the wedge
C_D	drag coefficient of the wedge
f	transformed stream function, defined in (2.30)
$\left.\begin{array}{l} f_0 \\ f_1 \\ f_2 \\ f_3 \end{array}\right\}$	functions of η appearing in the expansion of f in (3.10)
$\left.\begin{array}{l} F_S^* \\ F_N^* \end{array}\right\}$	tangential and normal force acting on either side of the wedge
h^*	enthalpy
H^*	total enthalpy
H	$= H^* / \frac{1}{2} u_\infty^{*2}$

$\left.\begin{array}{l} H_0 \\ H_1 \\ H_2 \\ H_3 \end{array}\right\}$ functions of η appearing in the expansion of H in (3.11)

$\left.\begin{array}{l} I_0 \\ I_1 \\ I_2 \\ I_3 \end{array}\right\}$ integrals defined in (3.30)

$\overline{I}$ integral defined in (3.68)

J   total number of x-stations

$\left.\begin{array}{l} J_1 \\ J_2 \\ J_3 \\ J_4 \end{array}\right\}$ integrals defined in (5.12), (5.15), (5.19)

k^* thermal conductivity

K   function defined in (1.6)

K_x ratio of consecutive stepsizes in x

K_t ratio of consecutive stepsizes in t

L^* length of the wedge

M   Mach number

N   total number of η-stations

p^* pressure

p $= p^*/p_\infty^*$

$$\left.\begin{array}{l} p_0 \\ p_1 \\ p_2 \\ p_3 \end{array}\right]$$ constants in the expansion of p in (3.7)

$\overline{p}$ $= p/(p_0\overline{x})$

Pr   Prandtl number $= \mu^* c_p^*/k^*$

q^* local heat transfer rate per unit area

Q^* heat transfer rate per unit width from either side of the wedge

Q   function defined in (3.52)

R^* gas constant

R   function defined in (4.14)

Re_{∞,x^*} local Reynolds number, defined in (1.8)

Re_{∞,L^*} Reynolds number evaluated at the end of the wedge

s   function defined in (3.74)

S^* constant in Sutherland's viscosity formula

t^* time

t $= t^* u_\infty^*/L^*$

T^* absolute temperature

T $= T^*/T_\infty^*$

u^* velocity component in the x^* direction

u $= u^*/u_\infty^*$

v^* velocity component in the y^* direction

v $= v^*/v_\infty^*$

x^* streamwise coordinate

x	$= x^*/L^*$
y^*	normal coordinate
y	$= y^*/L^*$
α	angle of attack
β	$= (\gamma-1)/\gamma$
γ	specific heat ratio
δ^*	boundary layer displacement thickness
δ	$= \delta^*/L^*$
$\left.\begin{array}{l}\delta_0\\[6pt]\delta_1\\[6pt]\delta_2\\[6pt]\delta_3\end{array}\right\}$	constants in the expansion of δ^* in (3.8)
$\bar{\delta}$	normalized function defined in (3.67)
Δ^*	displacement thickness of unsteady boundary layer, given by (2.37)
Δx	stepsize in x
Δt	stepsize in t
η	transformed normal coordinate
θ_b	angle of inclination of either side of the wedge
μ^*	coefficient of viscosity
μ	$= \mu^*/\mu^*_\infty$
ρ^*	density
ρ	$= \rho^*/\rho^*_\infty$
τ^*	shear stress at the surface

$\overline{\chi}$ hypersonic interaction parameter, defined in (1.7)

ψ stream function defined in (2.17)

Subscripts

∞ evaluation in the free stream

e   evaluation in the outer layer

b   evaluation on the surface of the wedge

i   indicates conditions before and after the impulsive

f   changes in the angle of attack

T   refers to the top and bottom surface of the

B   wedge

j   evaluation at the j-th x-station

k   evaluation at the k-th η-station

Superscïipt

(i)   evaluation at the i-th t-station

[m]   evaluation at the m-th iteration cycle

'   differentiation with respect to η

CHAPTER I
STATEMENT OF THE PROBLEM AND ASSOCIATED LITERATURE

1.1   Introduction

Wings with the cross section of narrow wedge are commonly
used as lifting surfaces in hypersonic vehicles. The behaviour of
such wings in steady flow conditions have been studied in great detail
over the past two decades. However, the question of maneuverability
and control of hypersonic vehicles often necessitates the study of
the flow in various unsteady situations. The present work deals with
one such problem. A slender two dimensional wedge wing moving at a
high Mach number is subjected to an impulsive change in the angle of
attack. The time history of the flow, till the final steady state is
reached, is analysed and the unsteady flow solutions are used to
determine the temporal variations in the lift, drag, heat transfer
rate and other characteristics of the wing.

The disturbances due to the presence of the wedge are confined
within a curved shock beyond which the free stream conditions prevail.
For a slender wedge with a sharp leading edge the shock is attached to
the leading edge. So the flows on the two sides of the wedge become
independent of each other, which can be considered separately. Thus
the problem under investigation reduces to the problem of finding the
unsteady hypersonic flow over an inclined flat plate after an instan-
taneous increase or decrease in the angle of inclination.

The hypersonic viscous flow over a slender body is characterized by the presence of a high temperature, low-density boundary layer adjacent to the body, which is considerably thicker than the corresponding boundary layers in subsonic or moderately supersonic flows. The displacement effects due to this thick boundary layer significantly changes the external inviscid flow and increases the pressure on the surface of the body. The flow in the boundary layer is, in turn, governed by the pressure (its streamwise gradient, in particular) and other external flow conditions. Thus the boundary layer and surrounding inviscid flow are mutually interdependent. This phenomenon which has been variously referred to in the literature as the hypersonic viscous interaction, viscid-inviscid interaction or shock-boundary layer interaction, is the basic feature that distinguishes the viscous flow at large Mach numbers from those at smaller Mach numbers. A review of literature on the interaction problem in two-dimensional hypersonic viscous flows over slender bodies is given in the following Section.

1.2 Review of Literature

Shen [1,2] first considered the viscous effects in the steady hypersonic flow over slender wedges. He considered the entire flow region between the wedge surface and the leading edge shock as the boundary layer and established the validity of the boundary layer equations in this region provided the ratio of the boundary layer thickness to the axial distance is much less than unity.

Detailed study of the hypersonic viscous flow by Lees and Probstein [3,4] helped to clarify some of the basic concepts. They

showed that the model postulated by Shen in which the boundary layer was

assumed to occupy the entire region between the body surface and the

shock, was inconsistant with the continuity condition. Figure 1.1 shows

the flow regions on an inclined flat plate according to the model in-

troduced by Lees and Probstein. The region between the shock and the

body surface is divided into two distinct regions, the external layer

and the boundary layer. In the external layer the effects of viscosity

are negligible, so that the flow in this region is governed by the

inviscid Euler equations. In the other region the flow is governed by

the boundary layer equations (Shen [1], Lees [5]). Thus the hypersonic

viscous interaction problem, mentioned earlier, has the following three

aspects :
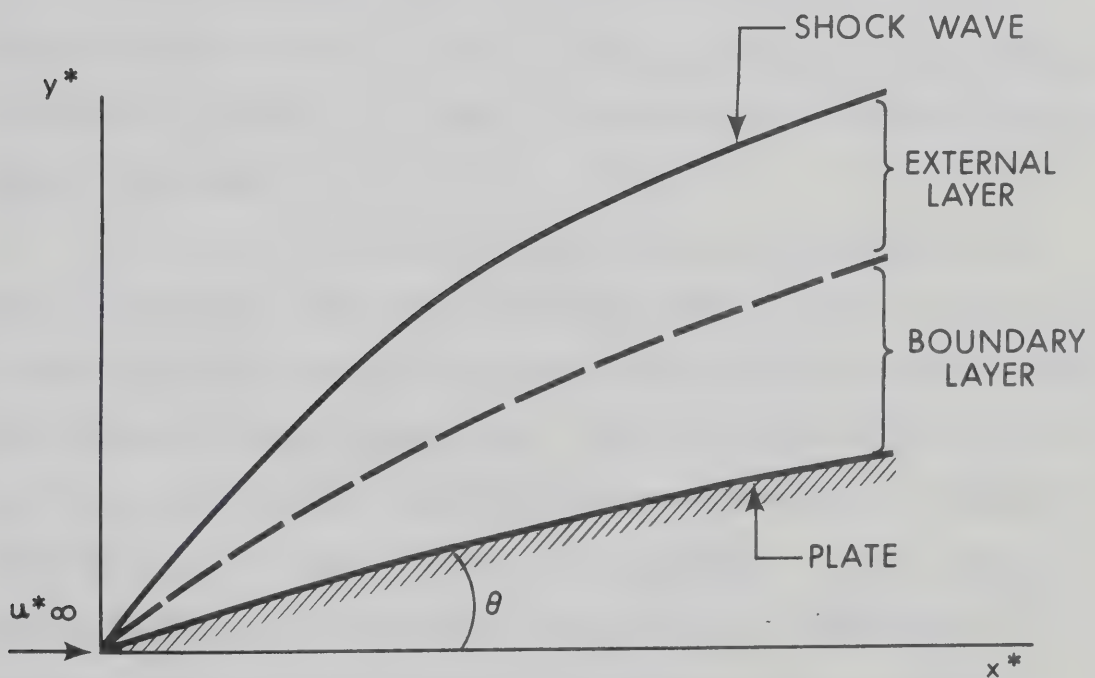
Figure 1.1   Flow Regions Over an Inclined Flat
Plate in Hypersonic Flow

(i)   The flow in the external layer can be considered as the in-
viscid hypersonic flow over an "effective body" given by the
boundary layer displacement thickness added to the original
body.

(ii) The distribution of pressure, tangential velocity and total
enthalpy at the edge of the "effective body" determines the
flow in the boundary layer.

(iii) The displacement thickness used to obtain the external
inviscid flow should be consistent with the displacement
thickness obtained from the solution of the boundary layer
equations.

Various methods used to tackle the interaction problem for
steady flow are reviewed in detail by Hayes and Probstein [6], Dorrance [7],
Stewartson [8], Moore [9]. The basic characteristics of these approaches
are outlined below.

The flow in the external layer, which is equivalent to the
inviscid hypersonic flow over a sharp-edged body of arbitrary shape can
be obtained by the method of characteristics, the shock expansion theory
and the tangent wedge approximation. The last method is the easiest of
the three, gives results of sufficient accuracy and has been employed
extensively in the hypersonic interaction problems. In the tangent
wedge approximation the pressure at any point on a·slender body of
thickness $y_e^*(x^*)$ is approximated by the pressure across an oblique
shock that produces the local flow deflection dy_e^*/dx^*. For free stream

Mach number $M_\infty \gg 1$ and for a slender body with $dy_e^*/dx^* \ll 1$, if the product $K(x^*) = M_\infty\, dy_e^*/dx^*$ remains finite, then the tangent wedge approximation gives the following results:

$$\frac{p_e^*(x^*)}{p_\infty^*} = 1 + \gamma K[\tfrac{\gamma+1}{4} K + \{(\tfrac{\gamma+1}{4} K)^2 + 1\}^{1/2}] + 0(M_\infty^{-2}) \qquad (1.1)$$

$$\frac{u_e(x^*)}{u_\infty^*} = 1 + 0(M_\infty^{-2}) \qquad (1.2)$$

$$\frac{H_e^*(x^*)}{\frac{1}{2} u^{*2}} = 1 + 0(M_\infty^{-2}) \qquad (1.3)$$

Linnel [10] obtained these results in a somewhat different form by assuming isentropic flow in the shock layer. Goldsworthy [11] later pointed out that the variation in entropy introduces errors of $0(M_\infty^{-2})$ only. For small and large values of K equation (1.1) can be expanded as:

$$\frac{p_e^*(x^*)}{p_\infty^*} = 1 + \gamma K + \frac{\gamma(\gamma+1)}{4} K^2 + \frac{\gamma(\gamma+1)^2}{32} K^3 + 0(K^5) \qquad (1.4)$$

and

$$\frac{p_e^*(x^*)}{p_\infty^*} = \frac{\gamma(\gamma+1)}{2} K^2 + \frac{3\gamma+1}{\gamma+1} - \frac{8\gamma}{(\gamma+1)^3} K^{-2} + 0(K^{-4}) \qquad (1.5)$$

Equations (1.4) and (1.5) are often used in place of the complete equation (1.1) for the sake of simplification.

For the hypersonic interaction problem K in the equation (1.1), (1.4) or (1.5) has to be replaced by:

$$K(x^*) = M_\infty [\frac{dy^*_b}{dx^*} + \frac{d\delta^*(x^*)}{dx^*}] \qquad (1.6)$$

where $y^*_b(x^*)$ defines the body surface and $\delta^*(x^*)$ is the boundary layer displacement thickness. Since the displacement thickness δ^* in (1.6) is not known a priori, the use of tangent wedge approximation still retains the basic iterative nature of the interaction problem. However, a great simplification is offered because the inviscid flow in the external layer need not be calculated explicitly. A disadvantage of using the tangent wedge approximation is that the vorticity in the external layer due to the curvature of the shock, which may affect the structure of the boundary layer, can not be accounted for. However, Hayes and Probstein [6] have pointed out that for a sharp-edged slender body the effects of the vorticity interaction can be neglected beyond a region very close to the leading edge.

Lees and Probstein [3,4] showed that the extent of the inter-action between the boundary layer and the inviscid external flow is characterized by the hypersonic interaction parameter $\overline{\chi}$, defined by

$$\overline{\chi} = M_\infty^3 (\frac{C}{Re_{\infty,x^*}})^{1/2} \qquad (1.7)$$

where

$$Re_{\infty,x^*} = \frac{\rho^*_\infty u^*_\infty x^*}{\mu^*_\infty} \qquad (1.8)$$

and C is the coefficient of the linear viscosity-temperature relation.
Two extreme cases corresponding to $\bar{\chi} \leq O(1)$ and $\bar{\chi} >> 1$ were called the
weak and strong interaction flows. The flow on a semi-infinite flat
plate in the two extreme cases of weak and strong interaction has re-
ceived considerable attention in the past. For the weak interaction
case [3,4,6] corresponding to a region far from the leading edge, the
appropriate expansion for the tangent-wedge approximation is given by
equation (1.4). It was assumed that the pressure and other inviscid
quantities varied slowly enough so that an approximate closed-form
expression for δ^* obtained from the zero-pressure gradient boundary
layer solutions could be substituted in the expansion (1.4), resulting
in a pressure distribution of the form $p^*/p^*_\infty = 1 + A\bar{\chi}$. A first order
correction to the skin friction was then calculated as a perturbation
to the zero-pressure gradient solution and it was shown that the heat
transfer was unaltered to first order.

In the strong interaction case, corresponding to a region
near the leading edge, equation (1.5) is the appropriate expansion of
the tangent wedge approximation. Using only the first term of equation
(1.5) an order of magnitude analysis shows that in the strong inter-
action region $p^* \alpha \bar{\chi}$ and $\delta^*/x^* \alpha \bar{\chi}^{-1/2}/M_\infty$. Since $\bar{\chi} \alpha x^{*-1/2}$, the
boundary layer admits similarity solution. Solutions for this zero-
order strong interaction theory were presented by Shen [2], Li and
Nagamatsu [12], Stewartson [8,12] and Dorrance [7] for an insulated
flat plate with Pr = 1. Li and Nagamatsu [14] later considered the
case of a constant temperature plate. The constants of proportionality
in the equations for p^* and δ^*, obtained by these authors were in general

agreement, the differences being mainly due to different methods of solving the boundary layer equations. In the works of Stewartson (and also Bush [15]) however, the tangent-wedge approximation was not used. Instead, it was shown that for $p* \propto x*^{-1/2}$ and $\delta* \propto x*^{3/4}$ the flows in both the boundary layer and the external layer admitted similar solutions. A solution based on the method of inner and outer expansion was presented in which it was possible to take into account the effects of vorticity in the external flow.

Lees and Probstein later generalized the strong and weak interaction theories for flow over a flat plate at non-zero angles of incidence [6]. The zero-order solutions are not affected and the effects of the non-zero angle of incidence appear through terms of higher order. In Section 3.2 the expansion scheme for the strong interaction case, outlined in Reference 6, is developed and solutions upto third order are presented.

In the strong and weak interaction theories mentioned above, the pressure variations were such that the boundary layer equations admitted similarity solutions. The partial differential equations then could be transformed into ordinary differential equations in suitable transformed variables. Such simplifications are not possible for moderately high values of $\overline{\chi}$. A theory valid for all values of $\overline{\chi}$ was presented by Nagakura and Naruse [16]. They considered the two-dimensional flow on an insulated slender body and used the Karman-Pohlhausen integral method to solve the boundary layer flow for an arbitrary pressure distribution. However, in the final expression the pressure at any point on the body was given implicitly through a

complicated nonlinear equation. This method is more suitable for the inverse problem of determining the body shape for a given pressure distribution than for the direct problem of determining the pressure distribution on a body of given shape.

An approximate method, originally suggested by Lees [17] and later modified by Moore [18] is often used in interaction problems for general values of $\bar{\chi}$. In this method, called the "local flat plate similarity" method the pressure gradient term in the momentum equation is neglected altogether, thus reducing the problem to the zero-pressure gradient Blassius problem. The basis of this assumption is the fact that the pressure gradient term in the momentum equation has a coefficient of the form $\gamma-1$ which may become very small for the high temperature gas in the boundary layer. The solutions for slender wedges presented by Cheng et al [19], Dewey [20] and Mirels and Lewellen [21] belong to this category. Other approximate theories include the works of Bertram and Blackstock [22] and White [23] where a displacement thick-ness distribution of the form $\delta^*/x^* = a\bar{\chi}p_\infty^*/(M_\infty p^*)$ was assumed. The coefficient a was found to remain approximately constant for the entire range of $\bar{\chi}$, depending only on the thermal conditions on the body. The pressure distribution $p^*(x^*)$ was then obtained from this relation and the tangent wedge equation (1.1). In spite of their approximate nature these theories often give quite useful and practical results.

Mann and Bradley [24] presented a different approach to the interaction problem which eliminated many of the approximations made in the references mentioned earlier. The flow over a flat plate at

zero incidence was considered. The non-similar boundary layer flow was obtained by numerically solving the partial differential equations. The external flow was solved by the method of characteristics. The two solutions were iterated till they converged within the required degree of accuracy.

Two other solutions of the interaction problem by Kurzrock and Mates [25] and Butler [26] should be mentioned because of their novel approach. In both works the steady flow over a flat plate at zero incidence was obtained as the asymptotic limit of the unsteady "impulsive-start-from-rest" problem. The complete unsteady Navier Stokes equations were solved numerically at discrete time steps over a region that extended beyond the shock surface. Thus the interaction between the external layer and the boundary layer did not appear explicitly. The intermediate timesteps were considered essentially as iteration steps for the final steady solution and the authors did not attribute any significance to the unsteady solution. These methods require too much computer time to be of practical use in the general case. However, the results are useful to confirm the validity of the boundary layer assumptions.

The foregoing discussion was on the interaction problem in steady hypersonic flows. In unsteady flows the interaction problem is further complicated because the lateral velocity of the unknown displacement surface also affects the external flow. Lighthill [27] presented an extension of the tangent wedge approximation to obtain the pressure on a slender moving body of shape $y_e^*(x^*,t^*)$ placed in an inviscid hypersonic stream. This extension was based on the "piston analogy" of

Hayes [28], who observed the equivalence between the steady two dimensional flow over an arbitrary body and the unsteady one-dimensional flow in front of a moving piston. The pressure in front of a piston moving with a velocity w^* in a stationary compressible medium is given by

$$\frac{p^*}{p^*_\infty} = 1 + \gamma \frac{w^*}{a^*_\infty} \left[\frac{\gamma+1}{4} \frac{w^*}{a^*_\infty} + \{(\frac{\gamma+1}{4} \frac{w^*}{a^*_\infty})^2 + 1\}^{1/2}\right] \tag{1.9}$$

where the subscript ∞ refers to conditions in the undisturbed gas. Equations 1.1 and 1.9 are analogous if one identifies w^* with the normal velocity component $u^*_e \, dy^*_e/dx^*$ induced because of the slope of the body. For a moving body an additional term $\partial y^*_e/\partial t^*$ is introduced in the normal velocity component. Thus the instantaneous pressure $p^*_e(x^*,t^*)$ on the body is given by equation 1.1 with

$$K(x^*,t^*) = \frac{w^*(x^*,t^*)}{a^*_\infty} \tag{1.10}$$

where

$$w^*(x^*,t^*) = u^*_e \, \frac{\partial y^*_e}{\partial x^*} + \frac{\partial y^*_e}{\partial t^*} \tag{1.11}$$

Miles [29] has discussed the above expression and several other variations arising from the expansions (1.4) and (1.5), for the unsteady pressure in inviscid hypersonic flow. The first two terms of the expansion (1.4) lead to the acoustic approximation formula, while the piston theory of Lighthill [27] correspond to the first four terms of (1.4).

For the unsteady interaction problem y^*_e in (1.11) should be

replaced by $(y_b^* + \Delta^*)$, where $\Delta^*(x^*,t^*)$ is the displacement thickness for the unsteady boundary layers, introduced by Moore and Ostrach [30].

Examples of unsteady interaction problem include the work of Rodkiewicz and Reshotko [31] who considered the unsteady weak interaction flow on a semi-infinite flat plate at zero-incidence after the free stream Mach number was impulsively increased by a small amount (of O(1%)). The pressure on the plate was assumed constant for calculating the unsteady boundary layer and a small unsteady perturbation in the pressure was calculated from the boundary layer solutions. This approach is justified because of the small change involved in the problem. Rodkiewicz and co-workers [32-37] later considered several variations of this problem.

Unsteady interaction problems involving lateral motion of the body are solely confined to cases of harmonic oscillations. King [38] and Orlik-Rückemann [39] considered the interaction on an oscillating slender wedge. These are examples of quasi-steady analysis, that is, the flow at any instant was assumed to be the steady flow corresponding to the conditions prevailing at that instant. Interaction problems involving impulsive lateral motion of the body are not available in literature.

1.3 Description of the Present Work

In the present work the tangent wedge approximation and its extension to the unsteady case, discussed in the last section, will be used to describe the interaction between the external flow and the boundary layer. The parameters defining the problem are the free stream

Mach number M_∞ Reynolds number $Re_{\infty,L*}$ based on the free stream conditions and the length of the wedge $L*$, the semi-wedge angle θ_w and the initial and final angles of attack α_i and α_f. In the problems considered M_∞ and $Re_{\infty,L*} \gg 1$ and the angles involved θ_w, α_i, $\alpha_f \ll 1$. However, their relative magnitudes are such that the combination $M_\infty^3/(Re_{\infty,L*})^{1/2}$ remains finite and the product $M_\infty|\theta| \leq O(1)$, where θ is the maximum deflection of the wedge surfaces. The thermal conditions on the wedge surface also affect the problem. Two types of thermal condition are used in this work - insulated wedge surface and the wedge surface maintained at a constant temperature. The fluid is assumed to be a perfect gas with constant c_p^*, γ and Pr. However, the assumptions Pr = 1 and $\gamma \to 1$, used in some of the earlier references, will not be made here.

In Chapter II, the governing equations and their transformations are presented. Chapter III is devoted to the problem of steady flow on an inclined flat plate. A four term series solution for the strong interaction region is described in Section 3.2. A more elaborate finite difference solution is presented in Section 3.3 and the results of the steady flow case are discussed in Section 3.4. In Chapter IV the unsteady flow on an inclined plate following an impulsive change in the angle of inclination is described. Initial conditions in time are derived from the steady solutions of Chapter III. The finite difference method of solution is described in detail. In Chapter V is indicated the utilization of the solutions on the two sides of the wedge yielding the unsteady characteristics of the two dimensional wedge wing.

CHAPTER II

THE GOVERNING EQUATIONS

2.1 Compressible Boundary Layer Equations for Two-Dimensional
Unsteady Flow

The governing equations for the flow in the boundary layer
are given by [8]:

Continuity equation:

$$\frac{\partial \rho^*}{\partial t^*} + \frac{\partial}{\partial x^*}(\rho^* u^*) + \frac{\partial}{\partial y^*}(\rho^* v^*) = 0 \qquad (2.1)$$

Momentum equations:

$$\rho^*(\frac{\partial u^*}{\partial t^*} + u^* \frac{\partial u^*}{\partial x^*} + v^* \frac{\partial u^*}{\partial y^*}) = -\frac{\partial p^*}{\partial x^*} + \frac{\partial}{\partial y^*}(\mu^* \frac{\partial u^*}{\partial y^*}) \qquad (2.2)$$

$$0 = \frac{\partial p^*}{\partial y^*} \qquad (2.3)$$

Energy equation:

$$\rho^*(\frac{\partial H^*}{\partial t^*} + u^* \frac{\partial H^*}{\partial x^*} + v^* \frac{\partial H^*}{\partial y^*}) = \frac{\partial p^*}{\partial t^*} + \frac{1}{Pr} \frac{\partial}{\partial y^*}(\mu^* \frac{\partial H^*}{\partial y^*})$$

$$+ (1 - \frac{1}{Pr}) \frac{\partial}{\partial y^*}(\mu^* u^* \frac{\partial u^*}{\partial y^*}) \qquad (2.4)$$

where $H^* = c_p^* T^* + u^{*2}/2$ is the total enthalpy. These equations, to-

gether with the equation of state:

$$p* = R* \, \rho* \, T* \qquad (2.5)$$

and the viscosity-temperature relation:

$$\mu* = \mu*(T*) \qquad (2.6)$$

define the complete set of equations governing the flow in the boundary layer. If we write

$$x = \frac{x*}{L*} \; , \; y = \frac{y*}{L*} \; , \; t = \frac{t* u_\infty^*}{L*}$$

$$u = \frac{u*}{u_\infty^*} \; , \; v = \frac{v*}{u_\infty^*} \; , \; p = \frac{p*}{p_\infty^*}$$

$$\rho = \frac{\rho*}{\rho_\infty^*} \; , \; T = \frac{T*}{T_\infty^*} \; , \; \mu = \frac{\mu*}{\mu_\infty^*}$$

and

$$H = \frac{H*}{\frac{1}{2} u_\infty^{*2}}$$

equations (2.1 - 2.6) take the non dimensional form:

$$\frac{\partial \rho}{\partial t} + \frac{\partial}{\partial x} (\rho u) + \frac{\partial}{\partial y} (\rho v) = 0 \qquad (2.7)$$

$$\frac{\partial u}{\partial t} + u \frac{\partial u}{\partial x} + v \frac{\partial u}{\partial y} = - \frac{\beta}{2} \frac{1}{\rho} \frac{\partial p}{\partial x} [H-u^2] + \frac{1}{Re_{\infty,L*}} \frac{1}{\rho} \frac{\partial}{\partial y} (\mu \frac{\partial u}{\partial y}) \qquad (2.8)$$

$$0 = \frac{\partial p}{\partial y} \qquad (2.9)$$

$$\frac{\partial H}{\partial t} + u \frac{\partial H}{\partial x} + v \frac{\partial H}{\partial y} = \beta \frac{1}{p} \frac{\partial p}{\partial t} [H - u^2]$$

$$+ \frac{1}{Re_{\infty,L*}} \frac{1}{\rho} [\frac{1}{Pr} \frac{\partial}{\partial y} (\mu \frac{\partial H}{\partial y}) + \frac{2(Pr-1)}{Pr} \frac{\partial}{\partial y} (\mu u \frac{\partial u}{\partial y})] \qquad (2.10)$$

$$p = \rho T \qquad (2.11)$$

and

$$\mu = \mu(T) \qquad (2.12)$$

where

$$\beta = \frac{\gamma - 1}{\gamma} \qquad (2.13)$$

and

$$Re_{\infty,L*} = \frac{u_{\infty}^* \rho_{\infty}^* L^*}{\mu_{\infty}^*} \qquad (2.14)$$

is the Reynolds number based on the length of the wedge and the free stream conditions.

The viscosity-temperature relation (2.12) is given by the Sutherland formula:

$$\mu = T^{3/2} \frac{1 + \frac{S^*}{T_{\infty}^*}}{T + \frac{S^*}{T_{\infty}^*}} \qquad (2.15)$$

where S* is a constant which has a value 110°K for air. The formula (2.15) is difficult to work with and a linear viscosity-temperature relation of the form

$$\mu = CT , \qquad (2.16)$$

suggested by Chapman and Rubesin [40] has been extensively used for compressible boundary layer problems. The constant C is taken as $T_b^{1/2}(1+S*/T_\infty^*)/(T_b+S*/T_\infty^*)$ where T_b is the non dimensional wall temperature. Thus the viscosity given by the approximation(2.16) correspond exactly to the Sutherland value at the wall, where the effects of viscosity are most pronounced.

2.2 Transformations of the Governing Equations

The governing equations are now transformed to bring them to a form suitable for numerical solution. The first step involves the introduction of the stream function, ψ, defined by

$$\rho u = \frac{\partial \psi}{\partial y} \tag{2.17}$$

and the application of Dorodnitsyn-Howarth transformation which used in conjunction with the linear viscosity-temperature relation (2.16) eliminates ρ from the transformed equations. In this transformation the independent variables x, y, t are changed to $\overline{x}$, $\overline{y}$, $\overline{t}$ where

$$\overline{x} = x \tag{2.18a}$$

$$\overline{y} = \int_{y_b}^{y} \rho \, dy \tag{2.18b}$$

$$\overline{t} = t \tag{2.18c}$$

For any function $\phi(x,y,t)$ one obtains the following relations:

$$\frac{\partial \phi}{\partial x} = \frac{\partial \phi}{\partial \overline{x}} + \frac{\partial \overline{y}}{\partial x} \frac{\partial \phi}{\partial \overline{y}} \tag{2.19a}$$

$$\frac{\partial \phi}{\partial y} = \rho \frac{\partial \phi}{\partial \overline{y}} \tag{2.19b}$$

$$\frac{\partial \phi}{\partial t} = \frac{\partial \overline{y}}{\partial t} \frac{\partial \phi}{\partial \overline{y}} + \frac{\partial \phi}{\partial \overline{t}} \; . \tag{2.19c}$$

Equations (2.17) and (2.7) then reduce to

$$u = \frac{\partial \psi}{\partial \overline{y}} \tag{2.20}$$

$$v = -\frac{1}{\rho} \left(\frac{\partial \psi}{\partial \overline{x}} + \frac{\partial \overline{y}}{\partial x} \frac{\partial \psi}{\partial \overline{y}} + \frac{\partial \overline{y}}{\partial t} \right) \tag{2.21}$$

Applying the relations (2.19) - (2.21) on equations (2.8) and (2.10) and making use of (2.9), (2.11) and (2.16) we obtain:

$$\frac{\partial^2 \psi}{\partial \overline{y} \partial \overline{t}} + \frac{\partial \psi}{\partial \overline{y}} \frac{\partial^2 \psi}{\partial \overline{x} \partial \overline{y}} - \frac{\partial \psi}{\partial \overline{x}} \frac{\partial^2 \psi}{\partial \overline{y}^2} = -\frac{\beta}{2} \frac{1}{p} \frac{\partial p}{\partial \overline{x}} \left[H - \left(\frac{\partial \psi}{\partial \overline{y}} \right)^2 \right] + \frac{Cp}{Re_{\infty,L^*}} \frac{\partial^3 \psi}{\partial \overline{y}^3} \tag{2.22}$$

and

$$\frac{\partial H}{\partial \overline{t}} + \frac{\partial \psi}{\partial \overline{y}} \frac{\partial H}{\partial \overline{x}} - \frac{\partial \psi}{\partial \overline{x}} \frac{\partial H}{\partial \overline{y}} = \beta \frac{1}{p} \frac{\partial p}{\partial \overline{t}} \left[H - \left(\frac{\partial \psi}{\partial \overline{y}} \right)^2 \right]$$

$$+ \frac{Cp}{PrRe_{\infty,L^*}} \left[\frac{\partial^2 H}{\partial \overline{y}^2} + 2(Pr-1) \left\{ \left(\frac{\partial^2 \psi}{\partial \overline{y}^2} \right)^2 + \frac{\partial \psi}{\partial \overline{y}} \frac{\partial^3 \psi}{\partial \overline{y}^3} \right\} \right] \tag{2.23}$$

The next step of transformation involves expanding the $\bar{y}$ dimension so that the derivatives with respect to $\bar{y}$ are brought to normalized forms. In the usual boundary layer problems where the pressure is a known function, it is possible to eliminate the term $Cp/Re_{\infty,L*}$, appearing in the equations (2.22) and (2.23), by suitably incorporating it in the transformed variables. This leads to equations with coefficients of $O(1)$ which are convenient to handle numerically. But in the present problem the pressure is an unknown function to be determined in accordance with the interaction equation. In order to obtain normalized coefficients in the transformed equations we introduce the function $\bar{p}(x,t)$ given by:

$$\bar{p}(x,t) = \frac{p(x,t)}{p_0\bar{X}} \tag{2.24}$$

where $p_0\bar{X}$ is the zero-order strong interaction solution for the steady state pressure and p_0 is a constant to be determined in the next Chapter. The function $\bar{p}$ is of $O(1)$.

The independent variables are now changed from $\bar{x}, \bar{y}, \bar{t}$ to $\bar{\bar{x}}, \eta, \bar{\bar{t}}$ where

$$\bar{\bar{x}} = \bar{x} \tag{2.25a}$$

$$\eta = \frac{\bar{y}}{2(p_0\bar{X}\ \bar{x})^{1/2}} \left(\frac{Re_{\infty,L*}}{C}\right)^{1/2} \tag{2.25b}$$

and

$$\bar{\bar{t}} = \bar{t} \tag{2.\,5c}$$

Noting that $\bar{x} = \bar{x}_{L*} \, x^{-1/2}$, where

$$\bar{x}_{L*} = M_\infty^3 \left(\frac{C}{Re_{\infty,L*}}\right)^{1/2} \tag{2.26}$$

is the interaction parameter evaluated at the end of the wedge, we can write

$$\eta = A \, \bar{y} \, \bar{x}^{-1/4} \tag{2.27}$$

where

$$A = \frac{1}{2} \left(\frac{Re_{\infty,L*}}{C \, p_0 \, \bar{x}_{L*}}\right)^{1/2} \tag{2.28}$$

is a constant. For any function $\phi(\bar{x}, \bar{y}, \bar{t})$ we have

$$\frac{\partial \phi}{\partial \bar{x}} = \frac{\partial \phi}{\partial \bar{\bar{x}}} - \frac{\eta}{4\bar{\bar{x}}} \frac{\partial \phi}{\partial \eta} \tag{2.29a}$$

$$\frac{\partial \phi}{\partial \bar{y}} = A \, \bar{\bar{x}}^{-1/4} \frac{\partial \phi}{\partial \eta} \tag{2.29b}$$

$$\frac{\partial \phi}{\partial \bar{t}} = \frac{\partial \phi}{\partial \bar{\bar{t}}} \tag{2.29c}$$

If we define

$$f(\bar{\bar{x}}, \eta, \bar{\bar{t}}) = A \, \bar{x}^{-1/4} \, \psi(\bar{x}, \bar{y}, \bar{t}) \tag{2.30}$$

and use the relations (2.29), then the equations (2.22) and (2.23) transform to

$$4\bar{x}\,\frac{\partial^2 f}{\partial\eta\,\partial\bar{\bar{t}}} + 4\bar{\bar{x}}\,[\frac{\partial f}{\partial\eta}\frac{\partial^2 f}{\partial\bar{\bar{x}}\partial\eta} - \frac{\partial f}{\partial\bar{\bar{x}}}\frac{\partial^2 f}{\partial\eta^2}] - f\,\frac{\partial^2 f}{\partial\eta^2} - \bar{p}\,\frac{\partial^3 f}{\partial\eta^3}$$

$$+ \beta[-1 + 2\,\frac{\bar{\bar{x}}}{\bar{p}}\,\frac{\partial\bar{p}}{\partial\bar{\bar{x}}}]\,[H - (\frac{\partial f}{\partial\eta})^2] = 0 \qquad (2.31)$$

and

$$4\bar{\bar{x}}\,\frac{\partial H}{\partial\bar{\bar{t}}} + 4\bar{\bar{x}}[\frac{\partial f}{\partial\eta}\frac{\partial H}{\partial\bar{\bar{x}}} - \frac{\partial f}{\partial\bar{\bar{x}}}\frac{\partial H}{\partial\eta}] - 4\beta\,\frac{\bar{\bar{x}}}{\bar{p}}\,\frac{\partial\bar{p}}{\partial\bar{\bar{t}}}\,[H - (\frac{\partial f}{\partial\eta})^2]$$

$$- \frac{\bar{p}}{Pr}\,[\frac{\partial^2 H}{\partial\eta^2} + 2(Pr-1)\{(\frac{\partial^2 f}{\partial\eta^2})^2 + \frac{\partial f}{\partial\eta}\frac{\partial^3 f}{\partial\eta^3}\}] - f\,\frac{\partial H}{\partial\eta} = 0 \qquad (2.32)$$

The coordinates x and t have not been distorted in the transformations. This facilitates the retrieval of physically significant results from the solutions of the transformed equations. Thus we can write (2.31) and (2.32) in the form

$$4x\,\frac{\partial^2 f}{\partial\eta\,\partial t} + 4x\,[\frac{\partial f}{\partial\eta}\frac{\partial^2 f}{\partial x\partial\eta} - \frac{\partial f}{\partial x}\frac{\partial^2 f}{\partial\eta^2}] - f\,\frac{\partial^2 f}{\partial\eta^2} - \bar{p}\,\frac{\partial^3 f}{\partial\eta^3}$$

$$+ \beta[-1 + 2\,\frac{x}{\bar{p}}\,\frac{\partial\bar{p}}{\partial x}]\,[H - (\frac{\partial f}{\partial\eta})^2] = 0 \qquad (2.33)$$

and $\qquad 4x\,\frac{\partial H}{\partial t} + 4x[\frac{\partial f}{\partial\eta}\frac{\partial H}{\partial x} - \frac{\partial f}{\partial x}\frac{\partial H}{\partial\eta}] - 4\beta\,\frac{x}{\bar{p}}\,\frac{\partial\bar{p}}{\partial t}\,[H - (\frac{\partial f}{\partial\eta})^2]$

$$- \frac{\bar{p}}{Pr}\,[\frac{\partial^2 H}{\partial\eta^2} + 2(Pr-1)\{(\frac{\partial^2 f}{\partial\eta^2})^2 + \frac{\partial f}{\partial\eta}\frac{\partial^3 f}{\partial\eta^3}\}] - f\,\frac{\partial H}{\partial\eta} = 0 \qquad (2.34)$$

It should be remembered that in the context of equations (2.33) and
(2.34)

$$\frac{\partial}{\partial x} \equiv \frac{\partial}{\partial x}\bigg|_{\eta,t}$$

$$\frac{\partial}{\partial t} \equiv \frac{\partial}{\partial t}\bigg|_{x,\eta}$$

whereas, in the context of equations (2.7) - (2.11)

$$\frac{\partial}{\partial x} \equiv \frac{\partial}{\partial x}\bigg|_{y,t}$$

$$\frac{\partial}{\partial t} \equiv \frac{\partial}{\partial t}\bigg|_{x,y}$$

However, for variables such as p, which are independent of y(and hence
independent of $\bar{y}$ and η) the partial derivative with respect to x
and t are same in both senses.

2.3 The Interaction Equation

For the unsteady flow over a flat plate inclined at a small
angle θ_b to the main flow, the shape of the "effective body" is given
by

$$y_e^*(x^*,t^*) = \theta_b\ x^* + \Delta^*(x^*,t^*) \tag{2.35}$$

From equation (1.11) the normal velocity component at the edge of this effective body is

$$w^*(x^*,t^*) = u_e^* \left[\theta_b + \frac{\partial \Delta^*}{\partial x^*}\right] + \frac{\partial \Delta^*}{\partial t^*}$$ (2.36)

Here $\Delta^*(x^*,t^*)$ is the displacement thickness for the unsteady boundary layer, introduced by Moore and Ostrach [30]. In terms of the present notations the differential equation for Δ^* becomes

$$\frac{\partial}{\partial x^*} \left[\rho_e^* u_e^* \Delta^* - \int_{y_b^*}^{y_e^*} (\rho_e^* u_e^* - \rho^* u^*)dy^*\right]$$

$$+ \frac{\partial}{\partial t^*} \left[\rho_e^* \Delta^* - \int_{y_b^*}^{y_e^*} (\rho_e^* - \rho^*)dy^*\right] = 0$$ (2.37)

Using the continuity equation for the external flow

$$\frac{\partial \rho_e^*}{\partial t^*} + \frac{\partial}{\partial x^*} (\rho_e^* u_e^*) = 0$$ (2.38)

equation (2.37) can be reduced to

$$\rho_e^*\left[\frac{\partial \Delta^*}{\partial t^*} + u_e^* \frac{\partial \Delta^*}{\partial x^*}\right] = \frac{\partial}{\partial x^*} \left[\rho_e^* u_e^* \int_{y_b^*}^{y_e^*} \left(1 - \frac{\rho^* u^*}{\rho_e^* u_e^*}\right)dy^*\right]$$

$$+ \frac{\partial}{\partial t^*} \left[\rho_e^* \int_{y_b^*}^{y_e^*} \left(1 - \frac{\rho^*}{\rho_e^*}\right) dy^*\right]$$ (2.39)

If we apply the transformations of the last section on the two integrals appearing in (2.39) it is found that

$$\int_{y_b^*}^{y_e^*} (1 - \frac{\rho^* u^*}{\rho_e^* u_e^*}) \, dy^* \approx \int_{y_b^*}^{y_e^*} (1 - \frac{\rho^*}{\rho_e^*}) \, dy^*$$

$$\approx \frac{(\gamma-1) \, L^*(\overline{\chi}_{L^*})^{1/2}}{\sqrt{p_0} \quad M_\infty} \quad \frac{x^{3/4}}{\overline{p}} \int_0^\infty [H - (\frac{\partial f}{\partial \eta})^2] \, d\eta \qquad (2.40)$$

Here terms of $O(M_\infty^{-2})$ have been neglected from the integrand of the last integral. Writing δ^* for both the integrals in (2.39) and using (2.38) once again, we obtain

$$\frac{\partial \Delta^*}{\partial t^*} + u_e^* \frac{\partial \Delta^*}{\partial x^*} = \frac{\partial \delta^*}{\partial t^*} + u_e^* \frac{\partial \delta^*}{\partial x^*} \qquad (2.41)$$

A further simplification is obtained if u_e^* is replaced by u_∞^* . This is consistent with the observation of Stewartson [8] and Goldsworthy [11] that

$$u_e = \frac{u_e^*}{u_\infty^*} = 1 + O(M_\infty^{-2}) \qquad (2.42)$$

when M_∞ is large but the product of M_∞ and the streamline deflection in the external flow remains finite. Therefore from (1.1), (1.11) and (2.35) we have

$$\overline{p}(x,t) = \frac{p}{p_0 \overline{x}}$$

$$= \frac{1}{p_0 \overline{x}} [1 + \gamma K \{ \frac{\gamma+1}{4} K + [(\frac{\gamma+1}{4} K)^2 + 1]^{1/2} \}] \qquad (2.43)$$

where

$$K(x,t) = M_\infty(\theta_b + \frac{\partial\delta}{\partial x} + \frac{\partial\delta}{\partial t})$$ (2.44)

and

$$\delta(x,t) = \frac{\delta^*}{L^*} = \frac{\gamma-1}{\sqrt{p_0}} \frac{\overline{X_L^*}^{1/2}}{M_\infty} \frac{x^{3/4}}{\overline{p}} \int\limits_0^\infty [H - (\frac{\partial f}{\partial \eta})^2] \, d\eta$$ (2.45)

The interaction problem can now be stated as follows: the functions $f(x,\eta, t)$ and $H(x,\eta,t)$ are to be solved from equation (2.33) and (2.34) for a function $\overline{p}(x,t)$ which is related to $f(x,\eta,t)$ and $H(x,\eta,t)$ through equations (2.43-45).

2.4 Boundary and Initial Conditions

The conditions on the wedge surface and at the outer edge of the boundary layer provide the boundary conditions in η. On the wedge surface both components of velocity are zero and the wedge is either insulated or held at a constant temperature. Thus,

at $y^* = y_b^*$

$$u^* = 0$$ (2.46a)

$$v^* = 0$$ (2.46b)

$$\frac{\partial T^*}{\partial y^*} = 0 \quad \text{(for insulated wedge surface)}$$ (2.46c)

or

$$T^* = T_b^* = \text{constant (for constant temperature wedge surface)}$$ (2.46d)

In terms of the transformed variables we have

at $\eta = 0$

$$f = 0 ,\tag{2.47a}$$

$$\frac{\partial f}{\partial \eta} = 0 ,\tag{2.47b}$$

$$\frac{\partial H}{\partial \eta} = 0\tag{2.47c}$$

$$\text{or} \quad H = H_b = \text{constant}\tag{2.47d}$$

where $H_b = c_p^* \, T_b^*/\frac{1}{2} u_\infty^{*2}$. At the edge of the boundary layer the tangential velocity and the total enthalpy in the boundary layer should match with the corresponding quantities in the external layer. Thus

at $y^* = y_e^*$

$$u^* = u_e^*\tag{2.48a}$$

$$H^* = H_e^*\tag{2.48b}$$

In terms of transformed variables we have

at $\eta \to \infty$

$$\frac{\partial f}{\partial \eta} = 1\tag{2.49a}$$

$$H = 1\tag{2.49b}$$

where terms of order M_∞^{-2} have been neglected.

In boundary layer problems it is customary to satisfy the conditions (2.49a,b) at a finite value $\eta = \eta_e$. The value of η_e is chosen sufficiently large, so that, in the resulting solution $|\partial^n f(\eta_e)/\partial \eta^n|$, $n \geq 2$ and $|\partial^k H(\eta_e)/\partial \eta^k|$, $k \geq 1$ can be made less than a predefined tolerance. From preliminary experiments it was found that, for the problems considered in the present work $\eta_e = 8$ was sufficient for a tolerance of 10^{-6}.

The initial conditions in x and t are discussed in Chapters III and IV.

CHAPTER III

THE STEADY FLOW ON AN INCLINED FLAT PLATE

3.1 Introduction

In this Chapter the steady hypersonic flow on a flat plate inclined at a small angle θ_b to the free stream will be considered. The solution of the steady problem will provide the initial conditions for the unsteady problem at $t = 0$ and also the final solution to which the unsteady flow should converge as $t \to \infty$.

Specializing the governing equations to the steady case, we have from equations (2.33) and (2.34)

$$\bar{p} \frac{\partial^3 f}{\partial \eta^3} + f \frac{\partial^2 f}{\partial \eta^2} - 4x \left[\frac{\partial f}{\partial \eta} \frac{\partial^2 f}{\partial x \partial \eta} - \frac{\partial f}{\partial x} \frac{\partial^2 f}{\partial \eta^2}\right]$$

$$= \beta\left[-1 + \frac{2x}{\bar{p}} \frac{d\bar{p}}{dx}\right] \left[H - \left(\frac{\partial f}{\partial \eta}\right)^2\right] \qquad (3.1)$$

and

$$\frac{\bar{p}}{Pr} \frac{\partial^2 H}{\partial \eta^2} + f \frac{\partial H}{\partial \eta} - 4x \left[\frac{\partial f}{\partial \eta} \frac{\partial H}{\partial x} - \frac{\partial f}{\partial x} \frac{\partial H}{\partial \eta}\right]$$

$$= \frac{2(1-Pr)}{Pr} \bar{p}\left\{\left(\frac{\partial^2 f}{\partial \eta^2}\right)^2 + \frac{\partial f}{\partial \eta} \frac{\partial^3 f}{\partial \eta^3}\right\} \qquad (3.2)$$

For the steady problem $\bar{p} = \bar{p}(x)$ is given by (2.43) with

$$K(x) = M_\infty\left(\theta_b + \frac{d\delta}{dx}\right) \qquad (3.3)$$

and $\delta = \delta(x)$ given by equation (2.45).

3.2   Series Expansion Solution of the Steady Problem*

A series expansion scheme for solving the steady strong interaction flow on an inclined flat plate, originally suggested by Lees and Probstein [6], is considered in this Section. Using appropriate expansions for p, δ, f and H in terms of the interaction parameter $\overline{\chi}$ and $K_b (= M_\infty \theta_b)$, the partial differential equations (3.1) and (3.2) are reduced to a sequence of ordinary differential equations. The unknown constants appearing in the expansions of p, δ, etc. are then determined from the solutions of these ordinary differential equations in accordance with the tangent wedge equation.

The zero-order term of this scheme correspond to the strong interaction similarity solution considered in references [6,7,8,12, 13,14] where the assumption Pr = 1 was made to simplify the energy equation. Solutions for higher order terms are not generally available. In this section solutions for terms up to third order are carried out for arbitrary values of Pr.

We start with the expansion

$$p = \frac{\gamma(\gamma+1)}{2} K^2 + \frac{3\gamma+1}{\gamma+1} - \frac{8}{(\gamma+1)^3} K^{-2} + 0(K^{-4}) \qquad (1.5)$$

of the tangent wedge equation (1.1). If we define the constant

---

$$K_b = M_\infty \theta_b \tag{3.4}$$

then from (3.3) we have

$$K(x) = K_b + M_\infty \frac{d\delta}{dx} \tag{3.5}$$

For the strong interaction region ($\bar{\chi} \gg 1$) an order of magnitude analysis [6] shows that

$$M_\infty \frac{\delta}{x} \alpha \; \bar{\chi}^{-1/2}$$

or $\qquad\qquad M_\infty \frac{d\delta}{dx} \alpha \; \bar{\chi}^{-1/2} \tag{3.6}$

Writing $K(x) = K_b + \text{constant} \; \bar{\chi}^{-1/2}$ and substituting in equation (1.5), we have for $\bar{\chi} \gg 1$

$$p(x) = p_0 \; \bar{\chi}[1 + \frac{p_1 K_b}{\bar{\chi}^{-1/2}} + \frac{p_2 + p_3 K_b^2}{\bar{\chi}} + 0(\bar{\chi}^{-3/2})] \tag{3.7}$$

where $p_i (i=0,1,2,3)$ are constants to be determined. Consistent with (3.7) we have for δ

$$\frac{\delta(x)}{x} = \frac{\delta_0 \; \bar{\chi}^{-1/2}}{M_\infty} [1 + \frac{\delta_1 K_b}{\bar{\chi}^{-1/2}} + \frac{\delta_2 + \delta_3 K_b^2}{\bar{\chi}} + 0(\bar{\chi}^{-3/2})] \tag{3.8}$$

where $\delta_i (i=0,1,2,3)$ are constants. On substituting (3.7) and (3.8) in (3.5) and (1.5) one obtains the following relations between the two

sets of constants:

$$p_0 = \frac{9}{32} \gamma(\gamma+1) \, \delta_0^{\,2} \tag{3.9a}$$

$$p_1 = \frac{8}{3} (\delta_1 + \frac{1}{\delta_0}) \tag{3.9b}$$

$$p_2 = \frac{10}{3} \delta_2 + \frac{32}{9} \frac{3\gamma+1}{\gamma(\gamma+1)^2} \frac{1}{\delta_0^{\,2}} \tag{3.9c}$$

$$p_3 = \frac{10}{3} \delta_3 + \frac{16}{9} (\delta_1 + \frac{1}{\delta_0})^2 \tag{3.9d}$$

In view of the expansions (3.7) and (3.8), Lees and Probstein [9] suggested the following expansions for f and H:

$$f(x,\eta) = f_0(\eta) + \frac{f_1(\eta) \, K_b}{\overline{\chi}^{-1/2}} + \frac{f_2(\eta) + f_3(\eta) \, K_b^{\,2}}{\overline{\chi}} + 0(\overline{\chi}^{-3/2}) \tag{3.10}$$

and

$$H(x,\eta) = H_0(\eta) + \frac{H_1(\eta) K_b}{\overline{\chi}^{-1/2}} + \frac{H_2(\eta) + H_3(\eta) K_b^{\,2}}{\overline{\chi}} + 0(\overline{\chi}^{-3/2}) \tag{3.11}$$

On inserting the expansions (3.7), (3.10) and (3.11) in the equations (3.1) and (3.2) and equating the terms of the same order on the two sides we get the following sets of coupled ordinary differential equations for $f_i(\eta)$, $H_i(\eta)$ (i=0,1,2,3):

$$f_0''' + f_0 f'' + \beta(H_0 - f_0'^2) = 0 \tag{3.12a}$$

$$H_0'' + Prf_0H_0' - 2(1-Pr)[(f_0')^2 + f_0'f_0''] = 0 \qquad (3.12b)$$

$$f_1''' + f_0f_1'' - f_0'f_1' + 2f_0''f_1 + \beta[H_1 - 2f_0'f_1']$$

$$= p_1[\frac{3}{2}\beta(H_0 - f_0'^2) + f_0f_0''] \qquad (3.13a)$$

$$H_1'' + Prf_0H_1' - Prf_0'H_1$$

$$- 2(1-Pr)[f_0'f_1'' + 2f_0''f_1' + f_0'''f_1'] + 2PrH_0'f_1$$

$$= p_1Prf_0H_0' \qquad (3.13b)$$

$$f_2''' + f_0f_2'' - 2f_0'f_2' + 3f_0''f_2 + \beta[H_2 - 2f_0'f_2']$$

$$= p_2[2\beta(H_0 - f_0'^2) + f_0f_0''] \qquad (3.14a)$$

$$H_2'' + Prf_0H_2' - 2Prf_0'H_2$$

$$- 2(1-Pr)[f_0'f_2'' + 2f_0''f_2' + f_0'''f_2'] + 3PrH_0'f_2$$

$$= p_2 Prf_0H_0' \qquad (3.14b)$$

$$f_3''' + f_0f_3'' - 2f_0'f_3' + 3f_0''f_3 + \beta(H_3 - 2f_0'f_3')$$

$$= p_3[2\beta(H_0 - f_0'^2) + f_0f_0'']$$

$$- p_1^2 \frac{\beta}{2} (H_0 - f_0'^2)$$

$$+ p_1 [\frac{\beta}{2} (H_1 - 2f_0'f_1') - f_1''']$$

$$- 2f_1 f_1'' + (1+\beta) f_1'^2 \tag{3.15a}$$

$$H_3'' + Prf_0 H_3' - 2Prf_0' H_3$$

$$- 2(1-Pr) [f_0'f_3'' + 2f_0''f_3' + f_0'''f_3] + 3PrH_0'f_3$$

$$= p_3 Prf_0 H_0'$$

$$+ p_1 [2(1-Pr) \{f_0'f_1'' + 2f_0''f_1' + f_0'''f_1\} - H_1'']$$

$$+ 2(1-Pr)\{f_1 f_1'' + (f_1')^2\} + Pr\{f_1' H_1 - 2f_1 H_1'\} \tag{3.15b}$$

Here the prime represents differentiation with respect to η. In equations (3.13) through (3.15) the unknown constants $p_i (i=1,2,3)$ appear in the inhomogeneous parts. To eliminate these unknowns we introduce a further change of variables:

$$\bar{f}_1 = \frac{f_1}{p_1}, \quad \bar{H}_1 = \frac{H_1}{p_1} \tag{3.16}$$

$$\bar{f}_2 = \frac{f_2}{p_2}, \quad \bar{H}_2 = \frac{H_2}{p_2} \tag{3.17}$$

$$\overline{f}_3 = (f_3 - p_3\overline{f}_2)/p_1^2 \ , \quad \overline{H}_3 = (H_3 - p_3\overline{H}_2)/p_1^2 \tag{3.18}$$

From equations (3.13) through (3.15) we obtain the following differential equations for $\overline{f}_i(\eta)$, $\overline{H}_i(\eta)$ (i=1,2,3):

$$L_i^{(1)}(\overline{f}_i) + \beta\overline{H}_i = F_i^{(1)}(\eta) \tag{3.19a}$$

$$L_i^{(2)}(\overline{H}_i) + L_i^{(3)}(\overline{f}_i) = F_i^{(2)}(\eta) \tag{3.19b}$$

The linear operators $L_i^{(j)}$ (i,j=1,2,3) are given by

$$L_i^{(1)} = \frac{d^3}{d\eta^3} + f_0\frac{d^2}{d\eta^2} - (a_i+2\beta)f_0'\frac{d}{d\eta} + b_if_0'' \tag{3.20}$$

$$L_i^{(2)} = \frac{d^2}{d\eta^2} + Prf_0\frac{d}{d\eta} - a_iPrf_0' \tag{3.21}$$

$$L_i^{(3)} = -2(1-Pr)(f_0'\frac{d^3}{d\eta^3} + 2f_0''\frac{d^2}{d\eta^2} + f_0'''\frac{d}{d\eta}) + b_iPrH_0' \tag{3.22}$$

with $a_1 = 1$, $a_2 = a_3 = 2$, $b_1 = 2$, $b_2 = b_3 = 3$. The functions $F_i^{(1)}$, $F_i^{(2)}$ are given by

$$F_i^{(1)}(\eta) = c_i\beta(H_0-f_0'^2) + f_0''f_0 \quad \text{for} \quad i = 1,2 \tag{3.23}$$

$$F_i^{(1)}(\eta) = (\overline{f}_1''-f_0'')(f_0-2\overline{f}_1) - f_1'[f_0'-(1+\beta)\overline{f}_1']$$

$$+ \frac{3}{2}\beta(\overline{H}_1-2f_0'\overline{f}_1') - 2\beta(H_0-f_0'^2) \quad \text{for} \quad i=3 \tag{3.24}$$

$$F_i^{(2)}(\eta) = PrH_0'f_0 \quad \text{for} \quad i=1,2 \tag{3.25}$$

$$F_i^{(2)}(\eta) = Pr(\overline{H}_1' - H_0')(f_0 - 2\overline{f}_1) + Pr\overline{H}_1(\overline{f}_1' - f_0')$$

$$+ 2(1-Pr)[(\overline{f}_1')^2 + \overline{f}_1\overline{f}_1''] \quad \text{for} \quad i=3 \tag{3.26}$$

with $c_1 = 1.5$ and $c_2 = 2$.

From (2.47) and (2.49) the boundary conditions can be written as

$$f_0(0) = 0 \tag{3.27a}$$

$$f_0'(0) = 0 \tag{3.27b}$$

$$H_0'(0) = 0 \quad \text{(for insulated surface)} \tag{3.27c}$$

or $\qquad H_0(0) = H_b \quad$ (for constant temperature surface) (3.27d)

$$f_0'(\eta_e) = 1 \tag{3.27e}$$

$$H_0(\eta_e) = 1 \tag{3.27f}$$

and for $\overline{f}_i$, $\overline{H}_i$ (i=1,2,3)

$$\overline{f}_i(0) = 0 \tag{3.28a}$$

$$\overline{f}_1'(0) = 0 \qquad (3.28b)$$

$$\overline{H}_i'(0) = 0 \quad \text{(for insulated surface)} \qquad (3.28c)$$

or $$\overline{H}_i(0) = 0 \quad \text{(for constant temperature surface)} \qquad (3.28d)$$

$$\overline{f}_1'(\eta_e) = 0 \qquad (3.28e)$$

$$\overline{H}_i(\eta_e) = 0 \qquad (3.28f)$$

In order to determine the unknown constants p_i, $\delta_i (i=0,1,2,3)$ we insert the expansions (3.7), (3.10) and (3.11) in (2.45) to obtain the following expression for δ:

$$\frac{\delta(x)}{x} = \frac{\gamma-1}{(p_0)^{1/2}} \frac{\overline{\chi}^{-1/2}}{M_\infty} [I_0 + p_1(I_1 - I_0) \frac{K_b}{\overline{\chi}^{-1/2}}$$

$$+ \{p_2(I_2 - I_0) + [p_2(I_2 - I_0) + p_1^2(I_3 - I_1 + I_0)]K_b^2\}/\overline{\chi}] \qquad (3.29)$$

where $$I_0 = \int_0^\infty (H_0 - f_0'^2) d\eta \qquad (3.30a)$$

$$I_1 = \int_0^\infty (\overline{H}_1 - 2f_0'\overline{f}_1') d\eta \qquad (3.30b)$$

$$I_2 = \int_0^\infty (\overline{H}_2 - 2f_0'\overline{f}_2') d\eta \qquad (3.30c)$$

$$I_3 = \int_0^\infty (\overline{H}_3 - 2f_0'\overline{f}_1' - \overline{f}_1'^2) d\eta \qquad (3.30d)$$

On comparing (3.29) with (3.8) one obtains

$$\delta_0 = \frac{\gamma-1}{(p_0)^{1/2}} I_0 \tag{3.31a}$$

$$\delta_1 = p_1(\frac{I_1}{I_0} - 1) \tag{3.31b}$$

$$\delta_2 = p_2(\frac{I_2}{I_0} - 1) \tag{3.31c}$$

$$\delta_3 = p_2(\frac{I_2}{I_0} - 1) + p_1^2[\frac{(I_3-I_1)}{I_0} + 1] \tag{3.31d}$$

Using (3.9) and (3.31) we now obtain the following expressions for the constants p_i:

$$p_0 = \frac{3}{4}(\gamma-1)[\frac{\gamma(\gamma+1)}{2}]^{1/2} I_0 \tag{3.32a}$$

$$p_1 = \frac{8 p_0^{1/2}}{(\gamma-1)(11I_0-8I_1)} \tag{3.32b}$$

$$p_2 = \frac{8(3\gamma+1)}{(\gamma^2-1)[2\gamma(\gamma+1)]^{1/2}(13I_0-10I_2)} \tag{3.32c}$$

$$p_3 = \frac{p_1^2(40I_3-40I_1+43I_0)}{(52I_0-40I_2)} \tag{3.32d}$$

Numerical method of solving the ordinary differential equations for f_0, H_0, $\bar{f}_i$, $\bar{H}_i$ (i=1,2,3) is described in the following subsection. From these solutions the integrals I_0, I_1, I_2, I_3 are

calculated. The constants p_i, $\delta_i (i=0,1,2,3)$ are then obtained from the equations (3.31) and (3.32).

3.2a Method of Solution

The equations for f_0, H_0 are nonlinear, while those for $\overline{f}_i$, $\overline{H}_i$ (i=1,2,3) are linear. The problems are of the boundary value type, that is, three conditions are specified at $\eta = 0$ and two conditions at $\eta = \eta_e$.

Let us first consider the zero-order problem

$$f_0''' + f_0 f_0'' + \beta(H_0 - f_0'^2) = 0 \qquad (3.12a)$$

$$H_0'' + Pr f_0 H_0' - 2(1-Pr)[(f_0'')^2 + f_0' f_0'''] = 0 \qquad (3.12b)$$

$$f_0(0) = 0 \; ; \; f_0'(0) = 0 \; ; \; H_0'(0) = 0 \text{ or } H_0(0) = \dot{H}_b \; ;$$

$$f_0'(\eta_e) = 1 \; ; \; H_0(\eta_e) = 1 \qquad (3.27)$$

Earlier workers often used the assumption Pr = 1, which eliminates the last term in (3.12b). For Pr = 1 and the insulated surface case, $H_0'(0) = 0$ (also for constant surface-temperature case with $H_b = 1$) equation (3.12b) has the constant solution $H_0(\eta) = 1$. The zero order problem in such cases reduces to the classical Falkner-Skan problem:

$$f_0''' + f_0 f_0'' + \beta(1 - f_0'^2) = 0 \qquad (3.33a)$$

$$f_0(0) = 0 \; ; \; f_0'(0) = 0 \; ; \; f_0'(\eta_e) = 1 \tag{3.33b}$$

In their work on similar solutions of compressible boundary layers, Cohen and Reshotko [41] have studied extensively problems of the type (3.12,27) for arbitrary values of β. It was shown that for positive values of β, the conditions (3.27) are sufficient to give a unique solution. In the present case $\beta = (\gamma-1)/\gamma$ is positive.

The nonlinear boundary value problem given by equations (3.12,27) can only be solved iteratively. In the method employed by Cohen and Reshotko, the differential equations were transformed to an integral system with f_0' as the independent variable. At each iteration stage a better approximation to the solutions was obtained by numerically integrating two functions that involved the current approximate solutions. In the present work we use a more direct approach, called the "shooting method", where the solution to the boundary value problem is obtained by solving a sequence of initial value problems.

We first consider the insulated surface case. The equations (3.12) can be solved as an initial value problem if all the elements of the row vector

$$c = [f_0(0), \; f_0'(0), \; f_0''(0), \; H_0(0), \; H_0'(0)] \tag{3.34}$$

are known. We first assume suitable approximations σ_1 and λ_1 for the unknown conditions $f_0''(0)$ and $H_0(0)$. With the initial condition

$$c_1 = [0, 0, \sigma_1, \lambda_1, 0] \tag{3.35}$$

the equations (3.12) are solved up to $\eta = \eta_e$ by the predictor-corrector method described in Appendix A. From the solution we note

$$A_1 = f_0'(\eta_e) - 1 \tag{3.36a}$$

and
$$B_1 = H_0(\eta_e) - 1 \tag{3.36b}$$

which represent the errors in satisfying the conditions at $\eta = \eta_e$. The equations are solved two more times with the initial conditions:

$$c_2 = [0, 0, \sigma_1 + \varepsilon, \lambda_1, 0] \tag{3.37a}$$

and
$$c_3 = [0, 0, \sigma_1, \lambda_1 + \varepsilon, 0] \tag{3.37b}$$

where ε is a small quantity. Let (A_2, B_2) and (A_3, B_3) be errors corresponding to (3.36) in the two cases. Interpolating from the above results we obtain more accurate approximations for the missing initial conditions:

$$\sigma_2 = \sigma_1 + \frac{\varepsilon(B_1 A_3 - B_3 A_1)}{A_1(B_2 - B_3) + A_2(B_3 - B_1) + A_3(B_1 - B_2)} \tag{3.38a}$$

$$\lambda_2 = \lambda_1 + \frac{\varepsilon(B_2 A_1 - B_1 A_2)}{A_1(B_2 - B_3) + A_2(B_3 - B_1) + A_3(B_1 - B_2)} \tag{3.38b}$$

The calculations are repeated with these values of the missing conditions. The iteration is stopped when $|A_1|$ and $|B_1|$ becomes less than a predefined tolerence. The initial approximations σ_1 and λ_1 are found by preliminary trials. The perturbation term ε is progressively reduced as the solution approaches convergence.

For constant surface temperature case the missing initial conditions are $f_0''(0)$ and $H_0'(0)$. The above iteration scheme is used with

$$c_1 = [0, 0, \sigma_1, H_b, \lambda_1] \qquad (3.39a)$$

$$c_2 = [0, 0, \sigma_1 + \varepsilon, H_b, \lambda_1] \qquad (3.39b)$$

$$c_3 = [0, 0, \sigma_1, H_b, \lambda_1 + \varepsilon] \qquad (3.39c)$$

The problems for $\overline{f}_i$, $\overline{H}_i$ $(i=1,2,3)$ are linear and therefore, can be solved directly. For each i we solve the following three initial value problems using the predictor-corrector method described in Appendix A:

$$L_i^{(1)}(f^{(1)}) + \beta H^{(1)} = F_i^{(1)}(\eta)$$

$$L_i^{(2)}(H^{(1)}) + L_i^{(3)}(f^{(1)}) = F_i^{(2)}(\eta)$$

$$f^{(1)}(0) = 0 \; ; \; f^{(1)'}(0) = 0 \; ; \; f^{(1)''}(0) = 0$$

$$H^{(1)}(0) = 0 \; ; \; H^{(1)'}(0) = 0 \tag{3.40}$$

$$L_i^{(1)}(f^{(2)}) + \beta H^{(2)} = 0$$

$$L_i^{(2)}(H^{(2)}) + L_i^{(3)}(f^{(2)}) = 0$$

$$f^{(2)}(0) = 0 \; ; \; f^{(2)'}(0) = 0 \; ; \; f^{(2)''}(0) = 1 \; ;$$

$$H^{(2)}(0) = 0 \; ; \; H^{(2)'}(0) = 0 \tag{3.41}$$

$$L_i^{(1)}(f^{(3)}) + \beta H^{(3)} = 0$$

$$L_i^{(2)}(H^{(3)}) + L_i^{(3)}(f^{(3)}) = 0$$

$$f^{(3)}(0) = 0 \; ; \; f^{(3)'}(0) = 0 \; ; \; f^{(3)''}(0) = 0 \; ;$$

$$H^{(3)}(0) = 1 \; ; \; H^{(3)'}(0) = 0 \quad \text{(for insulated surface)}$$

$$\text{or} \quad H^{(3)}(0) = 0 \; ; \; H^{(3)'}(0) = 1 \quad \text{(for constant-temperature surface)} \tag{3.42}$$

The solution can then be obtained from

$$\overline{f}_i = f^{(1)} + Af^{(2)} + Bf^{(3)} \tag{3.43a}$$

$$\overline{H}_i = H^{(1)} + AH^{(2)} + BH^{(3)} \tag{3.43b}$$

where the constants A, B are adjusted to satisfy the conditions $\bar{f}_i'(\eta_e) = 0$
and $\bar{H}_i(\eta_e) = 0$. A and B are given by

$$A = - \frac{f^{(1)'}(\eta_e)H^{(3)}(\eta_e) - f^{(3)'}(\eta_e)H^{(1)}(\eta_e)}{f^{(2)'}(\eta_e)H^{(3)}(\eta_e) - f^{(3)'}(\eta_e)H^{(2)}(\eta_e)} \qquad (3.44a)$$

$$B = - \frac{f^{(1)'}(\eta_e)H^{(2)}(\eta_e) - f^{(2)'}(\eta_e)H^{(1)}(\eta_e)}{f^{(3)'}(\eta_e)H^{(2)}(\eta_e) - f^{(2)'}(\eta_e)H^{(3)}(\eta_e)} \qquad (3.44b)$$

The FORTRAN program for the series solution is described in
Appendix A.

3.3 Finite Difference Solution for the Steady Problem

The series expansion solution discussed in Section 3.2 has
an error of order $\bar{\chi}^{-3/2}$. This solution is therefore suitable for
sufficiently high values of $\bar{\chi}$ only. In the problems considered in
the present work $\bar{\chi}_L*$ can be as low as O(1), which requires a more
accurate solution. In the current Section a finite difference method
is presented which refines the steady state series expansion solution.
The complete form of the tangent wedge equation is used.

For the finite difference solution it is necessary to specify
the initial values of $f(x_1,\eta)$, $H(x_1,\eta)$ and $\bar{p}(x_1)$ on some initial line
$x = x_1$. In numerical solutions of the steady boundary layer problems
[22,42-44] the usual practice is to specify these initial conditions
at x = 0. Since all the x-derivatives are multiplied by x, the partial
differential equations (3.1) and (3.2) reduce to ordinary differential

equations in η at $x = 0$. The solutions of these ordinary differential equations are then used as the initial values. This approach is questionable because it assumes the validity of the boundary layer equations at $x = 0$. In the present work an alternate approach in line with that used by Baxter and Flügge-Lotz [45] is employed. The values given by the series expansion solution on a line $x = x_1$ near the leading edge are used as the initial values. x_1 is given a value of the order 10^{-3}, which corresponds to $\bar{x} \sim O(10^2)$, so that the series expansion solutions are of sufficient accuracy at $x = x_1$. Lees [5] mentioned $(\delta^*/x^*)^2 \leq 10^{-1}$ as the limit of the applicability of the boundary layer equations. The present choice meets this criterion.

The initial conditions are, therefore,

$$f(x_1,\eta) = f_0(\eta) + \frac{p_1\bar{f}_1(\eta) \ K_b}{\bar{x}_1^{1/2}} + \frac{p_2\bar{f}_2(\eta)+[p_3\bar{f}_2(\eta)+p_1{}^2\bar{f}_3(\eta)]K_b{}^2}{\bar{x}_1} \quad (3.45a)$$

$$H(x_1,\eta) = H_0(\eta) + \frac{p_1\bar{H}_1(\eta) \ K_b}{\bar{x}_1^{1/2}} + \frac{p_2\bar{H}_2(\eta)+[p_3\bar{H}_2(\eta)+p_1{}^2\bar{H}_3(\eta)]K_b{}^2}{\bar{x}_1} \quad (3.45b)$$

$$\bar{p}(x_1) = 1 + \frac{p_1 K_b}{\bar{x}_1^{1/2}} + \frac{p_2+p_3 \ K_b{}^2}{\bar{x}_1} \quad (3.45c)$$

where $\bar{x}_1 = \bar{x}_L * x_1^{-1/2}$ and the other quantities are as defined in the previous Section.

The interaction between the boundary layer and the external layer is tackled by an iterative procedure. Each iteration cycle consists of the following two parts:

(i)   to solve equations (3.1,2), for any given $\bar{p}(x)$ distribution,
      in the region $x_1 \leq x \leq 1$, $0 \leq \eta \leq \eta_e$ subject to the initial
      conditions (3.45a,b) and boundary conditions (2.47) and (2.49),

(ii) to obtain a new $\bar{p}(x)$ distribution from the solutions $f(x,\eta)$,
      $H(x,\eta)$ of (i), making use of equations (2.43),(2.45), (3.3)
      and (3.45c).

The steps (i) and (ii) are repeated until $\bar{p}(x)$ converges
within a specified tolerance. Details of the two parts are given in
the sub-sections 3.3a and 3.3b.

3.3a Finite Difference Solution of the Boundary Layer Equations

From the series expansion solutions it can be observed that
the x-derivatives of different flow variables f, H, $\bar{p}$, etc. are large
for small values of x and the x-dependence decreases in the downstream
direction. For the same degree of accuracy a finite difference scheme
should therefore employ smaller stepsize near the leading edge. In
the present work we use the following arrangement of x-stations, in
which the stepsizes increase in the positive x-direction in geometric
progression:

$$\Delta x_1 = x_1 \tag{3.46a}$$

$$\Delta x_j = x_j - x_{j-1} = K_x \Delta x_{j-1}, \ j=2,3,\ldots,J \tag{3.46b}$$

Here K_x is a constant greater than 1 and J is an integer such that

$x_J = 1.$

In equations (3.1) and (3.2) the x-derivatives appear in the form $4x \, \partial\phi/\partial x$ where ϕ is a dummy function. A finite difference formula for this term for the present arrangement of x-stations can be written as:

$$\left[4x \frac{\partial\phi}{\partial x}\right]_j = B_j\phi_j - (B_j+C_j)\phi_{j-1} + C_j\phi_{j-2}, \quad j=2,3,\ldots J \qquad (3.47)$$

where ϕ_j represents $\phi(x_j)$ and the coefficients B_j, C_j are given by:

$$B_j = 4(K_x+1)/K_x \; , \; j=2$$

$$= \frac{4(2K_x+1)}{K_x+1} \frac{x_j}{\Delta x_j} \; , \; j=3,4,\ldots,J \qquad (3.48)$$

$$C_j = 0 \; , \; j=2$$

$$= \frac{4K_x^2}{K_x+1} \frac{x_j}{\Delta x_j} \; , \; j=3,4,\ldots,J \qquad (3.49)$$

This corresponds to three-point backward difference formula for $j=3,4,\ldots,J$ and two-point backward difference formula for $j=2$*. The truncation error involved in equation (3.47) is of the order $x_j\Delta x_j(\partial^2\phi/\partial x^2)_j$ for $j=2$ and $x_j\Delta x_j^2(\partial^3\phi/\partial x^3)_j$ for $j=3,4,\ldots,J$.

---

*For $j=2$, ϕ_{j-2}, is undefined. But since C_2 has been set equal to zero this does not present any problem. This arbitraryness has been introduced for the sake of uniformity at all x-stations, $j=2,3,\ldots,J$.

Substituting (3.47) in (3.1,2) we obtain

$$\overline{p}_j f_j''' + f_j''[(1+B_j)f_j - (B_j+C_j)f_{j-1} + C_j f_{j-2}]$$

$$- f_j'[(B_j+Q_j)f_j' - (B_j+C_j)f_{j-1}' + C_j f_{j-2}'] + Q_j H_j = 0 \qquad (3.50)$$

and

$$\frac{\overline{p}_j}{Pr} H_j'' + H_j'[(1+B_j)f_j - (B_j+C_j)f_{j-1} + C_j f_{j-2}]$$

$$- f_j'[B_j H_j - (B_j+C_j)H_{j-1} + C_j H_{j-2}]$$

$$+ 2 \overline{p}_j \frac{(Pr-1)}{Pr} [(f_j')^2 + f_j f_j''] = 0 \qquad (3.51)$$

In equations (3.50,51) the prime represents differentiation with respect to η and the function $Q(x)$ is defined by

$$Q(x) = \beta[1 - \frac{2x}{\overline{p}} \frac{d\overline{p}}{dx}] \qquad (3.52)$$

At any station $x = x_j$, f_{j-1}, H_{j-1}, f_{j-2} and H_{j-2} are all known functions of η and $\overline{p}_j$, Q_j, B_j, C_j are known constants. Thus equations (3.50,51) form a set of coupled nonlinear ordinary differential equations for f_j and H_j of the form:

$$\alpha_1 f''' + \alpha_2 ff'' + \phi_1(\eta)f'' + \alpha_3 f'^2 + \phi_2(\eta)f' + \alpha_4 H = 0 \qquad (3.53)$$

$$\alpha_5 H'' + \alpha_6 fH' + \phi_3(\eta)H' + \alpha_7 f'H + \phi_4(\eta)f' + \alpha_8[(f'')^2 + ff'''] = 0 \quad (3.54)$$

where the α's are known constants and the ϕ's are known functions of η. The boundary conditions are:

$$f(0) = 0$$

$$f'(0) = 0$$

$$H'(0) = 0$$

or $\qquad\qquad\qquad\qquad\qquad\qquad\qquad\qquad\qquad\qquad$ (3.55)

$$H(0) = H_b$$

$$f'(\eta_e) = 1$$

$$H(\eta_e) = 1$$

By solving the ordinary differential equation problem (3.53-55) at $x = x_2$, x_3, ...,x_J one can generate a numerical solution of the partial differential equations (3.1,2) in the region $x_1 \leq x \leq x_J$, $0 \leq \eta \leq \eta_e$. This approach, often called the "difference-differential method" in the literature, was originally suggested by Hartree and Womersley [46] and has been used extensively by Mann and Bradley [24] and Smith and co-workers [42,43,45] in boundary layer problems. Because of the use of backward difference formulas for the x-derivatives this implicit method is inherently stable [42].

Equations (3.53-55) can be considered as a fifth order non-linear boundary value problem with three conditions specified at $\eta = 0$ and the other two specified at $\eta = \eta_e$. Such a problem can only be solved iteratively. The method most commonly used is the "shooting method" described in Section 3.2 in connection with the problem for zero-order functions f_0, H_0.

The shooting method, although adequate for certain problems, has a severe limitation. In this method it is implicitly assumed that if the conditions at one boundary are perturbed by a small amount, the changes in the solution of the initial value problem near the other boundary will be of similar magnitude. But the equations (3.53,54) do not have such a behaviour. The coefficients of some terms in these equations involve the quantities B_j and C_j which are multiples of the term $x_j/\Delta x_j$. The stepsizes Δx_j are to be kept small to reduce the truncation errors of the finite difference scheme. This makes the term $x_j/\Delta x_j$, and therefore some of the coefficients of (3.53,54), quite large as the solution proceeds in the downstream direction. The presence of these large coefficients makes the solution extremely sensitive to small changes in the initial conditions [42]. While experimenting with the shooting method, the present author found situations where a change of $0(10^{-6})$ in $f''(0)$ could cause a change of $0(10^4)$ in $f'(\eta_e)$. The shooting method is obviously unsuitable in such cases. Cebeci and Keller [47] introduced a modification called "parallel shooting" which reduced this sensitivity in certain cases of the Falkner-Skan problem. However, for the problem under consideration,

this modification did not offer much advantage.

An alternative approach based on the "quasilinearization method" was developed for solving the problem (3.53-55). The quasi-linearization method, which is essentially an extension of the Newton-Raphson method of solving algebraic or transcendental equations (Bellman and Kalaba [48]), provides a powerful tool for solving nonlinear boundary value problems. Radbill [49,50], Libby and Chen [51] and Jaffee and Thomas [52] applied this method to equations arising from the boundary layer problems.

In the present case we formulate an iterative scheme, each cycle of which involves solving linearized forms of equations (3.53,54). These linear equations are solved by a finite difference method where the conditions at both boundaries could be used simultaneously. Bellman and Kalaba [48] and Kenneth and McGill [53] gave proof of convergence for second order boundary value problems. Similar analysis for the problems considered here are not available in the literature. However, at each iteration cycle we have to calculate two quantities which indicate how closely the current solution satisfies the original nonlinear equations. Examination of these terms indicate a uniform rapid convergence and also provides a suitable means of stopping the iteration after the necessary accuracy has been achieved.

At each station x_j we solve for a sequence of functions $f^{[m]}(\eta)$, $H^{[m]}(\eta)$, $m = 1,2,\ldots$ starting with a suitable initial assumption $f^{[0]}(\eta)$, $H^{[0]}(\eta)$, where each set of functions $f^{[m]}(\eta)$, $H^{[m]}(\eta)$, $m = 0,1,2,\ldots$ satisfies the boundary conditions (3.55). At any station

x_j the solutions of the preceeding station x_{j-1} are used as the initial assumption. Thus we set

$$f^{[0]}(\eta) = f_{j-1}(\eta) \tag{3.56a}$$

$$H^{[0]}(\eta) = H_{j-1}(\eta) \tag{3.56b}$$

If we introduce the functions $e^{(m)}(\eta)$ and $g^{(m)}(\eta)$ such that

$$e^{[m]}(\eta) = f^{[m]}(\eta) - f^{[m-1]}(\eta) \tag{3.57a}$$

$$g^{[m]}(\eta) = H^{[m]}(\eta) - H^{[m-1]}(\eta) \tag{3.57b}$$

then at the m th iteration cycle the momentum equation (3.50) gives the following linearized equation for $e^{[m]}$:

$$\zeta_1 e^{[m]\,\prime\prime\prime} + \sigma_1^{[m]}(\eta)e^{[m]\,\prime\prime} + \sigma_2^{[m]}(\eta)e^{[m]\,\prime} + \sigma_3^{[m]}(\eta)e^{[m]} = -F^{[m]}(\eta) \tag{3.58}$$

with the boundary conditions

$$e^{[m]}(0) = 0 \tag{3.59a}$$

$$e^{[m]\,\prime}(0) = 0 \tag{3.59b}$$

and

$$e^{[m]}{}'(\eta_e) = 0 \qquad\qquad (3.59c)$$

The coefficients in equation (3.58) are defined below:

$$\zeta_1 = \overline{p}_j \qquad\qquad (3.60a)$$

$$\sigma_1{}^{[m]}(\eta) = (1+B_j)f^{[m-1]}(\eta) - (B_j+C_j)f_{j-1}(\eta) + C_j f_{j-2}(\eta) \qquad (3.60b)$$

$$\sigma_2{}^{[m]}(\eta) = - 2(B_j+Q_j)f^{[m-1]}{}'(\eta)+(B_j+C_j)f'_{j-1}(\eta) - C_j f'_{j-2}(\eta) \qquad (3.60c)$$

$$\sigma_3{}^{[m]}(\eta) = (1+B_j)f^{[m-1]}{}''(\eta) \qquad\qquad (3.60d)$$

and

$$F^{[m]}(\eta) = \overline{p}_j\ f^{[m-1]}{}'''(\eta)$$

$$+ f^{[m-1]}{}''(\eta)\{(1+B_j)f^{[m-1]}(\eta)-(B_j+C_j)f_{j-1}(\eta) + C_j f_{j-2}(\eta)\}$$

$$- f^{[m-1]}{}'(\eta)\{(B_j+Q_j)f^{[m-1]}{}'(\eta)-(B_j+C_j)f'_{j-1}(\eta) + C_j f'_{j-2}(\eta)\}$$

$$+ Q_j\ H^{[m-1]}(\eta) \qquad\qquad (3.60e)$$

The function $F^{[m]}(\eta)$ represents the departure from satisfying the momentum equation (3.50) at the m th iteration cycle. The problem given by equations (3.58-60) is solved by a matrix method described

in detail in Appendix B. The solution $e^{[m]}(\eta)$ is then used to obtain the next iterate $f^{[m]}(\eta) = f^{[m-1]}(\eta) + e^{[m]}(\eta)$.

From the energy equation (3.51) we obtain the following linearized equation for $g^{(m)}$:

$$\zeta_2 g^{[m]''} + \sigma_4^{[m]}(\eta)g^{[m]'} + \sigma_5^{[m]}(\eta)g^{[m]} = -G^{[m]}(\eta) \qquad (3.61)$$

with the boundary conditions:

$$g^{[m]'}(0) = 0 \quad \text{for insulated surface} \qquad (3.26a)$$

or $\qquad\qquad g^{[m]}(0) = 0 \quad \text{for constant-temperature surface} \qquad (3.62b)$

and $\qquad\qquad\qquad\qquad g^{[m]}(\eta_e) = 0 \qquad\qquad\qquad\qquad (3.62c)$

The coefficients appearing in equation (3.61) are defined below:

$$\zeta_2 = \overline{p}_j/Pr \qquad (3.63a)$$

$$\sigma_4^{[m]}(\eta) = (1+B_j)f^{[m]}(\eta) - (B_j+C_j)f_{j-1}(\eta) + C_j f_{j-2}(\eta) \qquad (3.63b)$$

$$\sigma_5^{[m]}(\eta) = -B_j f^{[m]'}(\eta) \qquad (3.63c)$$

$$G^{[m]}(\eta) = \frac{\overline{p}_j}{Pr} H^{[m-1]''}(\eta)$$

$$+ H^{[m-1]''}(\eta)\{(1+B_j)f^{[m]}(\eta)-(B_j+C_j)f_{j-1}(\eta) + C_jf_{j-2}(\eta)\}$$

$$- f^{[m]''}(\eta)\{B_jH^{[m-1]}(\eta)-(B_j+C_j)H_{j-1}(\eta) + C_jH_{j-2}(\eta)\}$$

$$+ 2\bar{p}_j \frac{(Pr-1)}{Pr} \{(f^{[m]''}(\eta))^2 + f^{[m]'}(\eta)f^{[m]'''}(\eta)\} \qquad (3.63d)$$

Here again, the function $G^{[m]}(\eta)$ represents the departure from satis-
fying the energy equation (3.51) at the m th iteration cycle. The
problem defined by equations (3.61-63) are solved by a matrix method
details of which are described in Appendix B. The solution $g^{[m]}(\eta)$
is then used to obtain the next iterate $H^{[m]}(\eta) = H^{[m-1]}(\eta) + g^{[m]}(\eta)$.

The iteration is stopped after the m th cycle if

$$\max\{||e^{[m]}||,||g^{[m]}||,||F^{[m]}||,||G^{[m]}||\} \leq \epsilon \qquad (3.64)$$

where ϵ is a predefined tolerance and $||\phi||$ for any function $\phi(\eta)$ is

$$||\phi|| = \max_{0\leq\eta\leq\eta_e} \{|\phi(\eta)|\} \qquad (3.65)$$

Once the criterion (3.64) is satisfied the functions $f^{[m]}(\eta)$
and $H^{[m]}(\eta)$ are accepted as the solution at the station $x = x_j$, i.e.,

$$f_j(\eta) = f^{[m]}(\eta) \qquad (3.66a)$$

$$H_j(\eta) = H^{[m]}(\eta) \qquad (3.66b)$$

This completes the calculations at the j th station and the solution proceeds to the next station x_{j+1}.

For a tolerance $\varepsilon = 10^{-7}$, the number of iterations necessary was 2 in most cases and was never more than 4.

3.3b Solution of the Interaction Equation

From the solution of the boundary layer equations the pressure distribution can now be obtained using the equations (2.43), (2.45) and (3.3). We first introduce the normalized quantities $\bar{\delta}(x)$ and $\bar{I}(x)$:

$$\bar{\delta}(x) = M_\infty \frac{\delta(x)}{\delta_0 x_{L^*}^{-1/2}} x^{-3/4} \tag{3.67}$$

$$\bar{I}(x) = \frac{\int_0^\infty (H - f'^2) d\eta}{I_0} \tag{3.68}$$

δ_0 and I_0 are constants associated with the zero-order solution defined in the Section 3.2. In view of the relation (3.31a) between the constants δ_0, p_0 and I_0, equation (2.45) becomes

$$\bar{p}(x) = \frac{\bar{I}(x)}{\bar{\delta}(x)} \tag{3.69}$$

From (2.43) we recall

$$\bar{p}(x) = \frac{1}{p_0 \bar{x}} [1 + \gamma K \{\tfrac{\gamma+1}{4} K + [(\tfrac{\gamma+1}{4} K)^2 + 1]^{1/2}\}]$$

This relation can be inverted to give the following expression for K in terms of $\bar{p}$:

$$K(x) = \frac{(\bar{p}\ p_0\ \bar{x} - 1)}{[\gamma^2 + (\bar{p}p_0\bar{x} - 1)\ \frac{\gamma(\gamma+1)}{2}]^{1/2}} \tag{3.70}$$

Since $\bar{x} = \bar{x}_{L*}\ x^{-1/2}$, equation (3.70) can be written as

$$s(x) = \frac{\zeta_3\ \bar{I}/\bar{\delta} - x^{1/2}}{[\frac{\gamma(\gamma+1)}{2}\ \zeta_3\ \bar{I}/\bar{\delta} + \frac{\gamma(\gamma-1)}{2}\ x^{1/2}]^{1/2}} \tag{3.71}$$

where

$$s(x) = x^{1/4}\ K(x) \tag{3.72}$$

$$\zeta_3 = p_0\ \bar{x}_{L*} \tag{3.73}$$

and $\bar{p}$ has been replaced by $\bar{I}/\bar{\delta}$ from (3.69).

Now, from (3.3)

$$K(x) = M_\infty(\theta_b + \frac{d\delta}{dx})$$

Writing $K_b = M_\infty\theta_b$ and using the relations (3.67) and (3.72) we obtain

$$s(x) = K_b\ x^{1/4} + \zeta_4[\frac{3}{4}\ \bar{\delta} + x\ \frac{d\bar{\delta}}{dx}] \tag{3.74}$$

where

$$\zeta_4 = \delta_0\ \bar{x}_{L*}^{1/2} \tag{3.75}$$

Equation (3.74) gives the following differential equation for $\bar{\delta}$:

$$x \frac{d\bar{\delta}}{dx} + \frac{3}{4} \bar{\delta} - \frac{s(x)}{\zeta_4} + \frac{K_b \, x^{1/4}}{\zeta_4} = 0 \qquad (3.76)$$

The method of obtaining the pressure distribution $\bar{p}(x)$ from the solution of the boundary layer equations can now be described as follows.

From the solution of the boundary layer equations $f(x,\eta)$, $H(x,\eta)$ we calculate the $\bar{I}(x)$ distribution using equation (3.68). Equations (3.76) and (3.71) then defines a nonlinear first order ordinary differential equation for $\bar{\delta}$ with the initial condition: at $x = x_1$

$$\bar{\delta} = \bar{\delta}(x_1) = \frac{\int_0^\infty [H(x_1,\eta) - \{f'(x_1,\eta)\}^2] \, d\eta}{I_0 \, \bar{p}(x_1)} \qquad (3.77)$$

where $f(x_1,\eta)$, $H(x_1,\eta)$ and $\bar{p}(x_1)$ are those given in (3.45). We then solve for $\bar{\delta}(x)$ and obtain the pressure function $\bar{p}(x)$ from (3.69).

We solve the differential equation for $\bar{\delta}$ by an iterative method based on quasilinearization. Let $\bar{\delta}^{[n]}(x)$, $n = 0,1,2,...$ be a sequence of iterates satisfying the initial condition (3.77). If we define a sequence of functions

$$\tau^{[n]}(x) = \bar{\delta}^{[n]}(x) - \bar{\delta}^{[n-1]}(x), \quad n=1,2,... \qquad (3.78)$$

then $\tau^{[n]}(x)$ represents the correction to be added to the existing solution $\bar{\delta}^{[n-1]}(x)$. From (3.71, 76,77) we obtain the following linearized problem for $\tau^{[n]}(x)$:

$$x \frac{d\tau^{[n]}}{dx} + \sigma_6^{[n]}(x) \; \tau^{[n]} = - D^{[n]}(x) \tag{3.79}$$

$$\tau^{[n]}(x_1) = 0 \tag{3.80}$$

where

$$\sigma_6^{[n]}(x) = \frac{3}{4} - \frac{1}{\zeta_4} \left(\frac{\partial s}{\partial \bar{\delta}}\right)^{[n-1]}$$

$$= \frac{3}{4} + \left| \frac{\zeta_3 \bar{I} \left\{ \frac{\gamma(\gamma+1)}{4} \zeta_3 \frac{\bar{I}}{\bar{\delta}} + \frac{\gamma(3\gamma-1)}{4} x^{1/2} \right\}}{\zeta_4 \bar{\delta}^2 \left\{ \frac{\gamma(\gamma+1)}{2} \zeta_3 \frac{\bar{I}}{\bar{\delta}} + \frac{\gamma(\gamma-1)}{\delta^2} x^{1/2} \right\}^{3/2}} \right|^{[n-1]} \tag{3.81a}$$

and

$$D^{(n)}(x) = \left| x \frac{d\bar{\delta}}{dx} + \frac{3}{4} \bar{\delta} - \frac{s(x)}{\zeta_4} + \frac{K_b \; x^{1/4}}{\zeta_4} \right|^{[n-1]} \tag{3.81b}$$

The superscript [n-1] in the last terms of (3.81a,b) implies that the current iterate $\bar{\delta}^{[n-1]}$ is to be used in place of $\bar{\delta}$. The function $D^{[n]}(x)$ represents the departure from satisfying the differential equation at the end of the (n-1)th iteration cycle. $\tau^{[n]}(x)$ is solved at the stations x_j, $j=2,3,\ldots J$ by means of a finite difference method described in Appendix C. The next iterate $\bar{\delta}^{[n]} = \bar{\delta}^{[n-1]} + \tau^{[n]}$

is then calculated. The iteration is stopped when

$$\max \{||\tau^{[n]}||, ||D^{[n]}||\} \leq \varepsilon$$

where ε is a predefined tolerance and for any function $\phi(x)$

$$||\phi|| = \max_{1 \leq j \leq J} \{|\phi_j|\} . \qquad (3.82)$$

Once the criterion (3.82) is satisfied, $\overline{\delta}^{[n]}$ is accepted as the solution $\overline{\delta}$. We then calculate

$$\overline{p}_j = \overline{I}_j/\overline{\delta}_j , j=2,3,\ldots,J \qquad (3.83)$$

which gives the pressure distribution corresponding to the $\overline{I}$ distribution.

3.4 Results of the Steady Flow Problem

The results of the series solution method of Section 3.1 and 3.2 are presented in Tables 3.1 and 3.2 for Pr = 1.0 and Pr = 0.72 for γ = 1.4. Corresponding results available in the literature are mostly confined for the zero-order solution and for Pr = 1.0. Comparison with the available results are given in Table 3.3.

The lack of good agreement with the results of reference [13] is due to the fact that in Stewartson's work the tangent wedge approximation was not used. References [14] and [16] made use of

TABLE 3.1

RESULTS OF THE SERIES SOLUTION, Pr = 1.0, γ = 1.4

	Constant Temperature Surface				
	H_b = 1.0*	H_b = 0.75	H_b = 0.5	H_b = 0.25	H_b = 0.0
$f_0''(0)$	0.76275	0.70985	0.65555	0.59966	0.54192
$\overline{f_1}''(0)$	−0.43902	−0.38851	−0.33604	−0.28122	−0.22352
$\overline{f_2}''(0)$	−0.50238	−0.43317	−0.36097	−0.28517	−0.20488
$\overline{f_3}''(0)$	0.37567	0.32262	0.26704	0.20833	0.14559
$H_0'(0)$	0.0	0.12767	0.25152	0.37118	0.48618
$\overline{H_1}'(0)$	0.0	−0.049415	−0.095230	−0.13684	−0.17343
$\overline{H_2}'(0)$	0.0	−0.044431	−0.083600	−0.11648	−0.14164
$\overline{H_3}'(0)$	0.0	0.030704	0.057669	0.080050	0.096598
I_0	1.3091	1.0802	0.84660	0.60775	0.36291
I_1	0.60845	0.49842	0.38816	0.27797	0.16835
I_2	0.59464	0.48268	0.37213	0.26383	0.15905
I_3	−0.15318	−0.12451	−0.094934	−0.067762	−0.040542
δ_0	0.73394	0.66669	0.59022	0.50008	0.38643
δ_1	−0.80117	−0.88426	−1.0011	−1.1824	−1.5227
δ_2	−0.82398	−1.0034	−1.2861	−1.7975	−3.0026
δ_3	0.22395	0.27017	0.34326	0.47659	0.79750
p_0	0.50904	0.42008	0.32920	0.23632	0.14112
p_1	1.4969	1.6418	1.8486	2.1792	2.8402
p_2	1.5098	1.8139	2.2948	3.1765	5.3451
p_3	1.3067	1.5745	1.9986	2.7758	4.6750

*For Pr = 1.0, the constant-temperature surface case with H_b = 1.0 is identical with the insulated surface case.

TABLE 3.2

RESULTS OF THE SERIES SOLUTION, Pr = 0.72, γ = 1.4

	Insulated Surface*	Constant-temperature Surface				
		H_b = 1.0	H_b = 0.75	H_b = 0.5	H_b = 0.25	H_b = 0.0
$f_0''(0)$	0.73347	0.77184	0.71433	0.65514	0.59403	0.53065
$\overline{f}_1''(0)$	-0.40862	-0.44635	-0.39195	-0.33525	-0.27576	-0.21274
$\overline{f}_2''(0)$	-0.45843	-0.50958	-0.43573	-0.35844	-0.27690	-0.18994
$\overline{f}_3''(0)$	0.33730	0.38013	0.32374	0.26443	0.20143	0.13354
$H_0'(0)$	0.83244	-0.078114	0.037865	0.15023	0.25859	0.36245
$\overline{H}_1'(0)$	0.0082451	0.036826	-0.0096634	-0.052783	-0.091917	-0.12620
$\overline{H}_2'(0)$	0.012646	0.039139	-0.0040486	-0.042388	-0.074853	-0.099956
$\overline{H}_3'(0)$	-0.024620	-0.044235	-0.010735	0.019043	0.044208	0.063401
I_0	1.2175	1.3903	1.1316	0.86725	0.59655	0.31850
I_1	0.56600	0.64181	0.51791	0.39369	0.26953	0.14609
I_2	0.54984	0.62411	0.49885	0.37513	0.25400	0.13710
I_3	-0.17254	-0.17970	-0.14593	-0.11225	-0.079041	-0.047019
δ_0	0.70780	0.75637	0.68237	0.59737	0.49544	0.36201
δ_1	-0.83070	-0.77930	-0.86640	-0.99244	-1.1985	-1.6318
δ_2	-0.88748	-0.77852	-0.96141	-1.2609	-1.8406	-3.4377
δ_3	0.21841	0.20040	0.24380	0.31388	0.44639	0.78795
p_0	0.47342	0.54063	0.44001	0.33723	0.23196	0.12385
p_1	1.5524	1.4475	1.5976	1.8175	2.1863	3.0146
p_2	1.6183	1.4126	1.7194	2.2220	3.2053	6.0359
p_3	1.3305	1.1918	1.4507	1.8721	2.6830	4.8985

*For the insulated surface case the numbers given in the rows 5-8 are $H_0(0)$, $\overline{H}_1(0)$, $\overline{H}_2(0)$ and $\overline{H}_3(0)$ respectively.

TABLE 3.3

COMPARISON WITH THE AVAILABLE RESULTS (Pr=1.0, γ=1.4)

Source	P_0 (H_b=1.0)	P_2 H_b=1.0	$f''(0)$ H_b=1.0	P_0 (H_b=0.0)	$f_0''(0)$ (H_b=0.0)	$H_0'(0)$ (H_b=0.0)
Stewartson [13]	0.555	0.881				
Li et al [14]	0.514		0.766	0.149	0.539	0.408
Nagakura et al [16]	0.510	1.49	0.764			
Present work	0.50904	1.5098	0.76275	0.14112	0.54192	0.48618

the tangent wedge approximation. However, the method of solving the boundary layer equations were different in the two works. Li and Nagamatsu used analog computers while Nagakura and Naruse used von Karman's integral method. In references [13] and [16] a two term expression of the form

$$p = p_0 \, \overline{\chi} + \text{constant}$$

was obtained for the pressure on a flat plate at zero incidence. The constant term corresponds to $p_0 p_2$ in the present notation.

In Figures 3.1 to 3.8 the results of the series solution are compared with those of the finite difference solution. The finite difference solutions were carried out with the first station x_1 = 1./1024 and K_x = 1.15. This corresponds to 36 x-stations between x = 0.0 and x = 1.0. The step sizes in the η-direction were taken as 1./16 which

corresponds to 129 η-stations.

Figures 3.1 and 3.2 show the velocity and total enthalpy profiles at four different locations x = 0.25, 0.5, 0.75 and 1.0 along a flat plate at an angle 2° to the free stream with M_∞ = 20.0, $\overline{\chi}_L *$ = 8.0, Pr = 0.72, γ = 1.4 and H_b = 0.5. Since the error involved in the series solution are of order $\overline{\chi}^{-3/2}$ the agreement improves in the upstream direction. The overall agreement is good because of the high value of $\overline{\chi}_L *$. Figures 3.3 and 3.4 show the variation of the surface shear function f_b'', the surface enthalpy gradient H_b', the nondimensional pressure and displacement thickness p and δ along the plate obtained by the series solution and the finite difference solution. The series solution predicts lower values for f_b'', H_b' and p and higher values for δ, the discrepancies being of the order of 10%, 5%, 15% and 10% at x = 1.0.

The agreement between the series solution and the finite difference solution decreases with the decreasing values of $\overline{\chi}_L *$ because of the larger error terms in the series solution. The disagreement becomes significant for $\overline{\chi}_L * < 4$. In Figures 3.5 - 3.8 the results from the two solutions are compared for a flat plate inclined at an angle of 2° to the free stream with M_∞ = 10.0, Pr = 0.72, γ = 1.4 and H_b = 0.5 for $\overline{\chi}_L *$ = 2.0. The disagreement is quite noticeable as can be seen from the velocity and total enthalpy profiles in Figures 3.5 and 3.6. The variations of f_b'', H_b', p and δ along the plate are shown in Figures 3.7 and 3.8. The values predicted by the

series solution at x = 1.0 are about 70%, 20% and 25% less for f_b'', H_b' and p respectively while the value for δ is about 50% higher.

In the remaining figures of this section the results from the finite difference solutions are presented to show the effects of changing the parameters θ_b, H_b, $\overline{X}_L*$ on f_b'', H_b' , p and δ .

Figures 3.9 through 3.12 shows the distribution of f_b'', H_b', δ and p along the plate for θ_b = - 2°, 0°, 2°, 4°, 6° with Pr = 0.72, γ = 1.4, M_∞ = 20, H_b = 0.5 and $\overline{X}_L*$ = 8.

Figures 3.13 through 3.16 presents the effect of increasing $\overline{X}_L*$ on the distribution of f_b'', H_b', δ and p along the plate for Pr = 0.72, γ = 1.4, M_∞ = 10, H_b = 0.5 and θ_b = 2°.

Figure 3.17 through 3.20 shows the distribution of f_b'', H_b' δ and p along the plate for H_b = 0.0, 0.5, 1.0 with Pr = 0.72, γ = 1.4, M_∞ = 20, $\overline{X}_L*$ = 8.0 and θ_b = 2°.

Figure 3.1 Velocity Profiles at Different Location along the Plate
$M_\infty = 20.0$, $Pr = 0.72$, $\gamma = 1.4$, $H_b = 0.5$, $\overline{X}_{L*} = 8.0$, $\theta_b = 2°$
a: From Series Solution
b: From Finite Difference Solution

Figure 3.2 Total Enthalpy Profile at Different Locations along the Plate

$M_\infty = 20.0$, $Pr = 0.72$, $\gamma = 1.4$, $H_b = 0.5$, $\bar{X}_{L^*} = 8.0$, $\theta_b = 2°$

a: From Series Solution

b: From Finite Difference Solution

Figure 3.3 Variation of f''_b and H'_b along the Plate
$M_\infty = 20.0$, $Pr = 0.72$, $\gamma = 1.4$, $H_b = 0.5$, $\overline{X}_{L^*} = 8$, $\theta_b = 2°$

a: From Series Solution

b: From Finite Difference Solution

Figure 3.4 Variation of p and δ along the Plate

$M_\infty = 20$, $Pr = 0.72$, $\gamma = 1.4$, $H_b = 0.5$, $\overline{X}_{L^*} = 8.0$, $\theta_b = 2°$

a: From Series Solution

b: From Finite Difference Solution
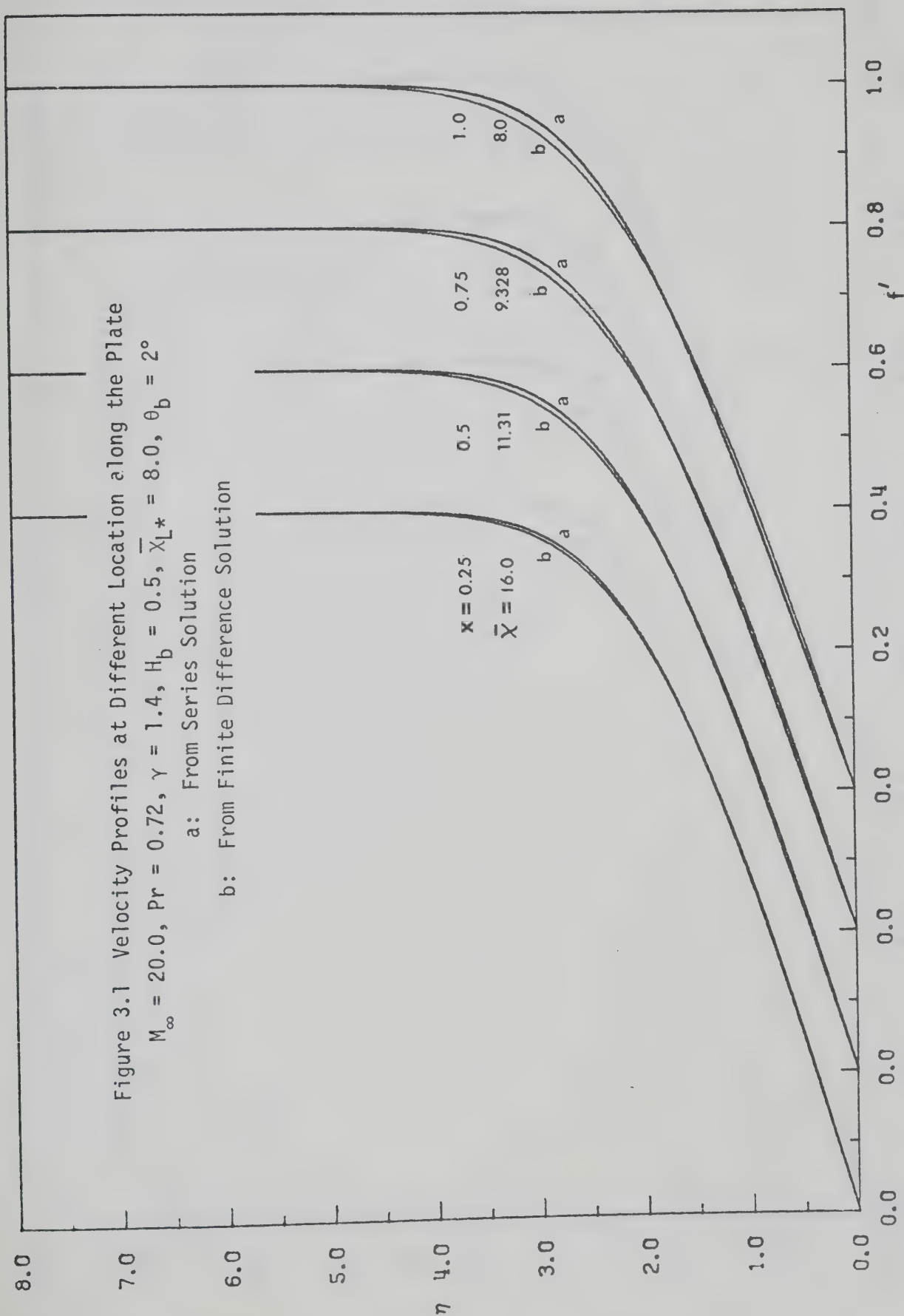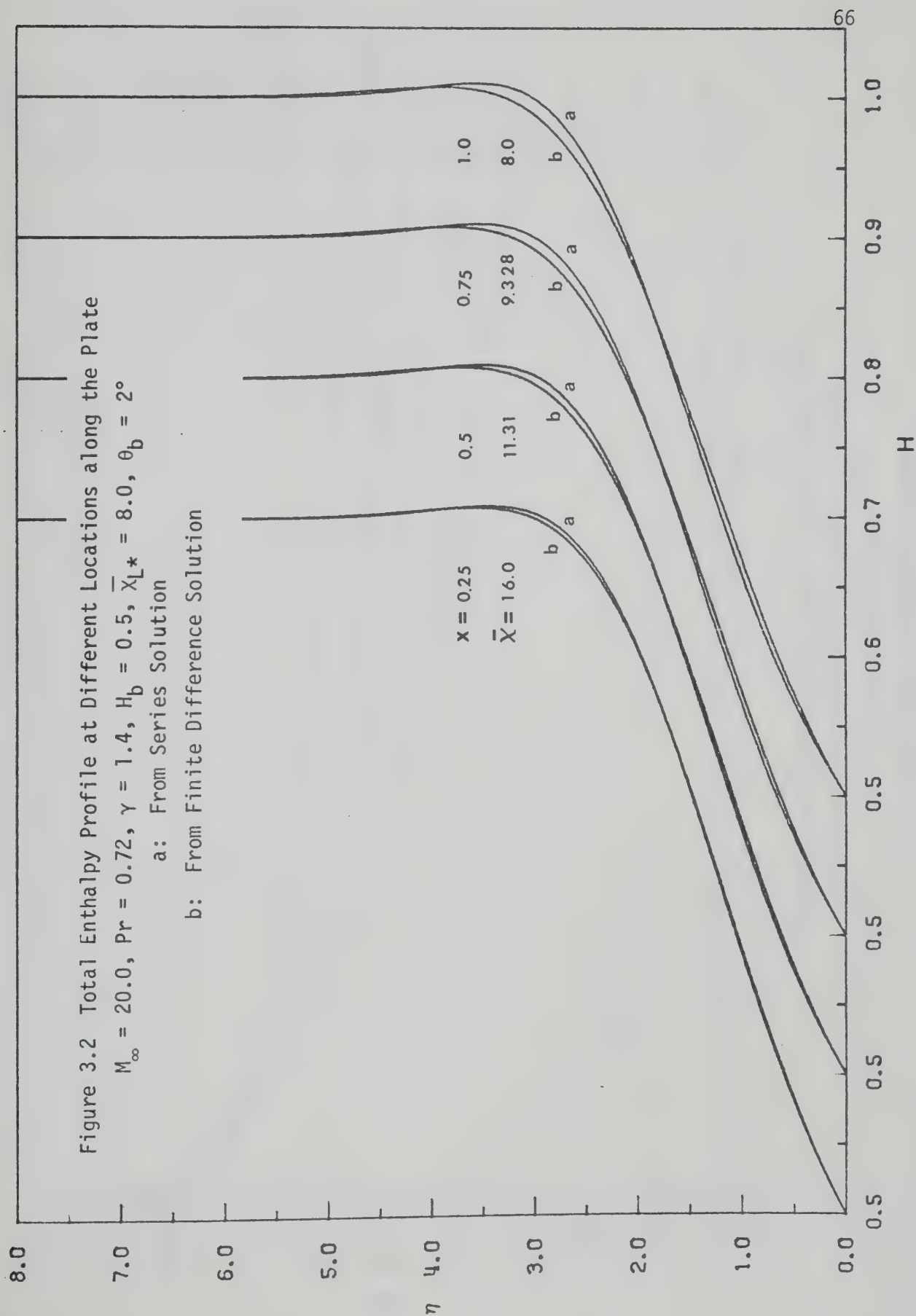
Figure 3.5 Velocity Profiles at Different Locations along the Plate
$M_\infty = 10.0$, $Pr = 0.72$, $\gamma = 1.4$, $H_b = 0.5$, $\bar{X}_{L*} = 2.0$, $\theta_b = 2°$
a: From Series Solution
b: From Finite Difference Solution

Figure 3.6 Total Enthalpy Profile at Different Locations along the Plate
$M_\infty = 10.0$, $Pr = 0.72$, $\gamma = 1.4$, $H_b = 0.5$, $\bar{X}_{L*} = 2.0$, $\theta_b = 2°$
a: From Series Solution
b: From Finite Difference Solution

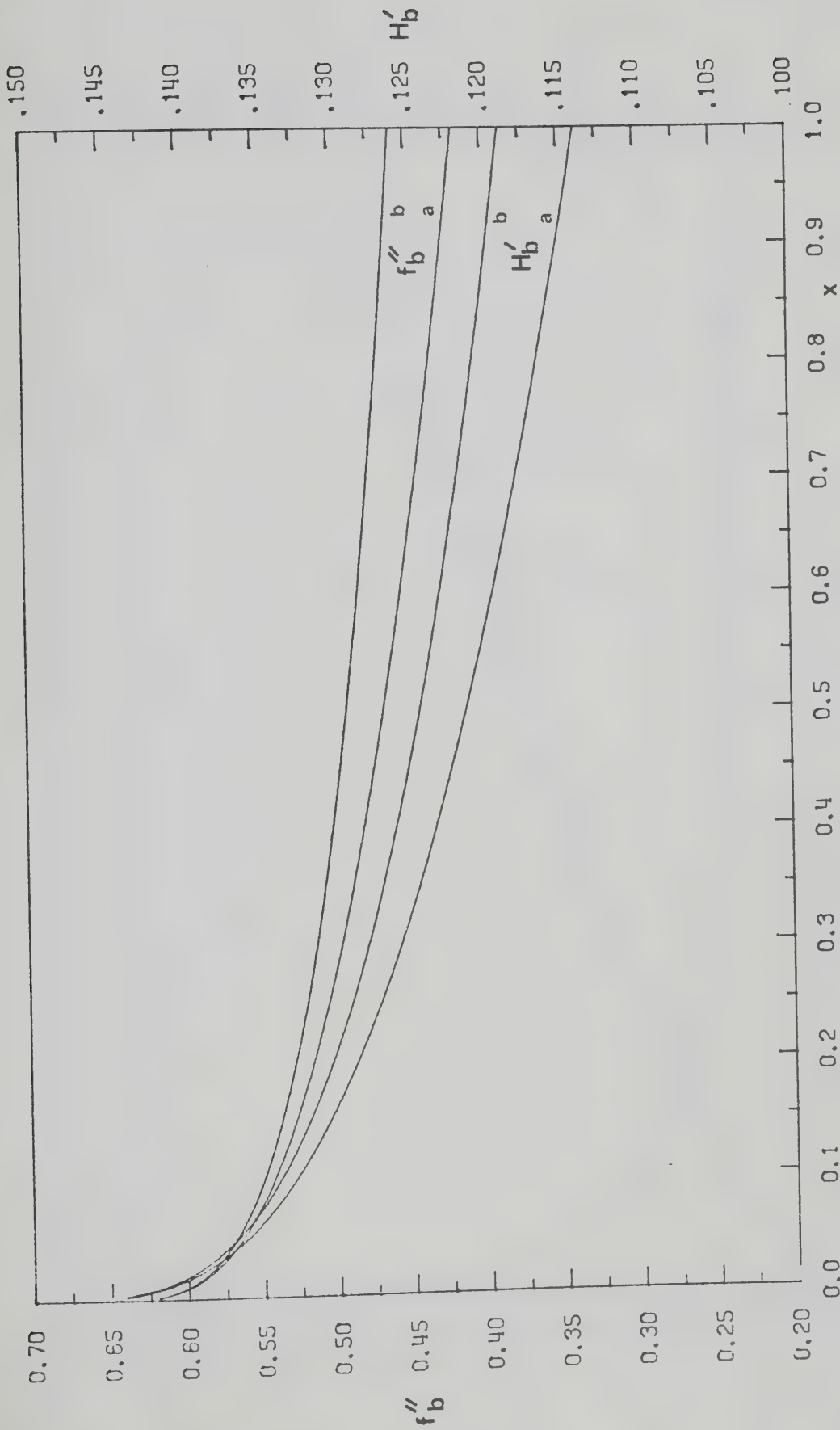Figure 3.7 Variation of f_b'' and H_b' along the Plate

$M_\infty = 10.0$, $Pr = 0.72$, $\gamma = 1.4$, $H_b = 0.5$, $\bar{X}_{L*} = 2.0$, $\theta_b = 2°$.

a: From Series Solution

b: From Finite Difference Solution

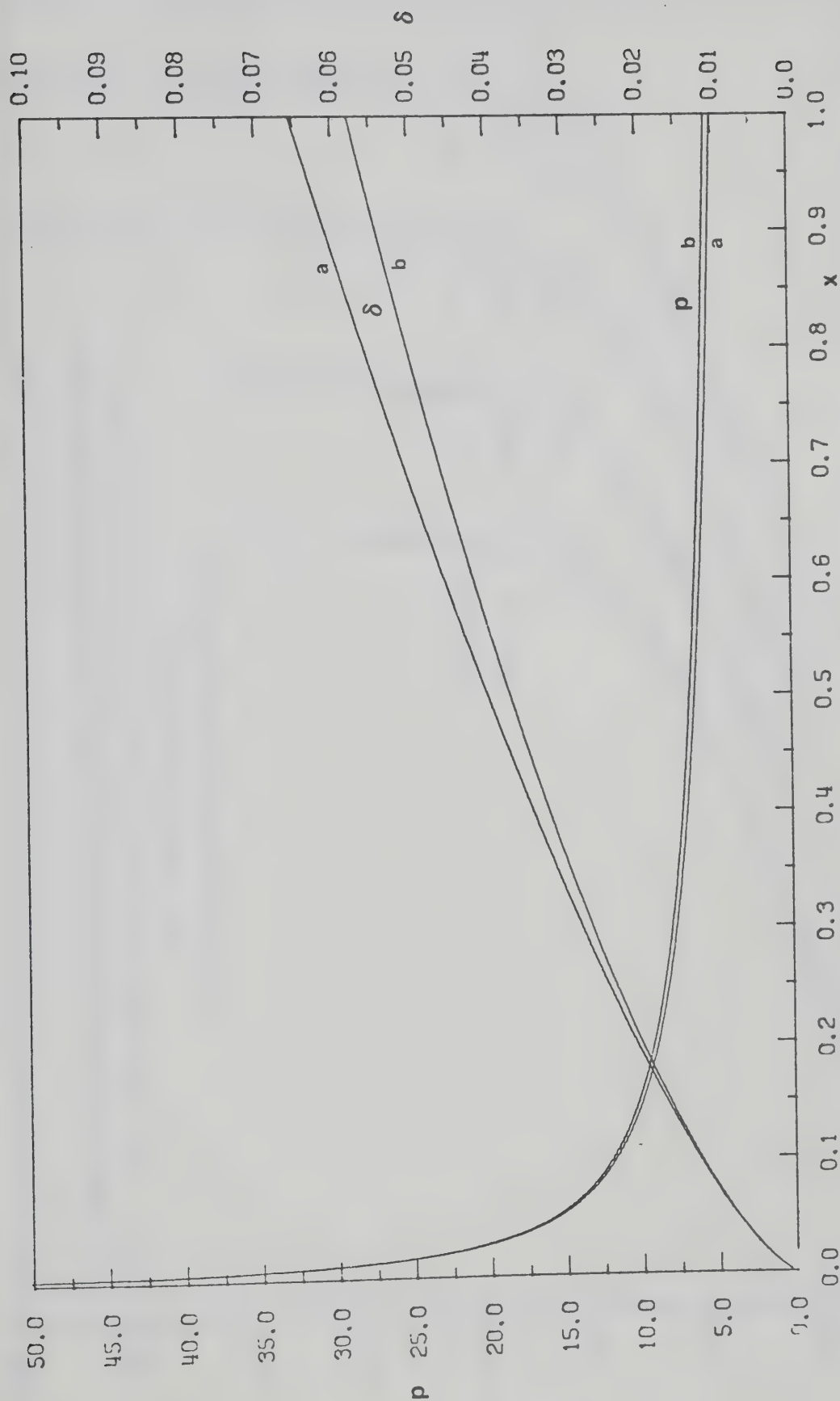Figure 3.8 Variation of p and δ along the Plate

$M_\infty = 10.0$, Pr $= 0.72$, $\gamma = 1.4$, $H_b = 0.5$, $\overline{X}_{L*} = 2.0$, $\theta_b = 2°$

a: From Series Solution

b: From Finite Difference Solution
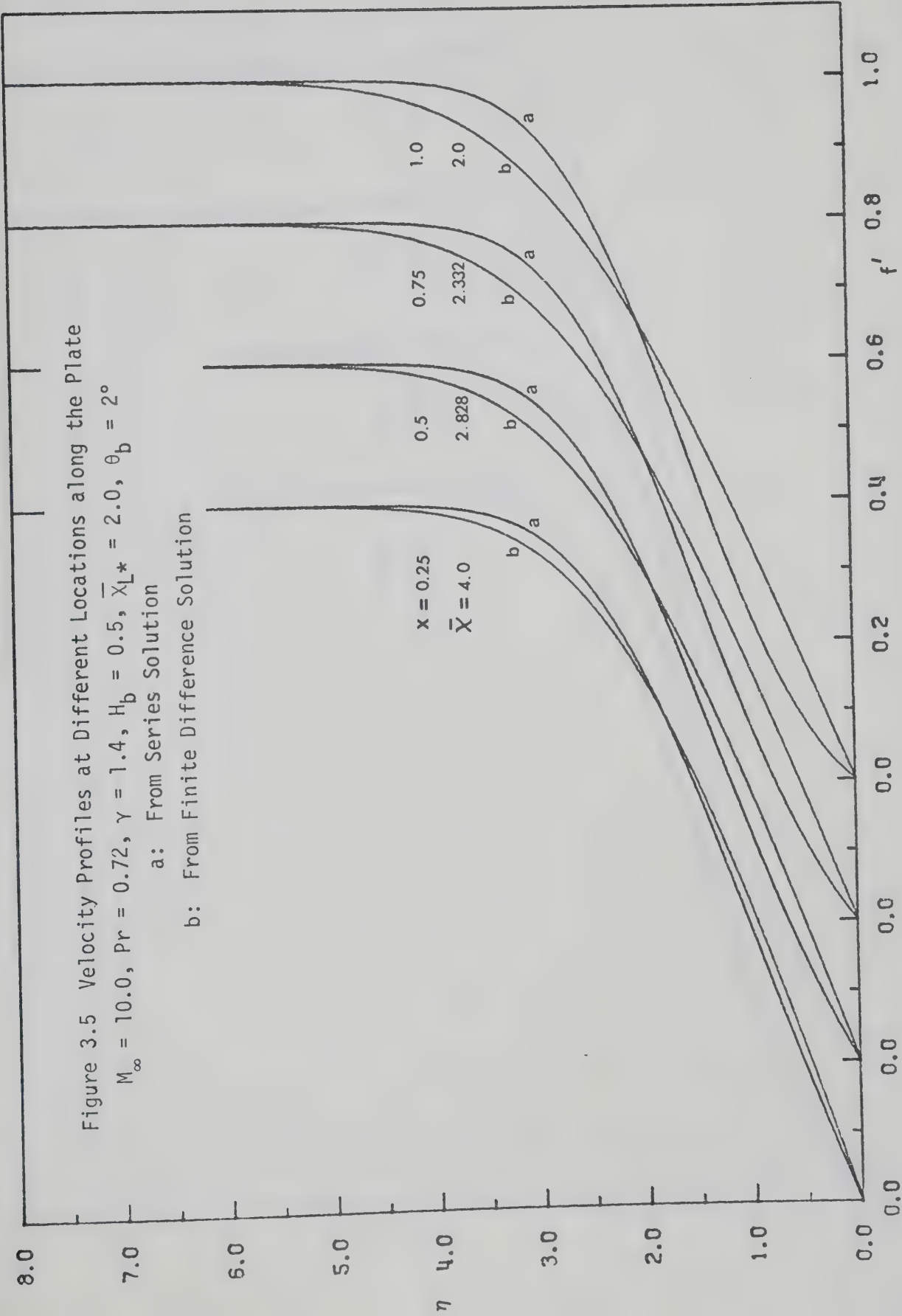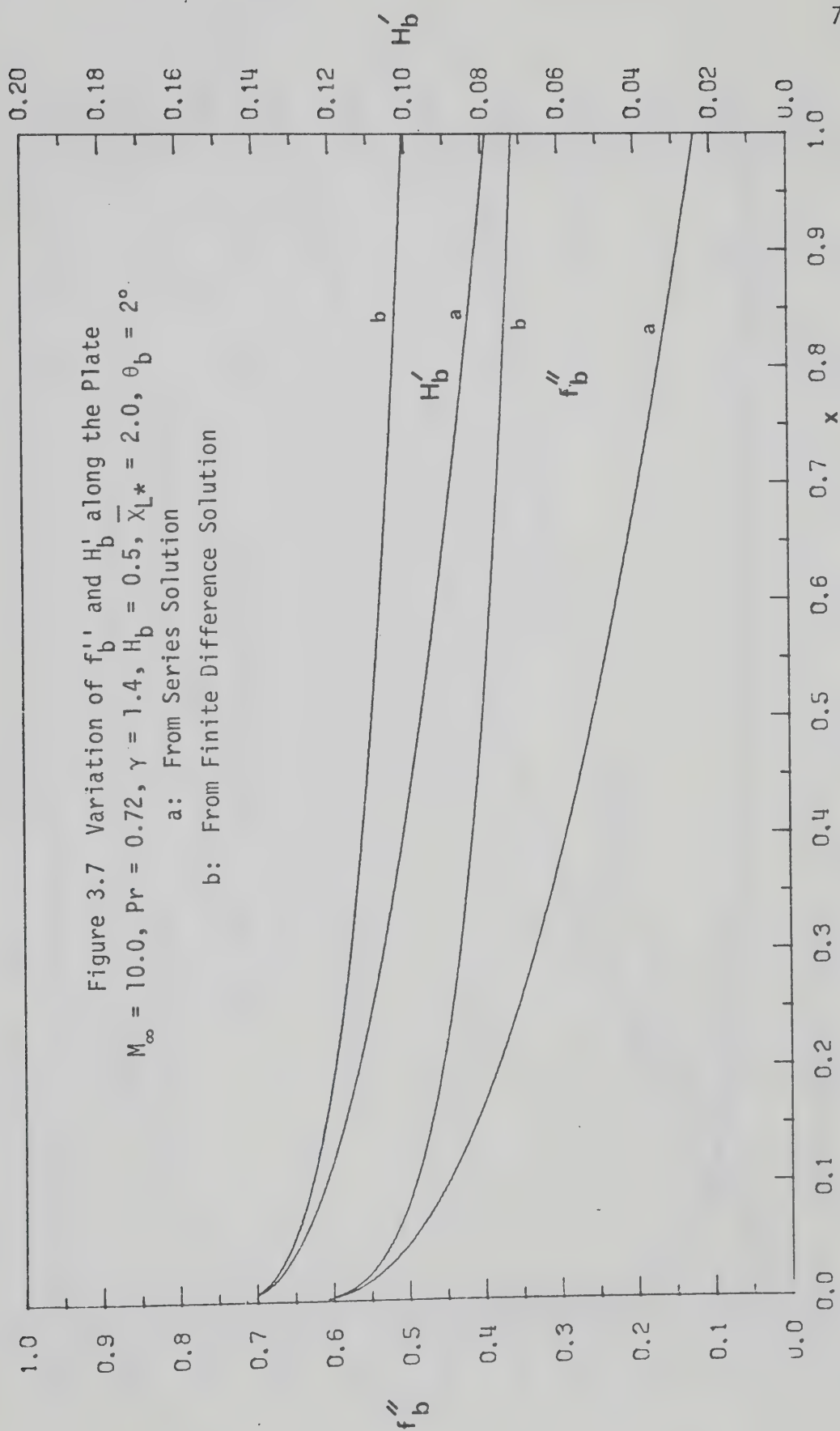
Figure 3.9 Variation of f_b'' along the Plate for Different θ_b

M_∞ = 20.0, Pr = 0.72, γ = 1.4, H_b = 0.5, $\bar{x}_{L*}$ = 8.0

Figure 3.10 Variation of H_b' along the Plate for Different θ_b

$M_\infty = 20.0$, $Pr = 0.72$, $\gamma = 1.4$, $\overline{\chi}_L* = 8.0$, $H_b = 0.5$

Figure 3.11 Variation of δ along the Plate for Different θ_b

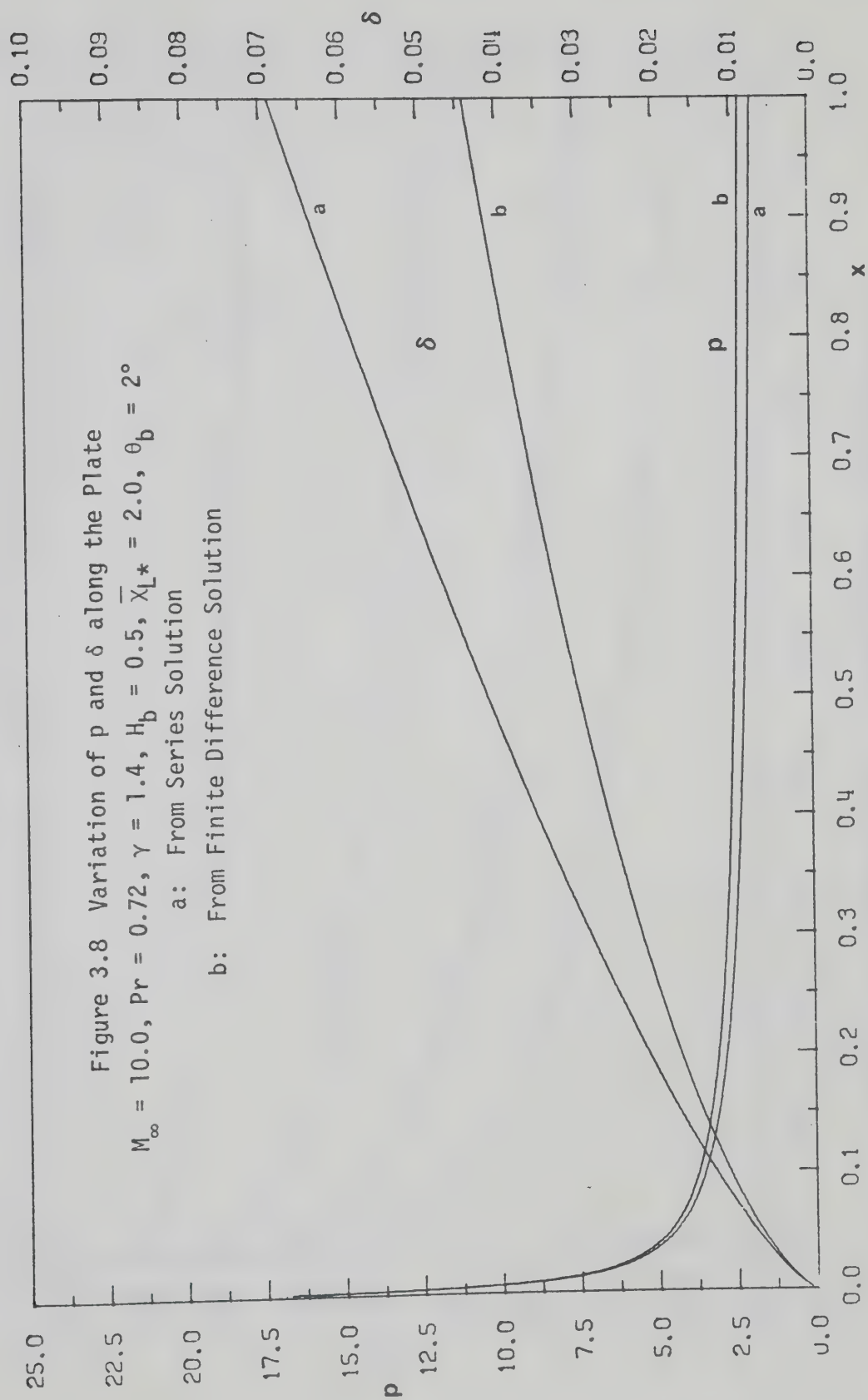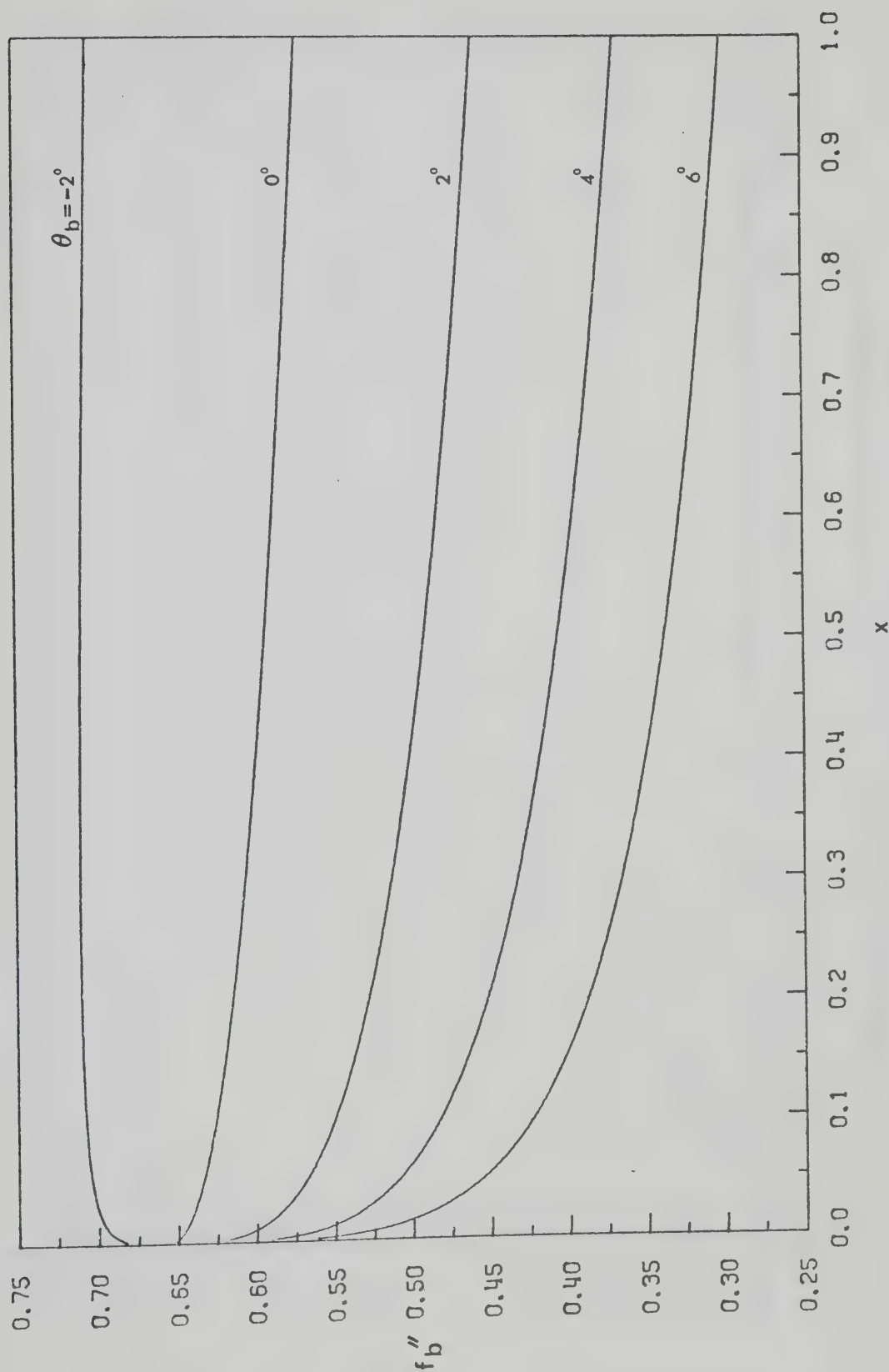$M_\infty = 20.0$, $Pr = 0.72$, $\gamma = 1.4$, $\bar{X}_{L*} = 8.0$, $H_b = 0.5$

Figure 3.12 Variation of p along the Plate for Different θ_b

$M_\infty = 20.0$, $Pr = 0.72$, $\gamma = 1.4$, $H_b = 0.5$, $\vec{x}_{L^*} = 8.0$

77

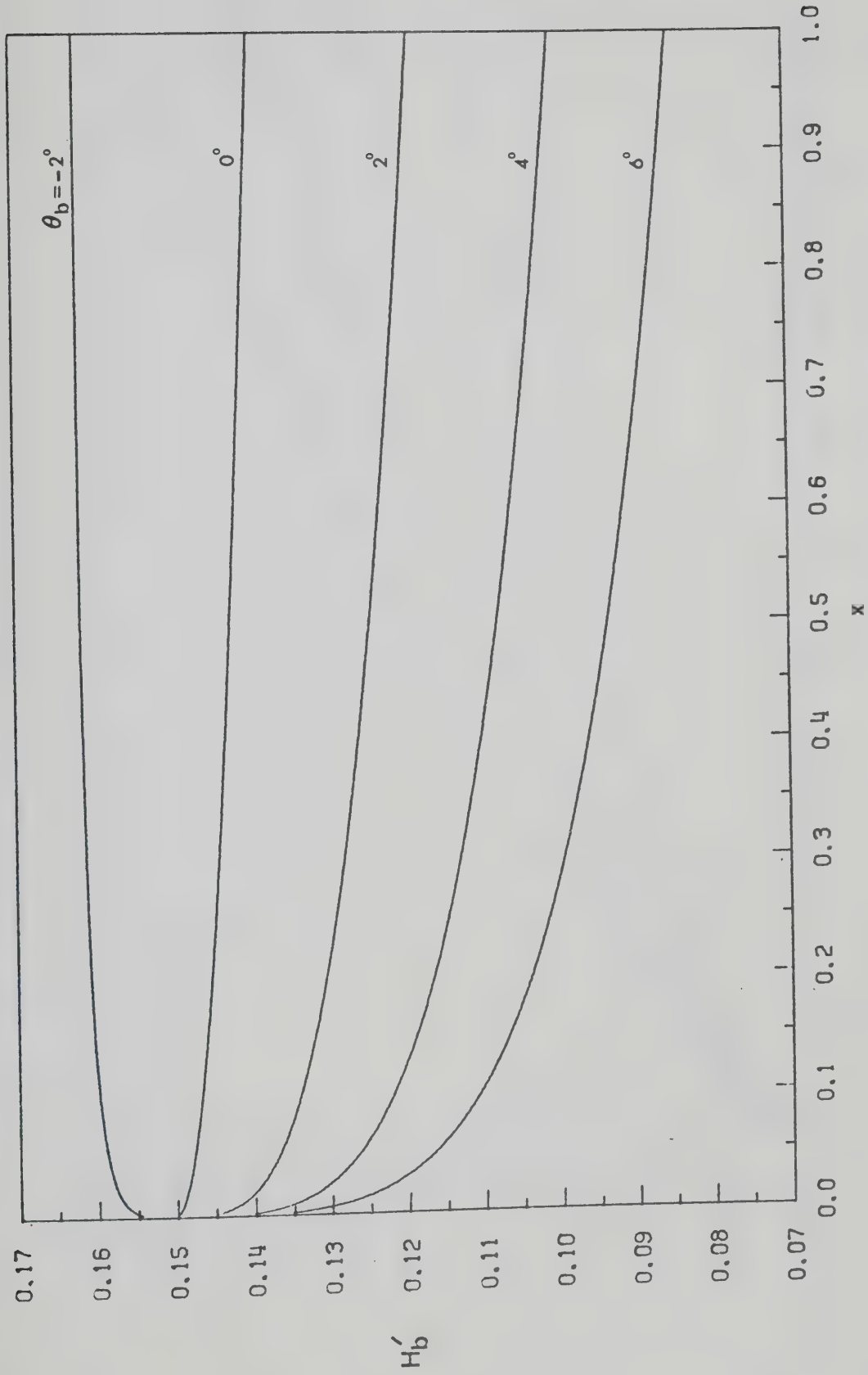

Figure 3.13 Variation of f_b'' along the Plate for Different $\bar{X}_{L*}$
$M_\infty = 10.0$, $Pr = 0.72$, $\gamma = 1.4$, $H_b = 0.5$, $\theta_b = 2°$
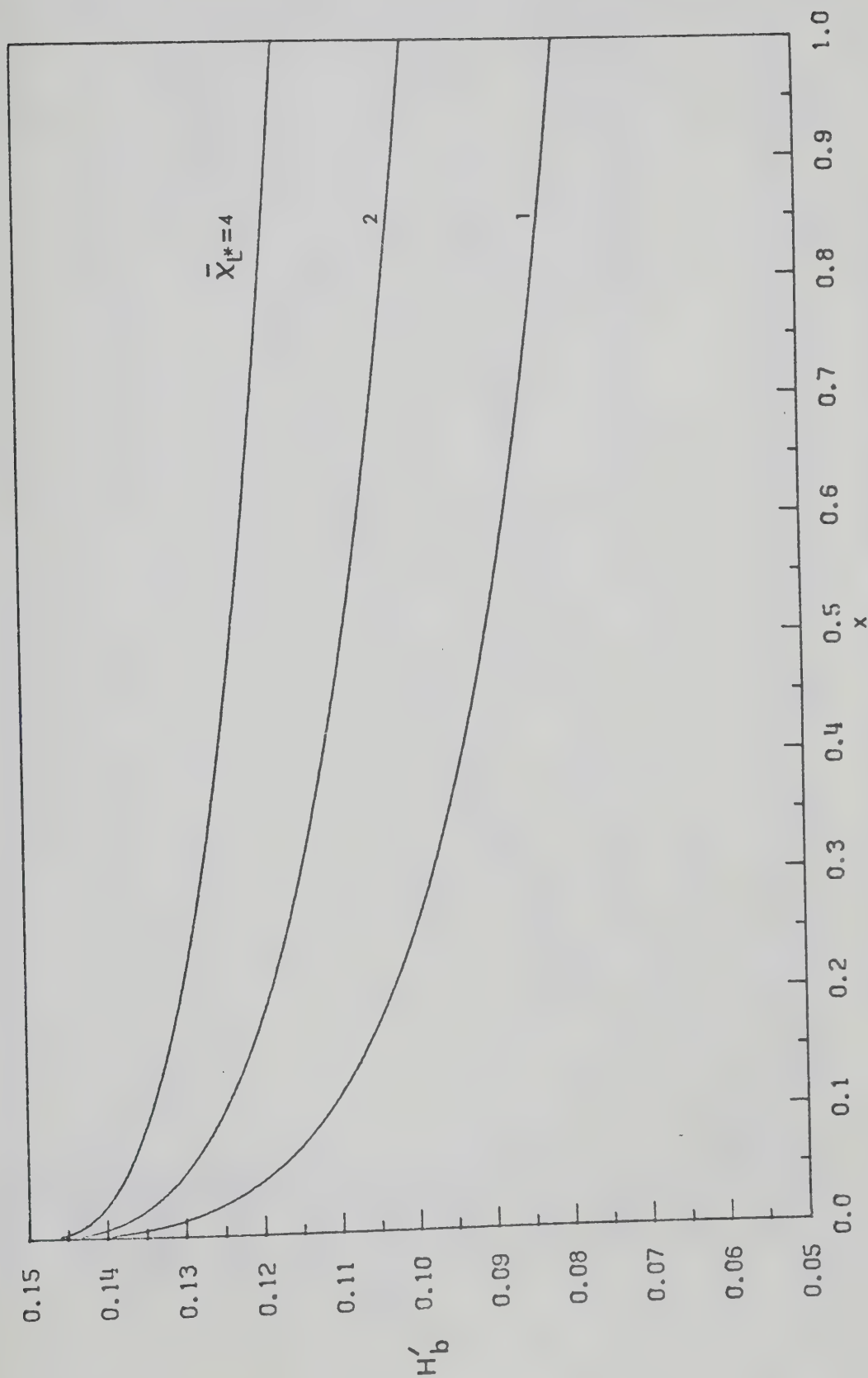
Figure 3.14 Variation of H_b' for Different $\bar{X}_{L*}$
$M_\infty = 10.0$, $Pr = 0.72$, $\gamma = 1.4$, $H_b = 0.5$, $\theta_b = 2°$
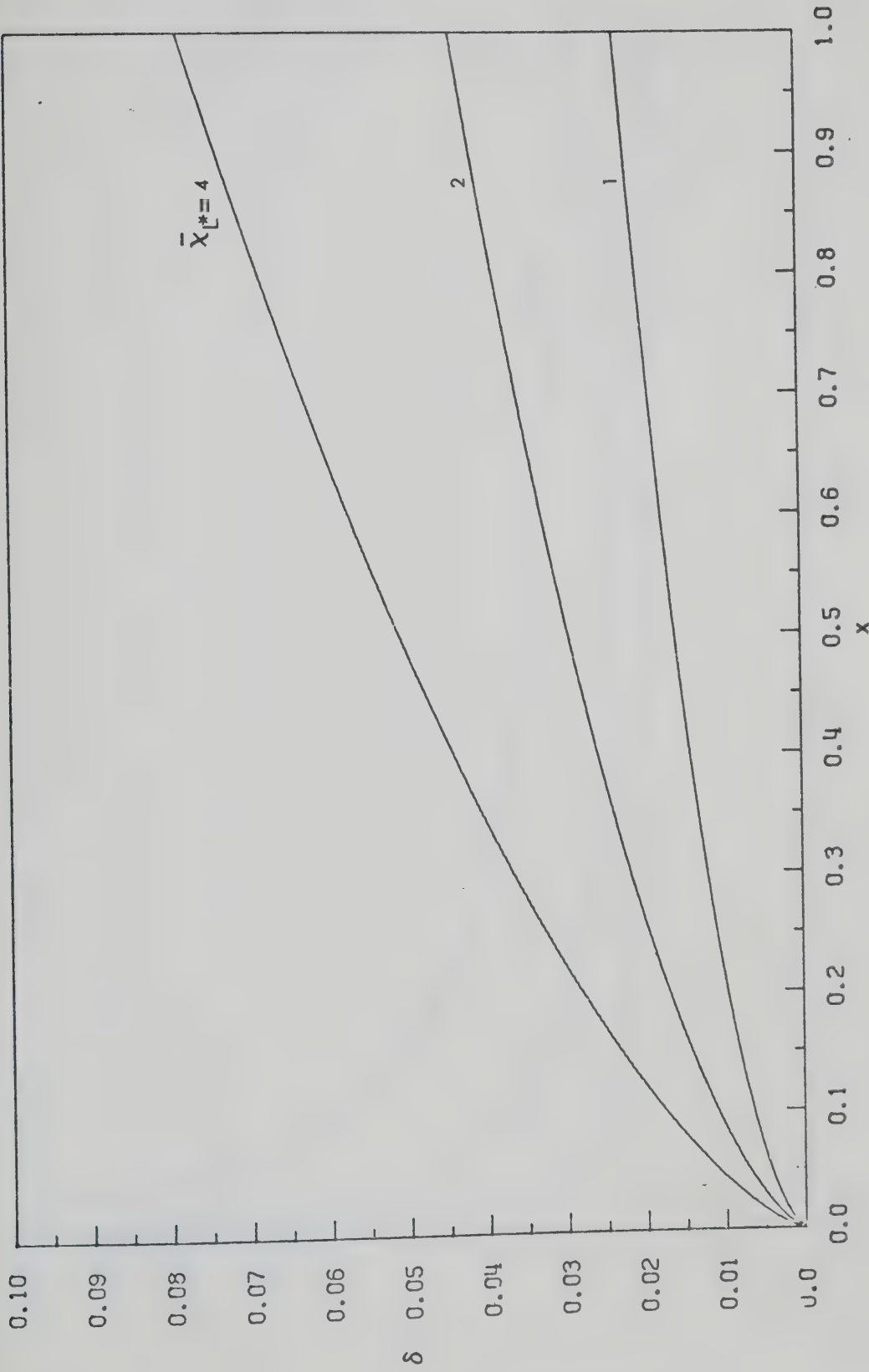
Figure 3.15 Variation of δ along the Plate for Different $\bar{x}_{L*}$

$M_\infty = 10.0$, $Pr = 0.72$, $\gamma = 1.4$, $H_b = 0.5$, $\theta_b = 2°$
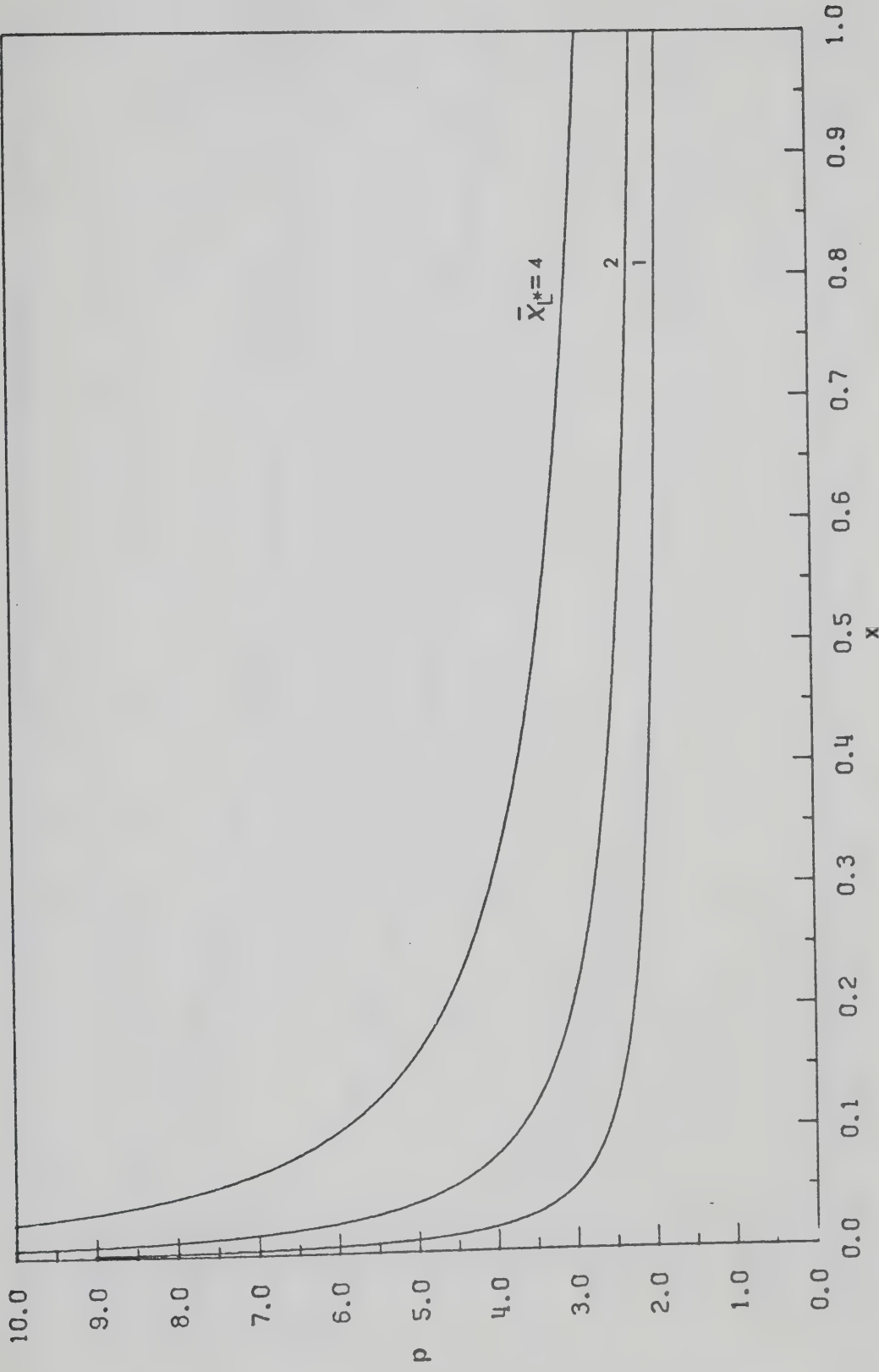
Figure 3.16 Variation of p along the Plate for Different $\bar{x}_{L*}$

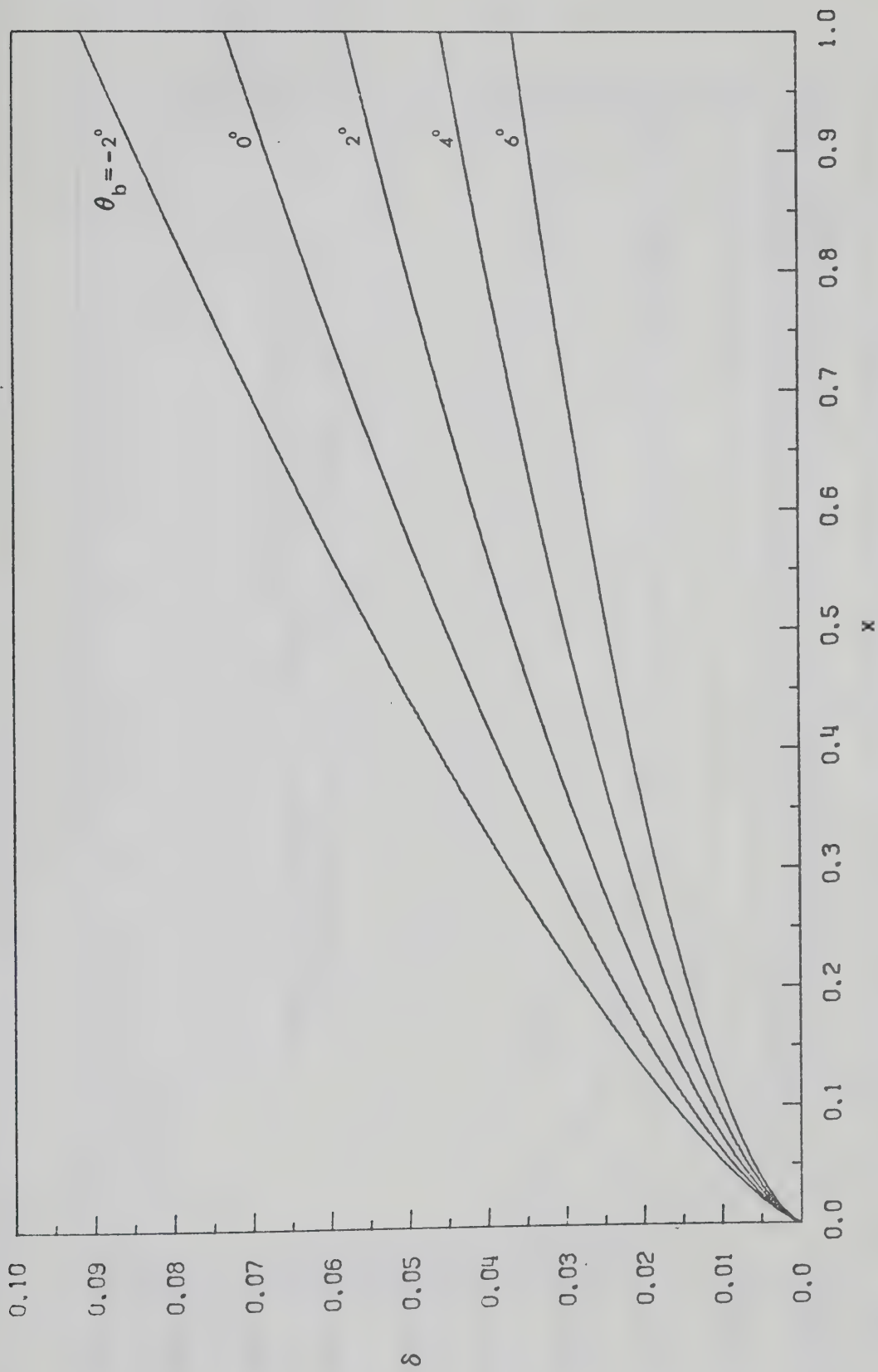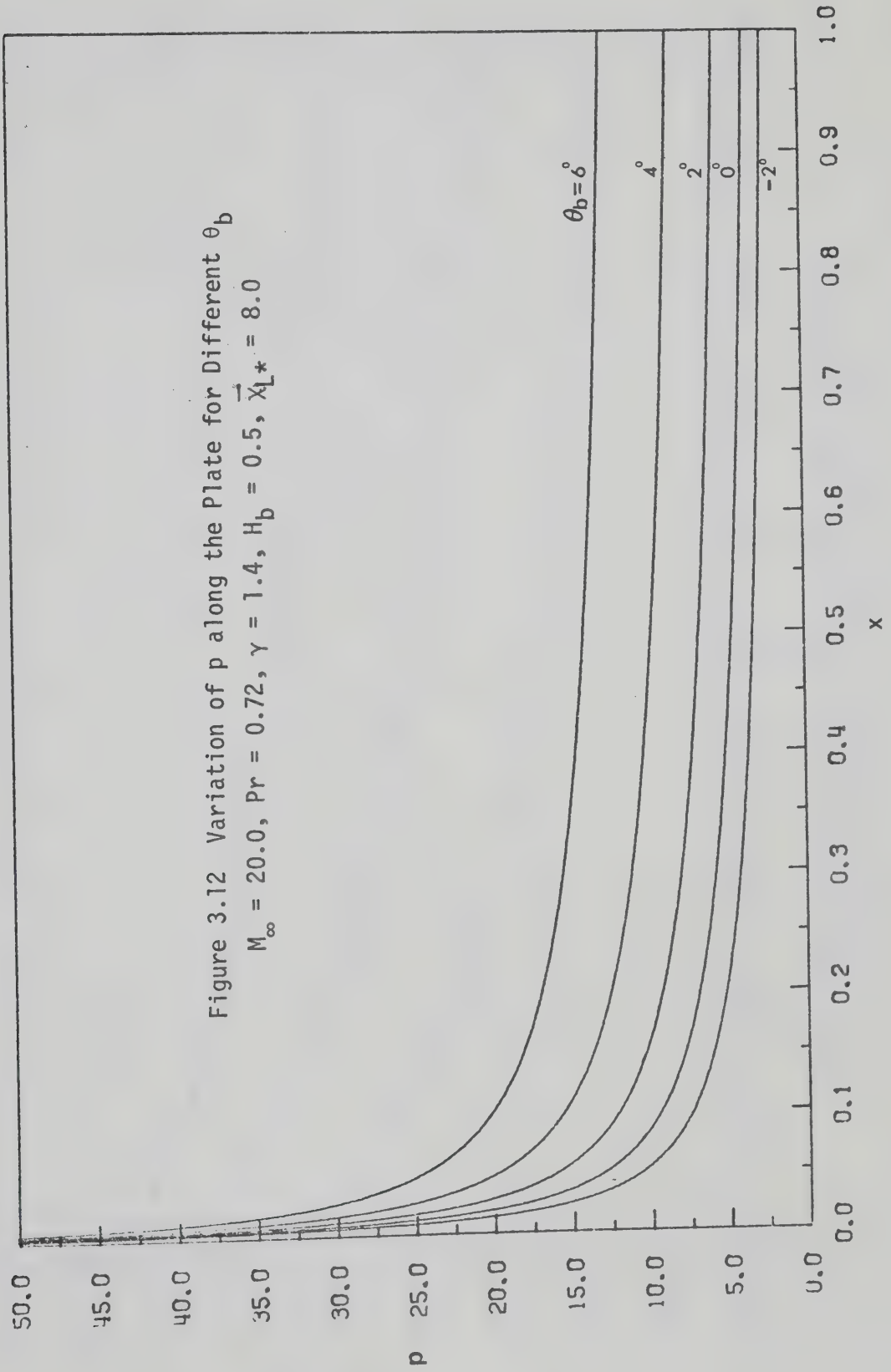$M_\infty = 10.0$, $Pr = 0.72$, $\gamma = 1.4$, $H_b = 0.5$, $\theta_b = 2°$

Figure 3.17 Variation of f_b'' along the Plate for Different H_b
$M_\infty = 20$, $Pr = 0.72$, $\gamma = 1.4$, $\overline{x}_{L*} = 8.0$, $\theta_b = 2°$

Figure 3.18 Variation of H_b' along the Plate for Different H_b
$M_\infty = 20$, $Pr = 0.72$, $\gamma = 1.4$, $\overline{X_L}* = 8.0$, $\theta_b = 2°$
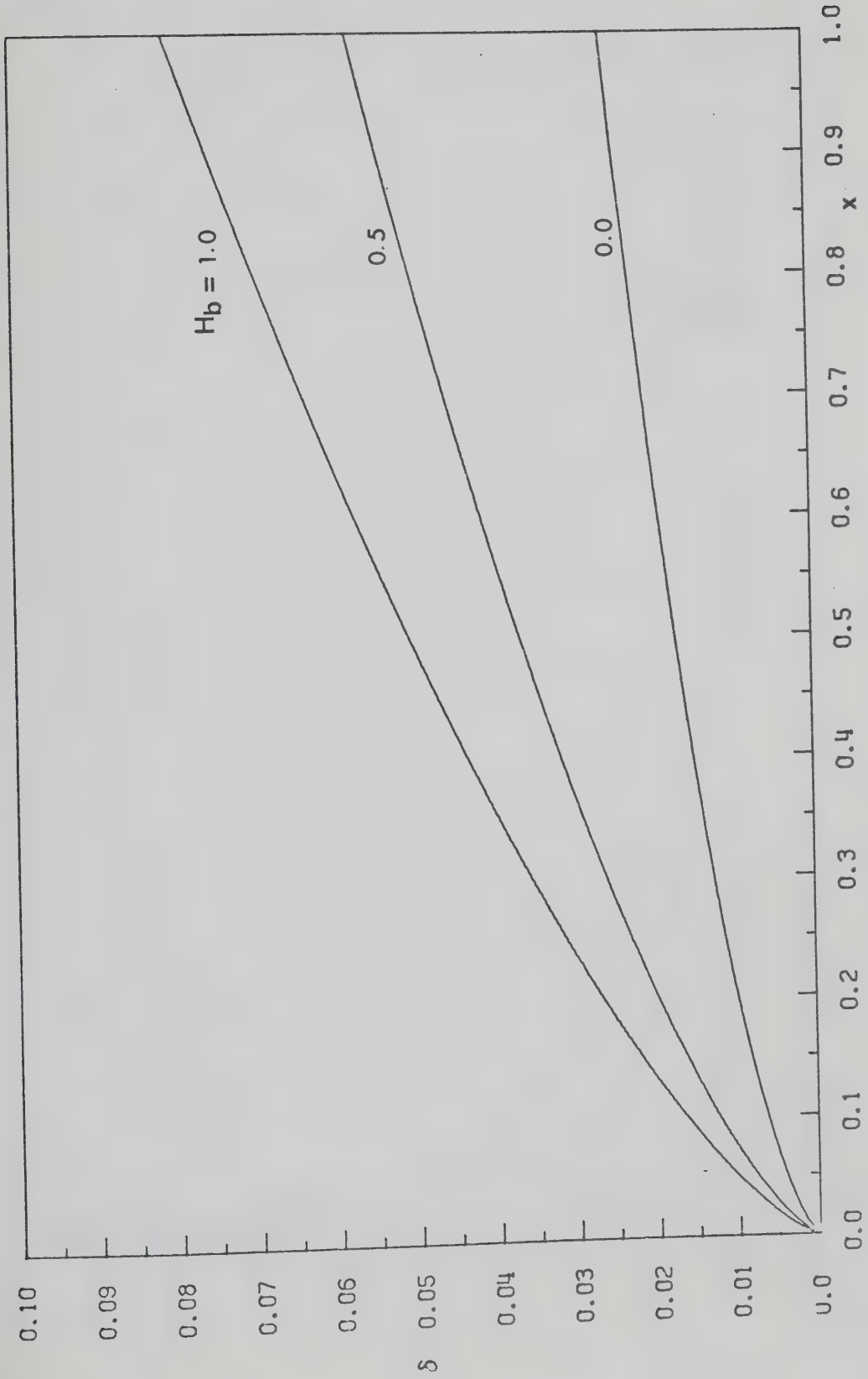
Figure 3.19 Variation of δ along the Plate for Different H_b
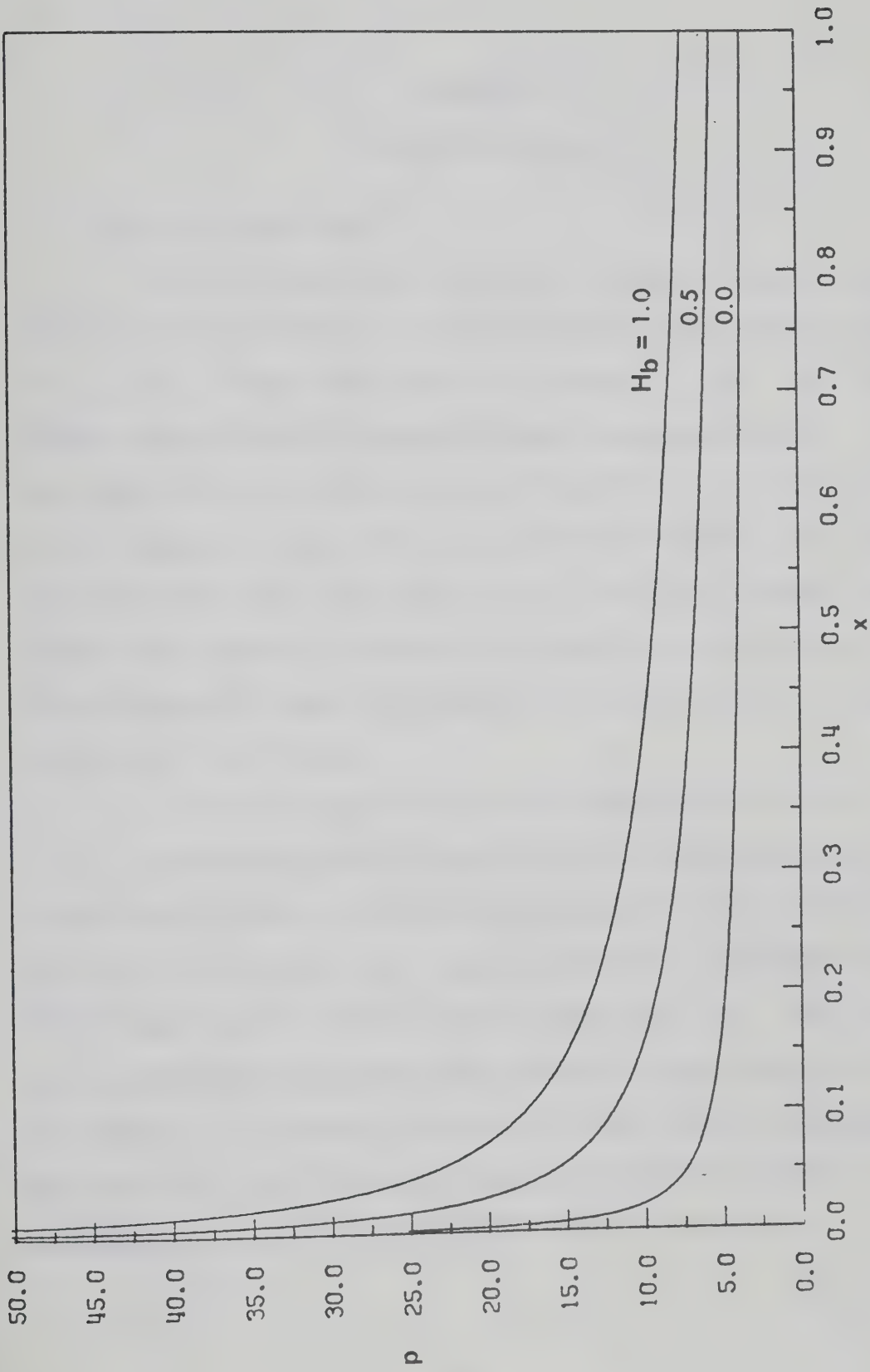
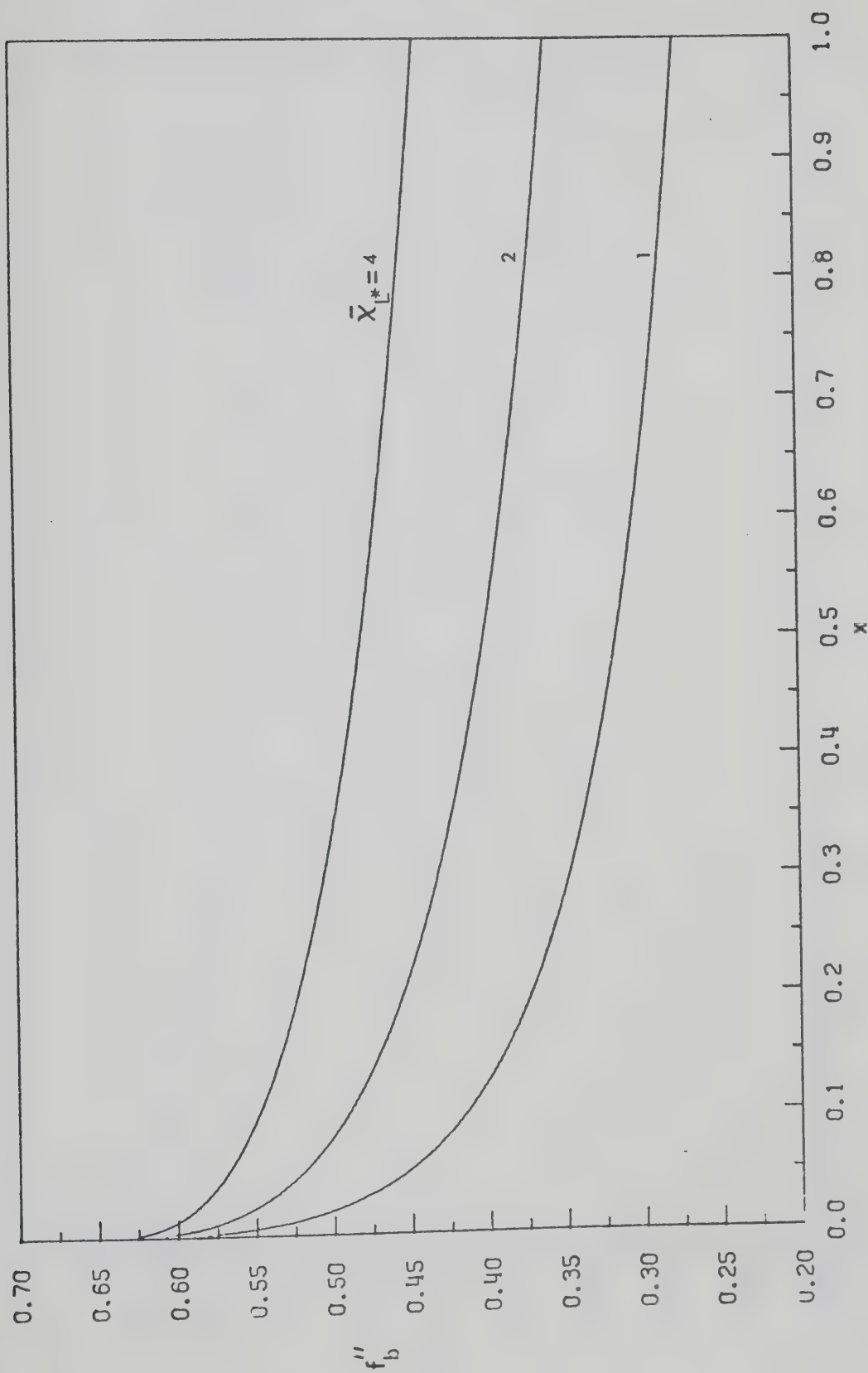$M_\infty = 20$, $Pr = 0.72$, $\gamma = 1.4$, $\overline{\chi}_L* = 8.0$, $\theta_b = 2°$

Figure 3.20 Variation of p along the Plate for Different H_b
$M_\infty = 20$, $Pr = 0.72$, $\gamma = 1.4$, $\overline{X}_L^* = 8.0$, $\theta_b = 2°$

CHAPTER IV
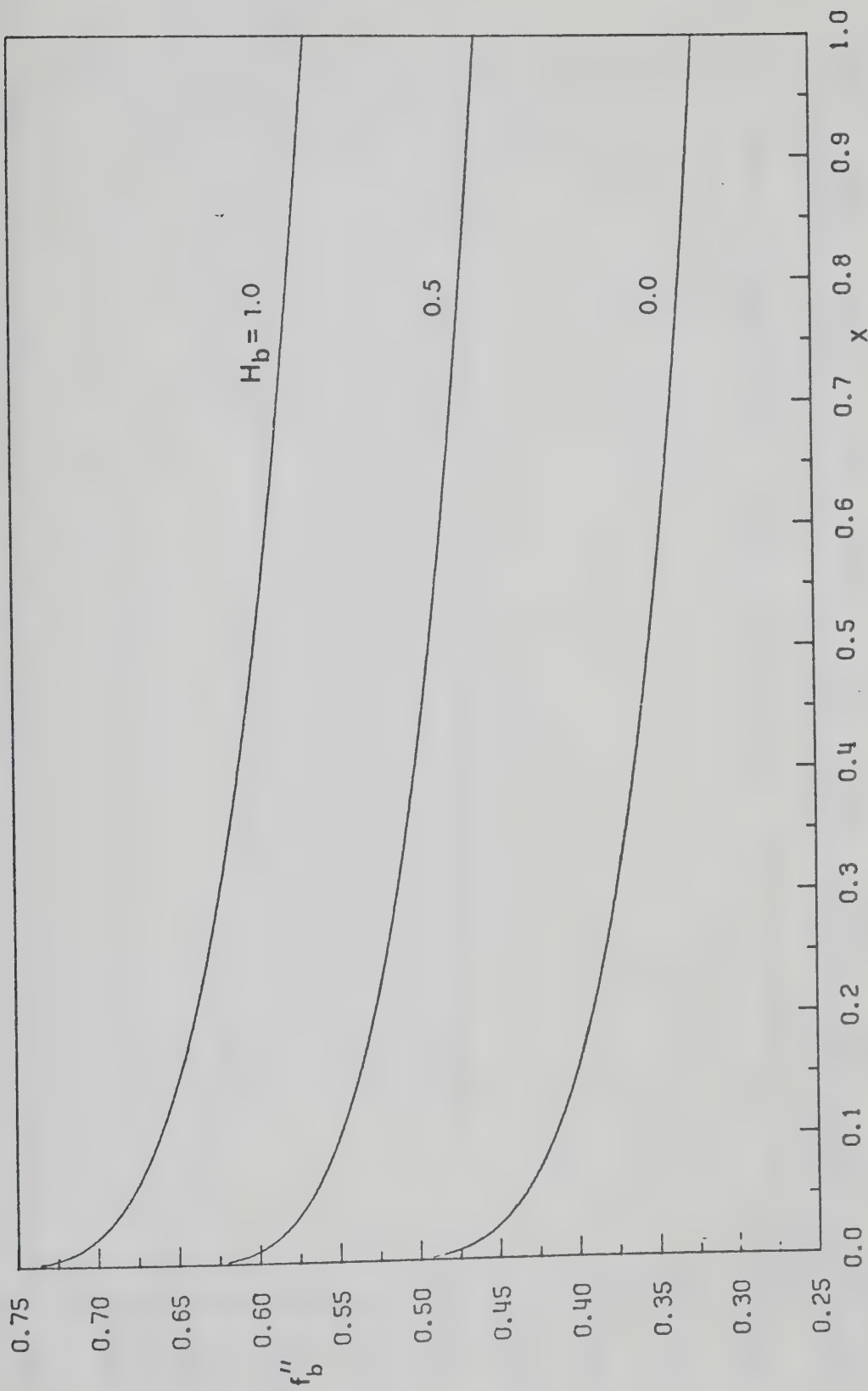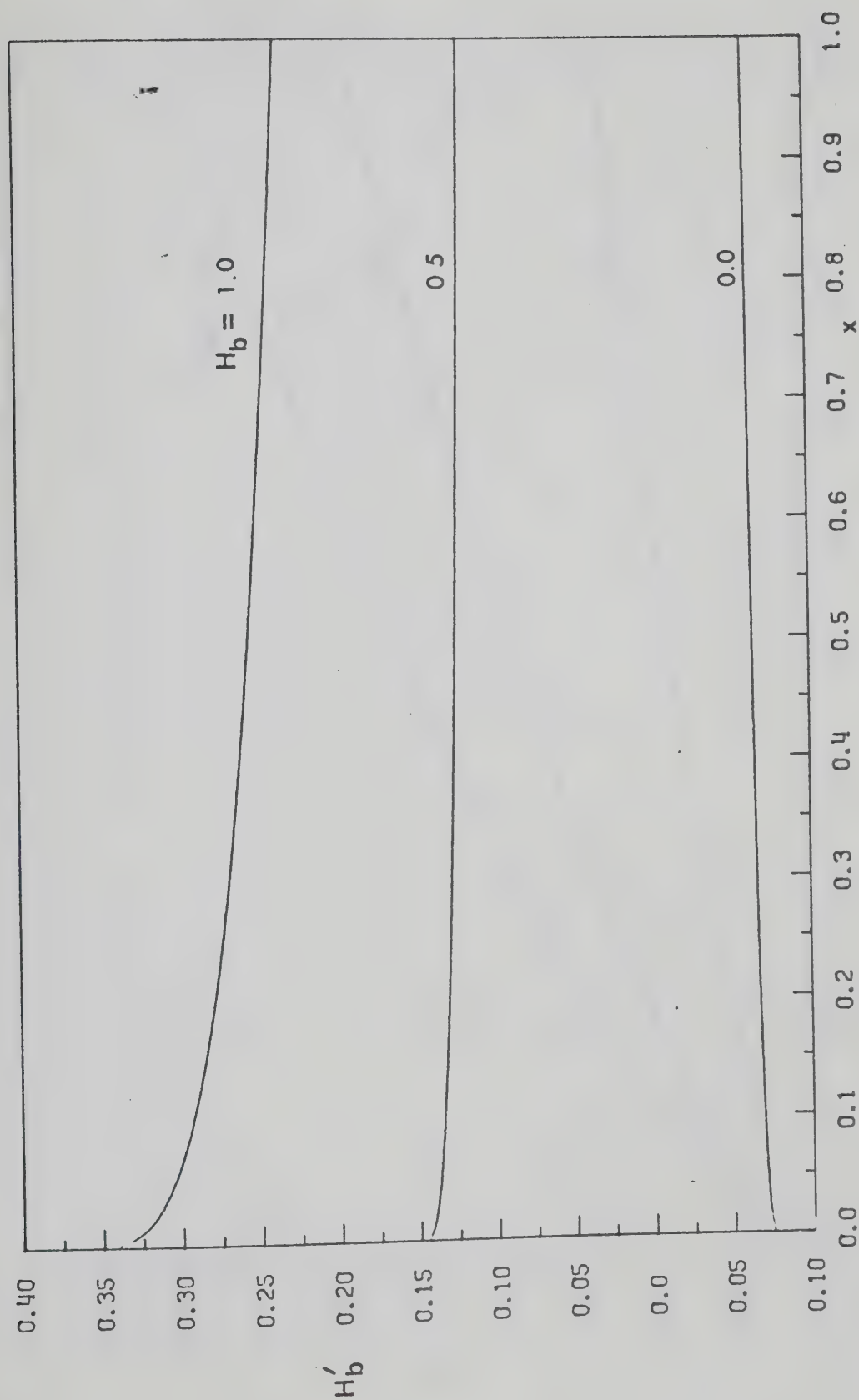
THE UNSTEADY PROBLEM

4.1 The Initial Conditions

In this chapter we consider the unsteady viscous flow on a plate, whose inclination to the free stream has been impulsively changed to $\theta_{b,f}$ at $t = 0$ from the original inclination $\theta_{b,i}$ at $t < 0$. The steady state solution of the last Chapter, corresponding to $\theta_b = \theta_{b,i}$, describes the flow on the plate prevailing at $t < 0$. At the instant of the impulsive change ($t=0$), the spatial distribution of the velocity and temperature field with respect to the flat plate is given by this steady state solution. However, the change in the inclination of the plate changes the shape of the effective body which in turn changes the pressure distribution.

The initial conditions in x are specified at $x = x_1$ for $t \geq 0$. In accordance with the approach in the steady problem, we assume that the series solution corresponding to $\theta_b = \theta_{b,f}$ gives the solution at $x = x_1$ for $t \geq 0$. This is equivalent to assuming that the final steady state is reached instantaneously at $x = x_1$. This assumption is justified because the close proximity to the leading edge makes the flow at $x = x_1$ extremely insensitive to the angle of inclination and the initial and final steady state solutions there differ by less than 1%. Thus the initial conditions in x are given by

for $t \geq 0$

$$f(x_1,\eta,t) = f_0(\eta) + \frac{\overline{f}_1(\eta)p_1K_{b,f}}{\overline{x}_1^{-1/2}} + \frac{p_2\overline{f}_2(\eta)+[p_3\overline{f}_2(\eta)+p_1^2\overline{f}_3(\eta)]K_{b,f}^2}{\overline{x}_1} \quad (4.1)$$

$$H(x_1,\eta,t) = H_0(\eta) + \frac{\overline{H}_1(\eta)p_1K_{b,f}}{\overline{x}_1^{-1/2}} + \frac{p_2\overline{H}_2(\eta)+[p_3\overline{H}_2(\eta)+p_1^2\overline{H}_3(\eta)]K_{b,f}^2}{\overline{x}_1} \quad (4.2)$$

$$\overline{p}(x_1,t) = 1 + \frac{p_1 \ K_{b,f}}{\overline{x}_1^{1/2}} + \frac{p_2+p_3 \ K_{b,f}^2}{\overline{x}_1} \quad (4.3)$$

where $\overline{x}_1 = \overline{x}_{L*} \ x_1^{-1/2}$ and $K_{b,f} = M_\infty \ \theta_{b,f}$.

The initial conditions in t are given by

for $x > x_1$

$$f(x,\eta,0) = f^{(0)}(x,\eta) \quad (4.4)$$

$$H(x,\eta,0) = H^{(0)}(x,\eta) \quad (4.5)$$

where $f^{(0)}$ and $H^{(0)}$ are the steady state solutions corresponding to $\theta_b = \theta_{b,i}$, obtained by the finite difference method of Section 3.3. The initial pressure distribution $\overline{p}(x,0) = \overline{p}^{(0)}(x)$ is calculated by the method of Section 3.3b using $K_{b,f}$ in place of K_b. The initial and boundary conditions are shown schematically in Figure 4.1.

4.2 Finite Difference Method for the Unsteady Problem

The unsteady equations are solved at discrete time-steps t_i, i=1,2,3,... with stepsizes increasing progressively in the positive t-direction:
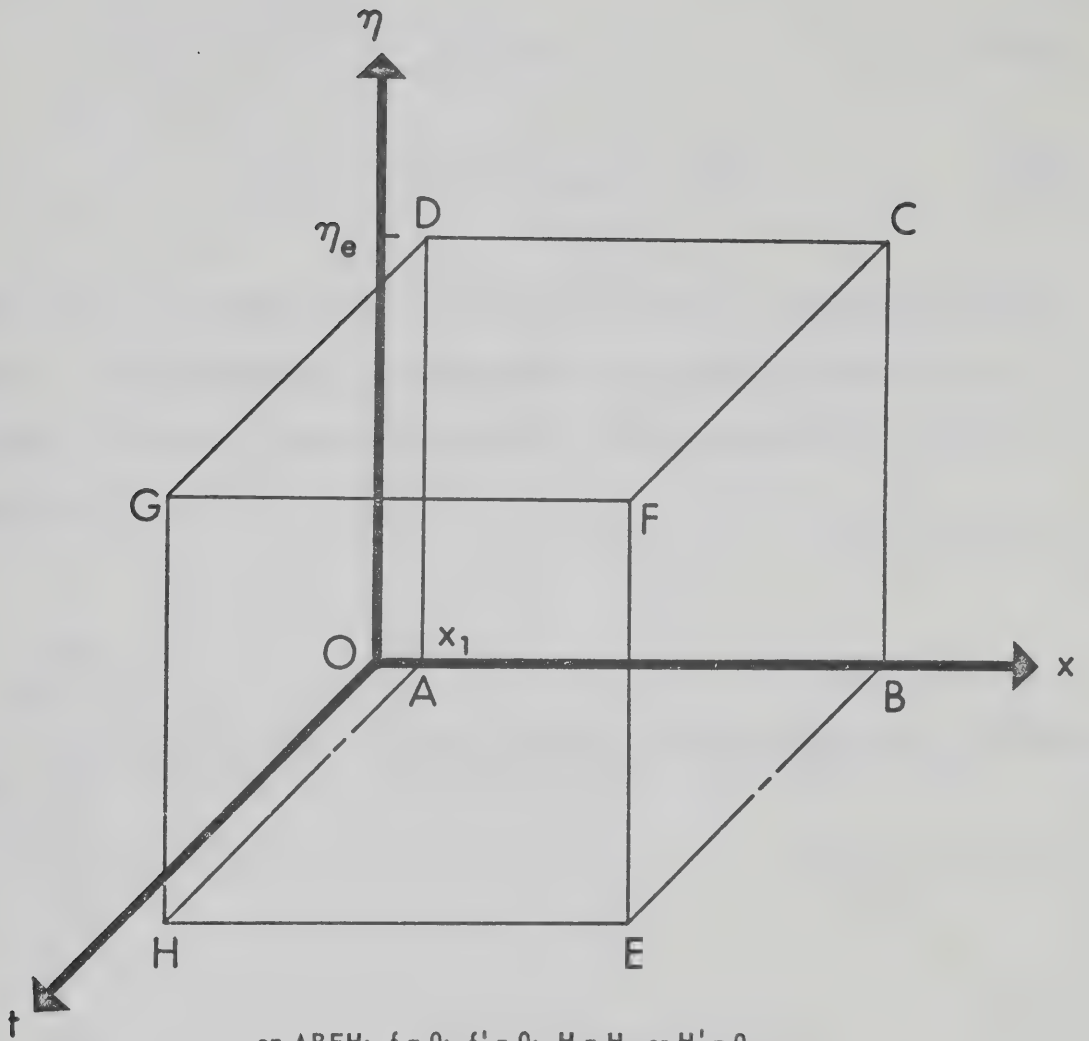
on ABEH: $f = 0$; $f' = 0$; $H = H_b$ or $H' = 0$

on FCDG: $f' = 1$; $H = 1$

on ABCD: $f = f^o$; $H = H^o$; $p = p^o$

on ADGH: $f = f_1$; $H = H_1$; $p = p_1$

Figure 4.1 Arrangement of the Boundary Conditions (Schematic)

$$t_1 = \Delta t_1 \qquad (4.6a)$$

$$t_i - t_{i-1} = \Delta t_i = K_t \Delta t_{i-1} \ , \ i=2,3,\ldots \qquad (4.6b)$$

Here the first timestep Δt_1 is of $0(10^{-3})$ and K_t is a constant greater than 1. The arrangement of x-stations is the same as that given in (3.46). Figure 4.2 shows schematically the arrangements of x and t stations.
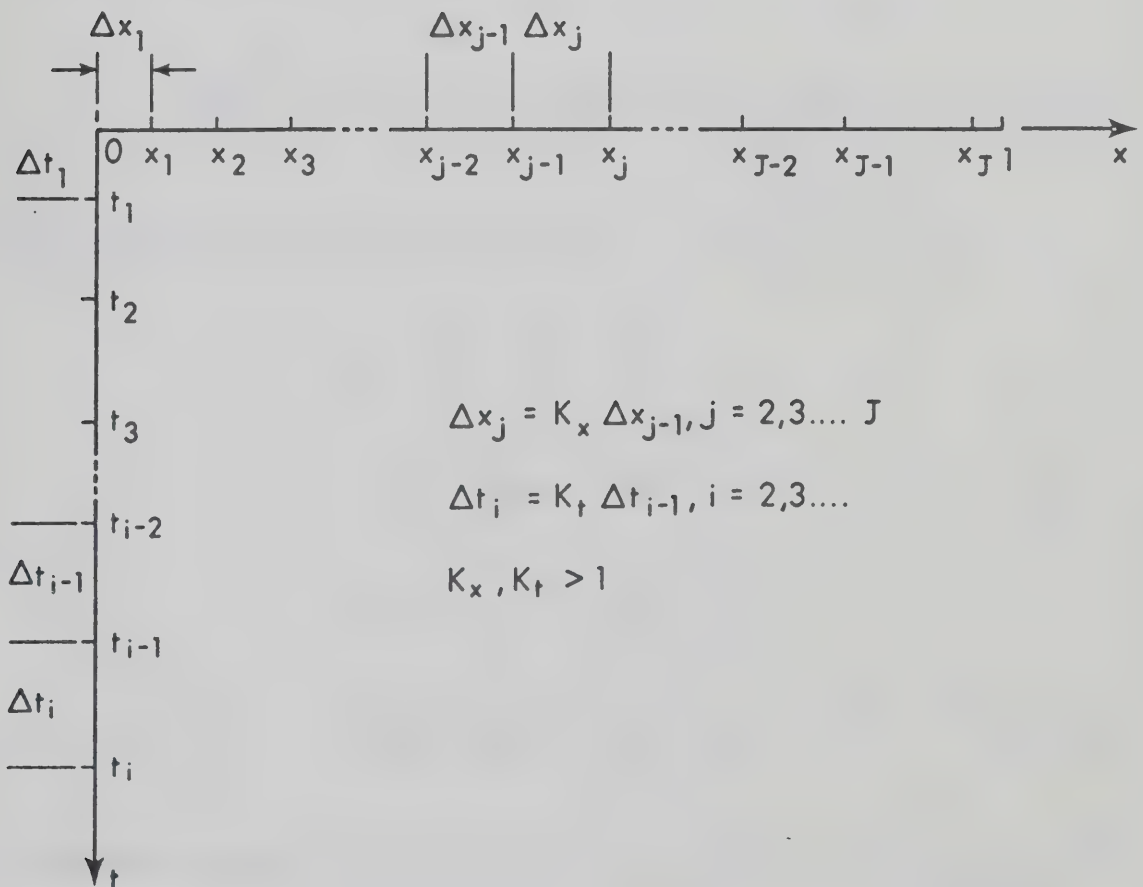
Figure 4.2 Schematic Arrangement of the x and t Stations

We introduce the notation

$$f^{(i)}(x,\eta) = f(x,\eta,t_i) \tag{4.7a}$$

$$H^{(i)}(x,\eta) = H(x,\eta,t_i) \tag{4.7b}$$

$$\bar{p}^{(i)}(x) = \bar{p}(x,t_i) \quad \text{etc.} \tag{4.7c}$$

For any function $\phi(t)$ the first derivative in the backward difference form can be written as:

$$\left(\frac{\partial\phi}{\partial t}\right)^{(i)} = u_i\phi^{(i)} - (u_i+v_i)\phi^{(i-1)} + v_i\phi^{(i-2)} \tag{4.8}$$

where the quantities u_i, v_i are given by

$$u_i = \frac{1}{\Delta t_i}\frac{K_t+1}{K_t} \quad \text{for } i = 1$$

$$= \frac{1}{\Delta t_i}\left(\frac{2K_t+1}{K_t+1}\right) \quad \text{for } i \geq 2 \tag{4.9}$$

$$v_i = 0 \quad \text{for } i = 1$$

$$= \frac{1}{\Delta t_i}\left(\frac{K_t^2}{K_t+1}\right) \quad \text{for } i \geq 2 \tag{4.10}$$

The truncation error in equation (4.8) is of the order of $\Delta t_i(\partial^2\phi/\partial t^2)^{(i)}$

for $i=1$ and $\Delta t_i{}^2 (\partial^2\phi/\partial t^2)^{(i)}$ for $i \geq 2$.

Using (4.8) equations (2.33) and (2.34) can be written as

$$\bar{p}^{(i)}(x)\frac{\partial^3 f}{\partial\eta^3} + f\frac{\partial^2 f}{\partial\eta^2} - 4x[\frac{\partial f}{\partial\eta}(\frac{\partial^2 f}{\partial x\partial\eta}+u_i) - \frac{\partial f}{\partial x}\frac{\partial^2 f}{\partial\eta^2}]$$

$$+ 4x[(u_i+v_i)\frac{\partial f^{(i-1)}}{\partial\eta} - v_i\frac{\partial f^{(i-2)}}{\partial\eta}] + Q^{(i)}(x)[H-(\frac{\partial f}{\partial\eta})^2] = 0 \quad (4.11)$$

$$\frac{\bar{p}^{(i)}(x)}{Pr}\frac{\partial^2 H}{\partial\eta^2} + f\frac{\partial H}{\partial\eta} - 4x[\frac{\partial f}{\partial\eta}\frac{\partial H}{\partial x} - \frac{\partial f}{\partial x}\frac{\partial H}{\partial\eta} + u_i H]$$

$$+ 4x[(u_i+v_i)H^{(i-1)} - v_i H^{(i-2)}] + R^{(i)}(x)[H-(\frac{\partial f}{\partial\eta})^2]$$

$$+ \frac{2(Pr-1)}{Pr}\bar{p}^{(i)}(x)\{(\frac{\partial^2 f}{\partial\eta^2})^2 + \frac{\partial f}{\partial\eta}\frac{\partial^3 f}{\partial\eta^3}\} = 0 \quad (4.12)$$

Here absence of any superscript in f and H indicates $f^{(i)}(x,\eta)$ and $H^{(i)}(x,\eta)$. $Q^{(i)}(x)$ and $R^{(i)}(x)$ are given by

$$Q^{(i)}(x) = \beta[1 - \frac{2x}{\bar{p}^{(i)}}\frac{\partial\bar{p}^{(i)}}{\partial x}] \quad (4.13)$$

and $$R^{(i)}(x) = 4\beta\frac{x}{\bar{p}^{(i)}}(\frac{\partial\bar{p}}{\partial t})^{(i)} \quad (4.14)$$

The use of backward difference formulas for the t-derivatives results in an implicit scheme which is inherently stable. At each time step $t = t_i$, $i=1,2,3,\ldots$ we approximate the functions $\bar{p}^{(i)}$, $Q^{(i)}$ and $R^{(i)}$ by extrapolating from the values at the previous time-steps. The partial differential equations (4.11,12) are then solved in the region $x_1 \leq x \leq x_J$, $0 \leq \eta \leq \eta_e$ using the initial conditions

(4.1-3) and the boundary conditions (2.47,49). The method described in Section 3.3a is followed. From the solution we then obtain $\bar{p}^{(i)}$ in accordance with the interaction equations (2.43-45). The solution then proceeds to the next time step $t = t_{i+1}$. The solution is continued till $\partial\bar{p}/\partial t$ becomes less than 10^{-5} in magnitude and is then compared with the steady state solution corresponding to $\theta = \theta_{b,f}$. The method of solution for the time steps t_1 and t_2 is different from that for the general time step t_i, $i \geq 3$. They are described in the following sub-sections.

4.2a General Case, $t = t_i$, $i \geq 3$

At the time steps $t_i (i \geq 3)$ we use the following extrapolation formulas for $\bar{p}^{(i)}$, $Q^{(i)}$ and $R^{(i)}$

$$\bar{p}^{(i)}(x) = (1+K_t)\bar{p}^{(i-1)}(x) - K_t\bar{p}^{(i-2)}(x) \qquad (4.15)$$

$$Q^{(i)}(x) = (1+K_t) Q^{(i-1)}(x) - K_t Q^{(i-2)}(x) \qquad (4.16)$$

$$R^{(i)}(x) = \frac{x}{\Delta t_i} z_1 \frac{[z_2\bar{p}^{(i-1)}(x)+z_3\bar{p}^{(i-2)}(x)+\bar{p}^{(i-3)}(x)]}{z_4\bar{p}^{(i-1)}(x) + \bar{p}^{(i-2)}(x)} \qquad (4.17)$$

where

$$z_1 = - 4\beta \frac{(2K_t+1) K_t^2}{(K_t+1)} \qquad (4.18a)$$

$$z_2 = \frac{2K_t^2+2K_t+1}{(2K_t+1)K_t^2} \qquad (4.18b)$$

$$z_3 = -\frac{(2K_t^2+K_t+1)(K_t+1)}{(2K_t+1)K_t^2} \tag{4.18c}$$

$$z_4 = -\frac{1+K_t}{K_t} \tag{4.18d}$$

The truncation errors in equations (4.15), (4.16) and (4.17) are of the order of $\Delta t_i^2 (\partial^2 p/\partial t^2)^{(i)}$, $\Delta t_i^2 (\partial^2 Q/\partial t^2)^{(i)}$ and $\Delta t_i^2 (\partial^3 p/\partial t^3)^{(i)}$ respectively.

With these values for $\bar{p}^{(i)}$, $Q^{(i)}$ and $R^{(i)}$ the equations (4.11) and (4.12) can now be solved in the region $x_1 \leq x \leq x_j$, $0 \leq \eta \leq \eta_e$. The method discussed in Section 3.3a is followed. The x-derivatives are replaced by backward difference formulas and the resulting ordinary differential equations are solved at the stations $x_j (j=2,J)$ using the iterative method based on quasilinearization. The linearized problems to be solved at the m th iteration cycle are given by (3.58-63) with the following exceptions:

$$\sigma_2^{[m]}(\eta) = -2(B_j+Q_j^{(i)})f^{[m-1]'}(\eta)+(B_j+C_j)f'_{j-1}(\eta)-C_jf'_{j-2}(\eta) - 4x_ju_i \tag{4.19a}$$

$$F^{[m]}(\eta) = \bar{p}_j^{(i)} f^{[m-1]'''}(\eta)$$

$$+ f^{[m-1]''}(\eta)\{(1+B_j)f^{[m-1]}(\eta)-(B_j+C_j)f_{j-1}^{(i)}(\eta) + C_jf_{j-1}^{(i)}(\eta)\}$$

$$- f^{[m-1]'}(\eta)\{(B_j+Q_j^{(i)})f^{[m-1]'}(\eta)-(B_j+C_j)f_{j-1}^{(i)'}(\eta)+C_jf_{j-2}^{(i)'}(\eta)\}$$

$$+ Q_j^{(i)} H^{[m-1]}(\eta)$$

$$- 4x_j \{u_i f^{[m-1]\prime}(\eta) - (u_i + v_i) f_j^{(i-1)\prime}(\eta) + v_i f_j^{(i-2)\prime}(\eta)\} \quad (4.19b)$$

$$\sigma_5^{[m]}(\eta) = - B_j f^{[m]\prime}(\eta) - 4x_j u_i + R_j^{(i)} \quad (4.20a)$$

$$G^{[m]}(\eta) = \frac{\overline{p}_j}{Pr} H^{[m-1]\prime\prime}(\eta)$$

$$+ H^{[m-1]\prime}(\eta)\{(1+B_j) f^{[m]}(\eta) - (B_j + C_j) f_{j-1}^{(i)}(\eta) + C_j f_{j-2}^{(i)}(\eta)\}$$

$$- f^{[m]\prime}(\eta)\{B_j H^{[m-1]}(\eta) - (B_j + C_j) H_{j-1}^{(i)}(\eta) + C_j H_{j-2}^{(i)}(\eta)\}$$

$$+ \frac{2(Pr-1)}{Pr} \overline{p}_j^{(i)} \{(f^{[m]\prime\prime}(\eta))^2 + f^{[m]\prime}(\eta)\, f^{[m]\prime\prime\prime}(\eta)\}$$

$$- 4x_j \{u_i H^{[m-1]}(\eta) - (u_i + v_i) H_j^{(i-1)}(\eta) + v_i H_j^{(i-2)}(\eta)\}$$

$$+ R_j^{(i)} \{H^{[m-1]}(\eta) - (f^{[m]\prime}(\eta))^2\} \quad (4.20b)$$

Here $f^{[m]}(\eta)$ and $H^{[m]}(\eta)$ are the m th iterate for $f_j^{(i)}(\eta)$ and $H_j^{(i)}(\eta)$. The extra terms in (4.19,20) over the corresponding expressions (3.60c,e) and (3.63c,d) result from the t-derivatives in (2.33,34). These extra terms do not present any additional difficulty and the matrix method described in Appendix B is used to solve the linearized equations for $e^{[m]}$ and $g^{[m]}$.

After solving $f_j^{(i)}(\eta)$ and $H_j^{(i)}(\eta)$ at all x-stations $x_j(j=2,J)$ we calculate

$$\bar{I}_j^{(i)} = \frac{\int_0^{\eta_e} [H_j^{(i)} - (f_j^{(i)'})^2] d\eta}{I_0} , \quad j=2,J \tag{4.21}$$

The pressure distribution $\bar{p}^{(i)}$ can now be obtained from the equation (2.43-45) by the method described in Section 3.3b. We first convert the problem into an ordinary differential equation for $\bar{\delta}^{(i)}$ in x. This is then solved iteratively using the method based on quasilinearization. The linearized problem at the n th iteration cycle is given by (3.79-81) with the following exceptions:

$$\sigma_6^{[n]}(x) = \frac{3}{4} + \{x \, u_i\}$$

$$+ \left| \frac{\zeta_3 \bar{I}^{(i)} [\frac{\gamma(\gamma+1)}{4} \zeta_3 \bar{I}^{(i)}/\bar{\delta} + \frac{\gamma(3\gamma-1)}{4} x^{1/2}]}{\zeta_4 \bar{\delta}^2 [\frac{\gamma(\gamma+1)}{4} \zeta_3 \bar{I}^{(i)}/\bar{\delta} + \frac{\gamma(\gamma-1)}{2} x^{1/2}]^{3/2}} \right|^{[n-1]} \tag{4.22}$$

$$D^{[n]}(x) = \left| x \frac{d\bar{\delta}}{dx} + \frac{3}{4} \bar{\delta} + x\{u_i \bar{\delta} - (u_i + v_i)\bar{\delta}^{(i-1)} + v_i \bar{\delta}^{(i-2)}\} \right.$$

$$\left. - \frac{\zeta_3 \bar{I}^{(i)}/\bar{\delta} - x^{1/2}}{\zeta_4 [\frac{\gamma(\gamma+1)}{2} \zeta_3 \bar{I}^{(i)}/\bar{\delta} + \frac{\gamma(\gamma-1)}{2} x^{1/2}]^{1/2}} + \frac{K_b \, x^{1/4}}{\zeta_4} \right|^{[n-1]} \tag{4.23}$$

The superscript [n-1] in the last terms of (4.22) and (4.23) implies that the current iterate $\bar{\delta}^{[n-1]}$ is to be used for $\bar{\delta}$. ζ_3 and ζ_4 are constants defined in (3.73) and (3.75). The terms inside the curly brackets result from the unsteady term $\partial \bar{\delta}/\partial t$ in equation (2.44). From the converged solution $\bar{\delta}^{(i)}$ we calculate the pressure distribution

$$\overline{p}_j^{(i)} = \frac{\overline{I}_j^{(i)}}{\overline{\delta}_j^{(i)}} \quad j=2,J \tag{4.24}$$

From this $\overline{p}^{(i)}$ we then calculate $Q_j^{(i)}$ $(j=2,J)$ using the finite difference formulas given in Appendix C.

4.2b Second Time Step

At the second time step $(i=2)$ the extrapolation formula (4.17) can not be used to approximate $R^{(2)}$. In order to maintain the same order of accuracy we use the following iterative scheme:
$p^{(2)}$ and $Q^{(2)}$ are obtained from (4.15) and (4.16) and $R^{(2)}$ is approximated by

$$R^{(2)}(x) = 4\beta \; \frac{x}{\Delta t_1} \; \frac{\overline{p}^{(1)}(x)-p^{(0)}(x)}{[(1+K_t)\overline{p}^{(1)}(x)-K_t\overline{p}^{(0)}(x)]} \tag{4.25}$$

The formula (4.25) has a truncation error of the order of $\Delta t_2 \; (\partial^2\overline{p}/\partial t^2)^{(2)}$. With these values of $\overline{p}^{(2)}$, $Q^{(2)}$ and $R^{(2)}$ the method described in Section 4.2a is followed to obtain a better approximation for $\overline{p}^{(2)}$ and $Q^{(2)}$. $R^{(2)}$ is then obtained from

$$R^{(2)}(x) = 4\beta \; \frac{x}{\Delta t_2} \; \frac{[(2K_t+1)\overline{p}^{(2)}(x)-(1+K_t)^2\overline{p}^{(1)}(x)+K_t^2\overline{p}^{(0)}(x)]}{(1+K_t) \; \overline{p}^{(2)}(x)}$$

$$\tag{4.26}$$

which has the same order of truncation error as equation (4.17). The calculations are repeated with these values of $\overline{p}^{(2)}$, $Q^{(2)}$ and $R^{(2)}$.

The iteration is continued till $\overline{p}^{(2)}$ converges within a predefined tolerance. Not more than three iterations was necessary to stabilize $\overline{p}^{(2)}$ to six significant digits.

4.2c First Time Step

At the first time step (i=1) we use the following iterative scheme:

We start with the assumption $\overline{p}^{(1)}(x) = \overline{p}^{(0)}(x)$, $Q^{(1)}(x) = Q^{(0)}(x)$, $R^{(1)}(x) = 0$ and follow the method described in Section 4.2a to obtain a better approximation for $\overline{p}^{(1)}$ and $Q^{(1)}$. $R^{(1)}(x)$ is then obtained from

$$R^{(1)}(x) = 4\beta \ \frac{x}{\Delta t_1} \ \frac{\overline{p}^{(1)}(x) - \overline{p}^{(0)}(x)}{\overline{p}^{(1)}(x)} \tag{4.27}$$

which has a truncation error of order $\Delta t_1 (\partial^2 \overline{p}/\partial t^2)^{(1)}$. We repeat the calculations with these values of $\overline{p}^{(1)}$, $Q^{(1)}$ and $R^{(1)}$.

The iteration is continued till $\overline{p}^{(1)}$ converges within a predefined tolerance. To stabilize $\overline{p}^{(1)}$ to six significant digits, the number of iterations necessary was between four and six.

4.3 Results of the Unsteady Problem

The variation of $\overline{p}$, $f''(0)$, and $H'(0)$ with time is presented in Figures 4.3 through 4.5. All curves are made for $Pr = 0.72$, $\gamma = 1.4$, $\overline{x}_{L*} = 8$, $M_\infty = 20$, and the change of angle from $2°$ to $6°$. The initial and final states are also indicated.

Figure 4.3 also indicates location of the condition $t^* u_\infty^*/x^* = 1$

which corresponds to the discontinuities quoted in the literature [8,31].

The discontinuity is avoided by suitable formulation of the variables,

and in particular by avoiding the variable of the type $t^*u_\infty^*/x^*$.

Figure 4.3 Variation of $\bar{p}$ with Time for $Pr = 0.72$, $\gamma = 1.4$, $\bar{X}_{L^*} = 8$, $M_\infty = 20$. Change of angle from 2° to 6°. (+ value at $t = 0$, x final steady state value, ● location of $t^*u^*_\infty/x^* = 1$)
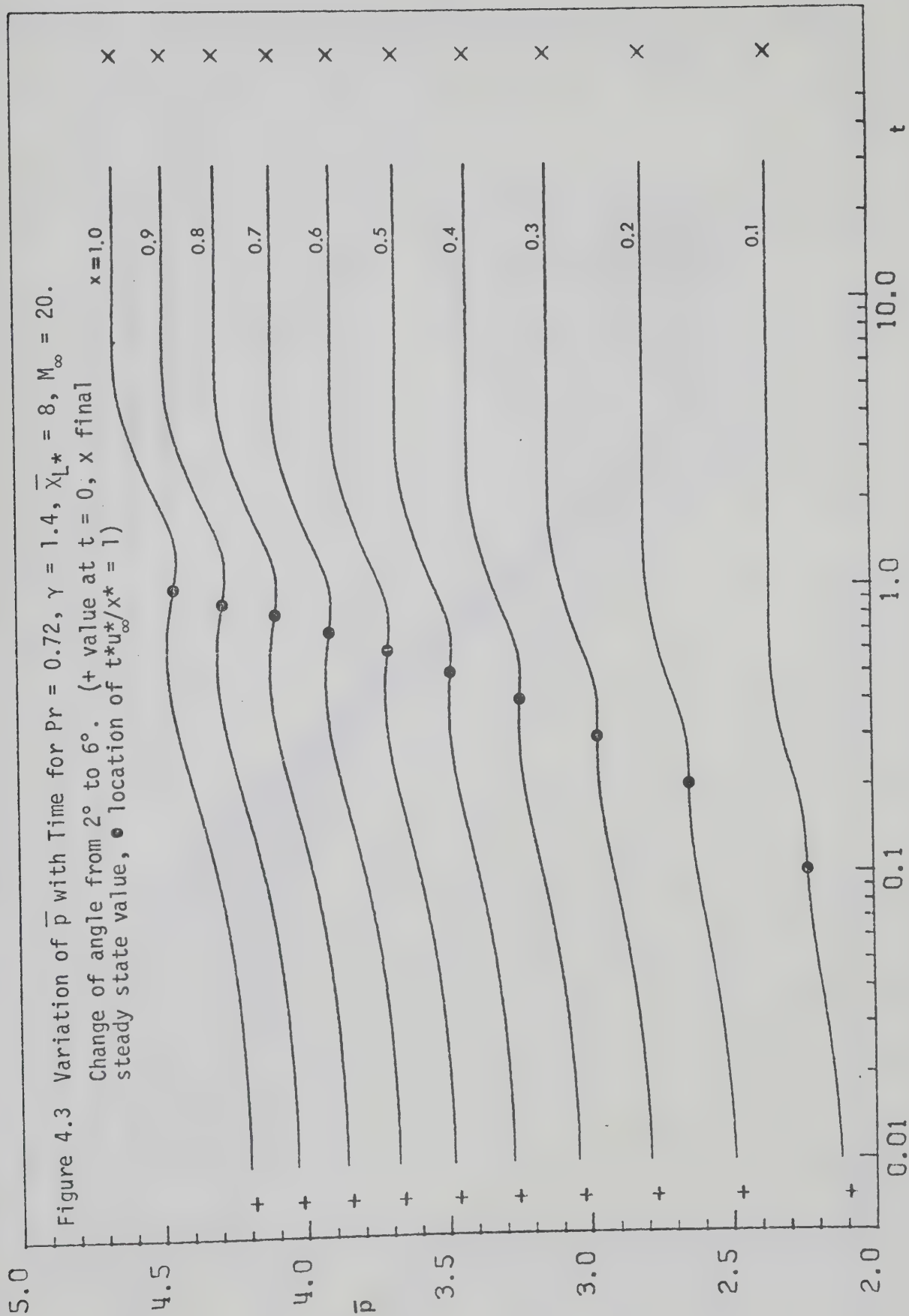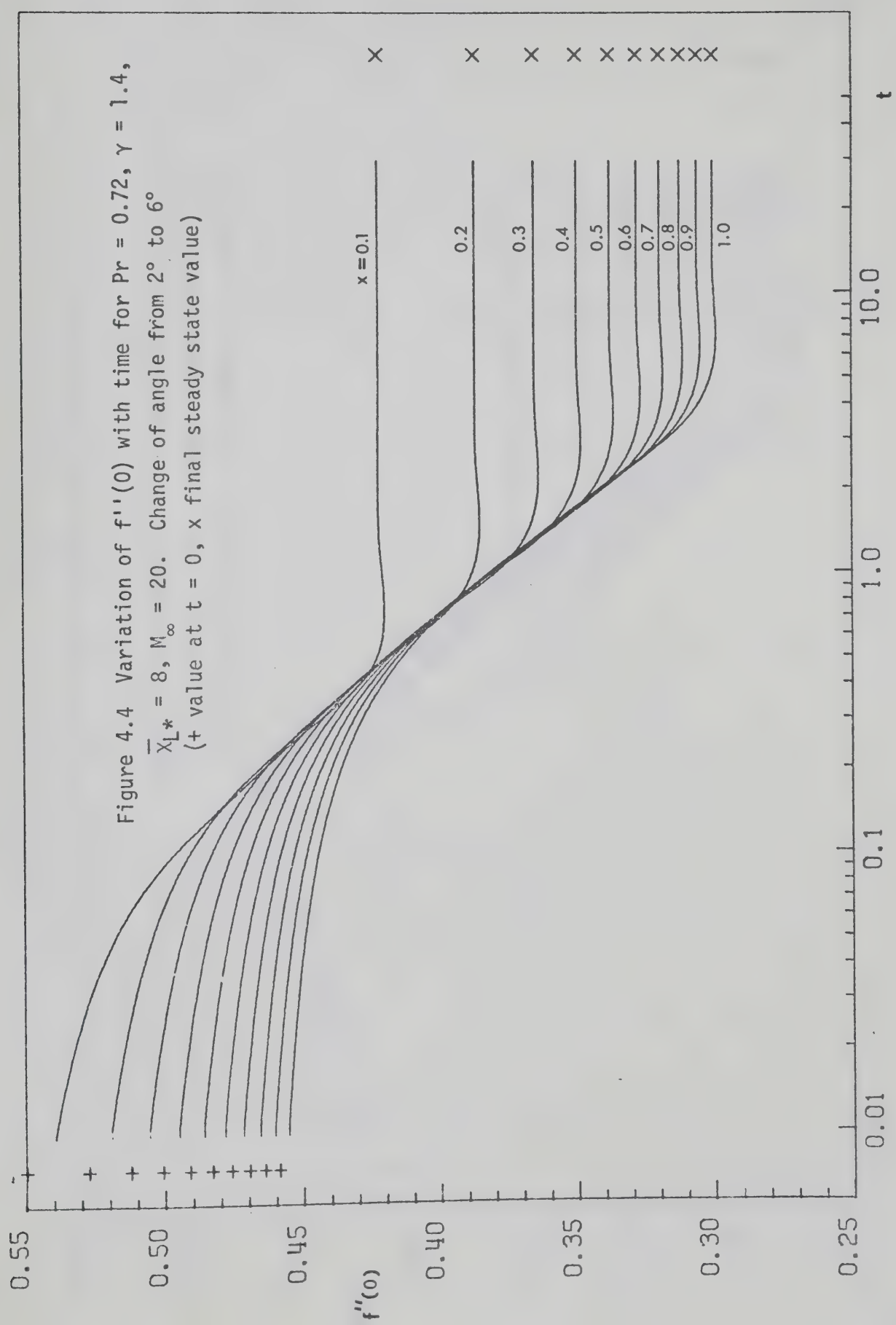
Figure 4.4 Variation of $f''(0)$ with time for $Pr = 0.72$, $\gamma = 1.4$, $\overline{X}_{L^*} = 8$, $M_\infty = 20$. Change of angle from $2°$ to $6°$ (+ value at $t = 0$, x final steady state value)

Figure 4.5 Variation of H'(0) with time for Pr = 0.72, γ = 1.4, $\overline{\chi}_{L*}$ = 8, M_∞ = 20. Change of angle from 2° to 6° (+ value at t = 0, x final steady state value)
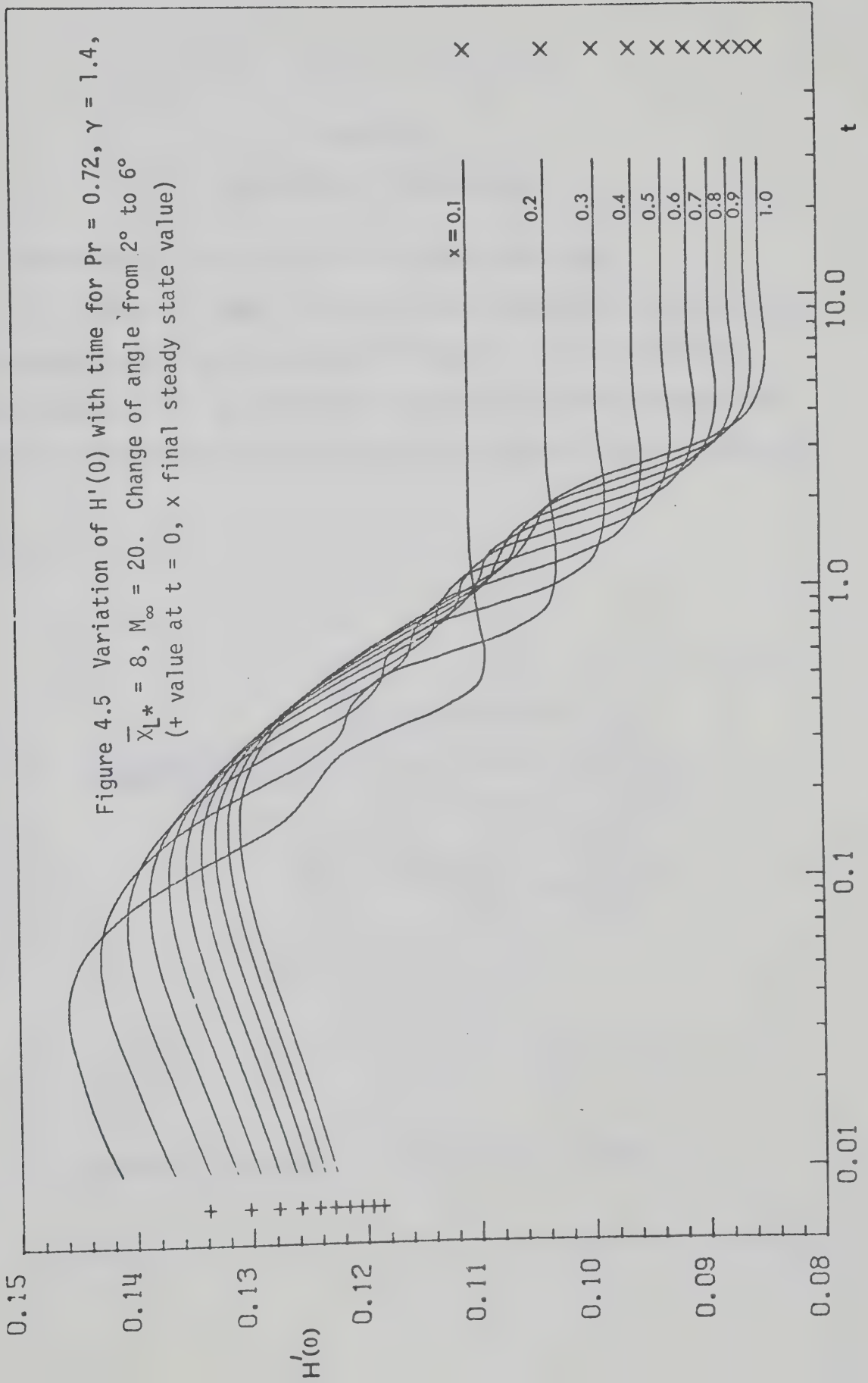
CHAPTER V

APPLICATION OF THE SOLUTIONS

5.1 Aerodynamic Characteristics of Slender Wedge Wings

Figure 5.1 shows the various forces acting on a slender wedge of semiwedge angle θ_w at an angle of attack α. If the subscripts T and B represent the top and bottom surfaces of the wedge respectively, then the total normal force per unit width acting on the two sides are
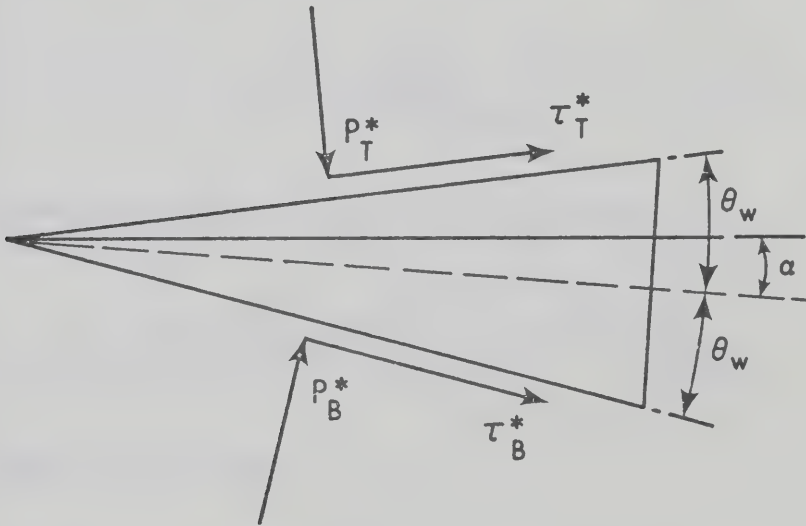
Figure 5.1 Aerodynamic Forces Acting on a Wedge

$$(F_N^*)_{T,B} = \int_0^{L^*} (p^*)_{T,B} \, dx^*$$

(5.1)

or

$$\frac{(F_N^*)_{T,B}}{\frac{1}{2} \rho_\infty^* u_\infty^{*2} L^*} = \frac{2p_0 \, \overline{X}_{L^*}}{\gamma M_\infty^2} \int_0^1 x^{-1/2} (\overline{p})_{T,B} \, dx$$

(5.2)

The total tangential force per unit width on the two sides are given by

$$(F_S^*)_{T,B} = \int_0^{L^*} (\tau^*)_{T,B} \, dx^*$$

(5.3)

where τ^* is the shear stress on the surface given by

$$\tau^* = \left(\mu^* \frac{\partial u^*}{\partial y^*} \right)_{y^*=y_b^*}$$

(5.4)

Using the transformations of Chapter II we can write

$$\tau^* = \frac{1}{2} \rho_\infty^* \, u_\infty^{*2} \, p_0^{1/2} \frac{\overline{X}_{L^*}^{3/2}}{M_\infty^3} \, x^{-3/4} \, \overline{p} \, \frac{\partial^2 f}{\partial \eta^2} \Big|_{\eta=0}$$

(5.5)

Therefore from (5.3) we have

$$\frac{(F_S^*)_{T,B}}{\frac{1}{2} \rho_\infty^* u_\infty^{*2} L^*} = \frac{p_0^{1/2} \overline{X}_{L^*}^{3/2}}{M_\infty^3} \int_0^1 x^{-3/4} \left(\overline{p} \, \frac{\partial^2 f}{\partial \eta^2} \Big|_{\eta=0} \right)_{T,B} dx$$

(5.6)

The lift and drag coefficients of the wedge wing can now be given as

$$C_L = \frac{(F_N*)_B - (F_N*)_T - (F_S*)_B \theta_B + (F_S*)_T \theta_T}{\frac{1}{2} \rho_\infty^* u_\infty^{*2} L^*} \tag{5.7}$$

$$C_D = \frac{(F_S*)_B + (F_S*)_T + (F_N*)_B \theta_B + (F_N*)_T \theta_T}{\frac{1}{2} \rho_\infty^* u_\infty^{*2} L^*} \tag{5.8}$$

where

$$\theta_B = \theta_W + \alpha \tag{5.9a}$$

$$\theta_T = \theta_W - \alpha \tag{5.9b}$$

Using (5.2) and (5.6) we have

$$C_L = \frac{2p_0 \bar{X}_L*}{\gamma M_\infty^2} [J_{1,B} - J_{1,T}] - \frac{p_0^{1/2} \bar{X}_L*^{3/2}}{M_\infty^3} [J_{2,B} \theta_B - J_{2,T} \theta_T] \tag{5.10}$$

$$C_D = \frac{p_0^{1/2} \bar{X}_L*^{3/2}}{M_\infty^3} [J_{2,B} + J_{2,T}] + \frac{2p_0 \bar{X}_L*}{\gamma M_\infty^2} [J_{1,B} \theta_B + J_{1,T} \theta_T] \tag{5.11}$$

where J_1, J_2 represent the integrals

$$J_1 = \int_0^1 x^{-1/2} \bar{p} \, dx \tag{5.12a}$$

$$J_2 = \int_0^1 [x^{-3/4} \bar{p} \frac{\partial^2 f}{\partial \eta^2} |_{\eta=0}] \, dx \tag{5.12b}$$

The lift to drag ratio is given by C_L/C_D.

The position of the aerodynamic centre is given by

$$
x_{ac}^* = \frac{\int_0^{L*} x^* p_B^* \, dx^* - \int_0^{L*} x^* p_T^* \, dx^*}{C_L \frac{1}{2} \rho_\infty^* u_\infty^{*2} L^*}
\tag{5.13}
$$

or in the nondimensional form

$$
x_{ac} = \frac{x_{ac}^*}{L^*} = \frac{J_{3,B} - J_{3,T}}{(J_{1,B} - J_{1,T}) - \frac{\gamma}{2} \frac{\overline{X}_L^{*1/2}}{p_0^{1/2} M_\infty} (J_{2,B} \theta_B - J_{2,T} \theta_T)}
\tag{5.14}
$$

Here J_3 represents the integral

$$
J_3 = \int_0^1 x^{1/2} \overline{p} \, dx
\tag{5.15}
$$

The rate of heat transfer to the wedge per unit area at any point of the surface is given by

$$
q^* = \left(k^* \frac{\partial T^*}{\partial y^*} \right)_{y^* = y_b^*}
\tag{5.16}
$$

Making use of the transformations of Chapter II we can write

$$
\frac{q^*}{\frac{1}{2} \rho_\infty^* u_\infty^{*3}} = \frac{1}{2Pr} \, p_0^{1/2} \frac{\overline{X}_L^{*3/2}}{M_\infty^3} \left[x^{-3/4} \, \overline{p} \, \frac{\partial H}{\partial \eta} \Big|_{\eta=0} \right]
\tag{5.17}
$$

If Q^* denote the total heat transfer rate per unit width to one side of the wedge, then

$$\frac{(Q^*)_{T,B}}{\frac{1}{2}\rho_\infty^* u_\infty^{*3} L^*} = \frac{1}{2Pr} \ P_0^{1/2} \ \frac{\overline{X}_L^{*\,3/2}}{M_\infty^3} \ (J_4)_{T,B} \tag{5.18}$$

where J_4 represents the integral

$$J_4 = \int\limits_0^1 (x^{-3/4} \ \frac{1}{\overline{p}} \ \frac{\partial H}{\partial \eta} \ \Big|_{\eta=0}) \ dx \tag{5.19}$$

The integrals J_1, J_2, J_3, J_4 are of the form

$$\int\limits_0^1 x^\omega \ \phi(x) \ dx \tag{5.20}$$

Because of the special arrangement of the x-stations used in the numerical method, the function $\phi(x)$ is given as a set of values ϕ_j at the abscissae x_j, $j=1,2,\ldots J$. A modification of the Simpson's rule to evaluate the integrals of the form (5.20) is described in Appendix D.

BIBLIOGRAPHY

1. Shen, S.F., "An Estimate of the Viscosity Effects on the Hyper-
        sonic Flow over an Insulated Wedge", Jour. Math. Phys.,
        Vol. 31, No. 3, p. 192, 1952.

2. Shen, S.F., "On the Boundary-Layer Equations in Hypersonic Flow",
        Journal Aero. Sci., Vol. 19, No. 7, p. 500, July 1952.

3. Lees, L. and Probstein, R.F., "Hypersonic Viscous Flow over a
        Flat Plate", Princeton University, Aeronautical Engineering
        Laboratory, Report No. 195, April 1952.

4. Lees, L., and Probstein, R.F., "Hypersonic Flows of a Viscous
        Fluid", Princeton University Monograph, 1953.

5. Lees, L., "On the Boundary-Layer Equations in Hypersonic Flow
        and Their Approximate Solutions", Journal Aero. Sci.,
        Vol. 20, No. 2, p. 143, February 1953.

6. Hayes, W.D. and Probstein, R.F., "Hypersonic Flow Theory",
        Academic Press, New York, 1959.

7. Dorrance, W.H., "Viscous Hypersonic Flow", McGraw-Hill Book Co.,
        Inc., 1962.

8. Stewartson, K., "The Theory of Laminar Boundary Layers in Com-
        pressible Fluids", Oxford Mathematical Monographs, Oxford
        University Press, 1964.

9.   Moore, F.K., "Hypersonic Boundary Layer Theory", In High Speed
     Aerodynamics and Jet Propulsion, Vol. IV, Princeton
     University Press, 1964.

10. Linnell, R.D., "Two-Dimensional Airfoils in Hypersonic Flows:,
     J urnal Aero. Sci., Vol. 16, No. 1, p. 22, January 1949.

11. Goldworthy, F.A., "Two-Dimensional Rotational Flow at High Mach
     Number Past Thin Aerofoils", Quart. Journal Mech. and
     Applied Math., Vol. V, Pt. 1, p. 54, 1952.

12. Li, T.Y. and Nagamatsu, H.T., "Shock-Wave Effects on the Laminar
     Skin Friction of an Insulated Flat Plate at Hypersonic
     Speeds", Journal Aero. Sci., Vol. 20, No. 5, p. 345,
     May 1953.

13. Stewartson, K., "On the Motion of a Flat Plate at High Speed
     in a Viscous Compressible Fluid - II. Steady Motion",
     Journal Aero. Sci., Vol. 22, No. 5, p. 303, May 1955.

14. Li, T.Y., and Nagamatsu, H.T., "Hypersonic Viscous Flow on
     Noninsulated Flat Plate", Proc. Fourth Midwestern Conf.
     Fluid Mech., p. 273, Purdue University, 1955.

15. Bush, W.B., "Hypersonic Strong-Interaction Similarity Solutions,
     Journal Fluid Mech. Vol. 25, Part 1, p. 51, 1966.

16. Nagakura, T. and Naruse, H., "An Approximate Solution of the
     Hypersonic Laminar Boundary-Layer Equations and its
     Application", Journal Phys. Soc. Japan, Vol. 12, No. 11,
     p. 1298, Nov. 1957.

17. Lees, L., "Laminar Heat Transfer over Blunt-Nosed Bodies at
    Hypersonic Flight Speeds", Jet Propulsion, Vol. 26, No. 4,
    p. 259, April 1956.

18. Moore, F.K., "On Local Flat-Plate Similarity in the Hypersonic
    Boundary Layer", J. Aerospace Sci., Vol. 28, No. 10,
    p. 753, October 1961.

19. Cheng, H.K., Hall, J.G., Golian, T.C. and Hertzberg, A., "Boundary-
    Layer Displacement and Leading-Edge Bluntness Effects in
    High-Temperature Hypersonic Flow", Journal Aerospace Sci.,
    Vol. 28, No. 5, p. 353, May 1961.

20. Dewey, C.F., "Use of Local Similarity Concepts in Hypersonic
    Viscous Interaction Problems", A.I.A.A. Journal, Vol. 1,
    No. 1, p. 20, January 1963.

21. Mirels, H. and Lewellen, "Hypersonic Viscous Interaction Theory
    for Wedge Wings", Journal of Spacecraft and Rockets,
    Vol. 4, No. 4, p. 492, April 1967.

22. Bertram, M.H. and Blackstock, T.A., "Some Simple Solutions to
    the Problem of Predicting Boundary-Layer Self-Induced
    Pressures", NASA Technical Note D-798, April 1961.

23. White, F.M., "Hypersonic Laminar Viscous Interactions on Inclined
    Flat Plates", ARS Journal, Vol. 32, p. 780, May 1962.

24. Mann, W.M. and Bradley, R.J., "Hypersonic Viscid-Inviscid In-
    teraction Solutions for Perfect-Gas and Equilibrium Real-
    Air Boundary-Layer Flow",

25. Kurzrock, J.W. and Mates, R.E., "Exact Numerical Solutions of the Time-Dependent Compressible Navier-Stokes Equations", Cornell Aeronautical Laboratory Report No. AG-2026-W-1, February 1966.

26. Butler, T.D., "Numerical Solution of Hypersonic Sharp-Leading-Edge Flows", Physics of Fluids, Vol. 10, p. 1205, 1967.

27. Lighthill, M.J., "Oscillating Aerofoils at High Mach Number, Journal Aero. Sci., Vol. 20, No. 6, p. 402, June 1953.

28. Hayes, W.D., "On Hypersonic Similitude", Quart. Appl. Math., Vol. 5, p. 105, 1947.

29. Miles, J.W., "Unsteady Flow at Hypersonic Speeds". In "Hypersonic Flow", Butterworths Scientific Publications, London, p. 185, 1960.

30. Moore, F.K. and Ostrach, S., "Displacement Thickness of the Unsteady Boundary Layer", Journal Aero. Sci., Vol. 24, No. 1, p. 77, January 1957.

31. Rodkiewicz, C.M. and Reshotko, E., "Time-Dependent Hypersonic Viscous Interactions", Scientific Report AFOSR 67-2451, Case Inst. of Tech., FTAS/TR-67-28, November 1967. (See also Reshotko, E. and Rodkiewicz, C.M., "Pressure induced by Weak Interaction with Unsteady Boundary Layers", AIAA Journal, Vol. 7, No. 8, p. 1609, August 1969).

32. Gupta, R.N., "The Weak Interaction Induced Pressure due to the Stepwise-Deceleration of a Flat Plate in Hypersonic Flow", M.Sc. Thesis, University of Alberta, 1968.

33. Gupta, R.N., "Strong Viscous Interaction in Unsteady High Speed Flows", Ph.D. Thesis, University of Alberta, 1970.

34. Rodkiewicz, C.M. and Gupta, R.N., "Time-Dependent Shear Stress and Temperature Distribution over an Insulated Flat Plate Moving at Hypersonic Speed", C.A.S.I. Transactions, Vol. 4, No. 1, p. 20, March 1971.

35. Gupta, R.N. and Rodkiewicz, C.M., "Unsteady Boundary-Layer Induced Pressures at Hypersonic Speeds", Physica of Fluids, Vol. 14, No. 7, p. 1332, July 1971.

36. Luft, B., "Prandtl Number Dependence of the Unsteady Compressible Boundary Layer", M.Sc. Thesis, University of Alberta, 1971.

37. Netterville, D., "The Unsteady Slip-flow Boundary Layer at High Mach Number", M.Sc. Thesis, University of Alberta, 1972.

38. King, W.S., "Low Frequency, Large Amplitude Fluctuations of the Laminar Boundary Layer", AIAA Journal, Vol. 4, No. 6, p.

39. Orlik-Rückemann, K.J., "Stability Derivatives of Sharp Wedges in Viscous Hypersonic Flow", National Aeronautical Establishment, Ottawa, Report LR 421, 1965 (See also AIAA Journal, Vol. 4, No. 6, June 1966).

40. Chapman, D.R. and Rubesin, M.W., "Temperature and Velocity Profiles in the Compressible Laminar Boundary Layer with Arbitrary Distribution of Surface Temperature", Journal Aero. Sci., Vol. 16, No. 9, p. 547, Sept. 1949.

41. Cohen, C.B. and Reshotko, E., "Similar Solutions for the Compressible Laminar Boundary Layer with Heat Transfer and Pressure Gradient", NACA Report No. 1293, 1956.

42. Smith, A.M.O. and Clutter, D.W., "Solution of the Incompressible Laminar Boundary Layer Equations", Douglas Aircraft Company, Report No. ES40446, July 1961.

43. Clutter, D.W. and Smith, A.M.O., "Solution of the General Boundary-Layer Equations for Compressible Laminar Flow, Including Transverse Curvature", Douglas Aircraft Company, Report No. LB 31088, October 1964.

44. Cebecci, T. and Smith, A.M.O., "A Finite-Difference Method for Calculating Compressible Laminar and Turbulent Boundary Layers", ASME Paper No. 70-FE-A, 1970.

45. Baxter, D.C. and Flügge-Lotz, I., "Compressible Laminar Boundary Layer Behavior Studied by a Finite Difference Method", ZAMP, Vol. IXb, p. 81, 1958.

46. Hartree, D.R. and Womersley, J.R., "A Method for the Numerical or Mechanical Solution of Certain Types of Partial Differential Equations", Proc. Roy Soc., Series A, Vol. 161, No. 906, p. 353, August 1937.

47. Cebeci, T. and Keller, H.B., "Shooting and Parallel Shooting Methods for Solving the Falkner-Skan Boundary-Layer Equation", J.urnal of Computational Physics, Vol. 7, No. 2, p. 289, April 1971.

48. Bellman, R.E. and Kalaba, R.E., "Quasilinearization and Non-linear Boundary-Value Problems", American Elsevier Publishing Company, Inc., New York, 1965.

49. Radbill, J.R., "Application of Quasilinearization to Boundary-Layer Equations", A.I.A.A. Journal, Vol. 2, No. 10, p. 1860, Oct. 1964.

50. Radbill, J.R. and McCue, G.A., "Quasilinearization and Nonlinear Problems in Fluid and Orbital Mechanics", American Elsevier Publishing Company, Inc., New York, 1970.

51. Libby, P.A. and Chen, K.K., "Remarks on Quasilinearization Applied in Boundary-Layer Calculations, A.I.A.A. Journal, Vol. 4, No. 5, p. 937, May 1966.

52. Jaffe, N.A. and Thomas, J., "Application of Quasi-Linearization and Chebyshev Series to the Numerical Analysis of the Laminar Boundary-Layer Equations", A.I.A.A. Journal, Vol. 8, No. 3, p. 483, March 1970.

53. McGill, R. and Kenneth, P., "A Convergence Theorem on the Iterative Solution of Non-linear Two-point Boundary-value Systems", Proceedings of the XIVth International Astronautical Federation Congress, Paris, p. 173, 1963.

54. Romanelli, M.J., "Runge-Kutta Methods for the Solution of Ordinary Differential Equations" in "Mathematical Methods for Digital Computers", edited by Ralston, A. and Wilf, H.S., John Wiley and Sons, Inc., 1967.

55. Wilkinson, J.H., "Error Analysis of Direct Methods of Matrix
        Inversion", Association of Computing Machinery Journal, 8,
        pp. 281-330, 1961.

56. Forsythe, G.E. and Moler, C.B., "Computer Solution of Linear
        Algebraic System", Prentice Hall, Inc., 1967.

APPENDIX A

NUMERICAL METHODS FOR THE SERIES SOLUTION

In this appendix we describe the numerical procedure for solving the coupled initial value problem of the form

$$f''' = F(f,f',f'',H,\phi_1(\eta)) \tag{A.1a}$$

$$H'' = G(H,H',f,f',f'',f''',\phi_2(\eta)) \tag{A.1b}$$

with the initial values $f(0)$, $f'(0)$, $f''(0)$, $H(0)$ and $H'(0)$ specified. ϕ_1 and ϕ_2 represent known functions of η. A predictor-corrector method using the Falkner extrapolation formula for predictor and the Adams interpolation formula for corrector is employed. This scheme was originally chosen by Smith and Clutter [42] because of its suitability in high order problems of the form (A.1).

We divide the interval $\eta = 0$ to $\eta = \eta_e$ by (N-1) uniform steps of size h. For any function $\phi(\eta)$ we use the notation

$$\phi_k = \phi(\eta_k) \tag{A.2}$$

where
$$\eta_k = (k-1)h , \quad k=1,2,3,\ldots,N \tag{A.3}$$

Let us consider the general situation where the solution has

progressed up to η_k , $k \geq 4$. Extrapolating from the known values of f, H and their derivatives at the last four η-stations, we predict the un-known values at the station k+1. Representing the extrapolated values with the superscript ~ , the Falkner extrapolation formulas can be written as:

$$\tilde{f}''_{k+1} = f''_k + \frac{h}{24} [55f'''_k - 59f'''_{k-1} + 37f'''_{k-2} - 9f'''_{k-3}] \qquad (A.4a)$$

$$\tilde{f}'_{k+1} = f'_k + \frac{h}{24} [55f''_k - 59f''_{k-1} + 37f''_{k-1} - 9f''_{k-3}] \qquad (a.4b)$$

$$\tilde{f}_{k+1} = f_k + hf'_k + \frac{h^2}{360} [323f''_k - 264f''_{k-1} + 159f''_{k-2} - 38f''_{k-3}] \qquad (A.4c)$$

$$\tilde{H}'_{k+1} = H'_k + \frac{h}{24} [55H''_k - 59H''_{k-1} + 37H''_{k-2} - 9H''_{k-3}] \qquad (A.4d)$$

$$\tilde{H}_{k+1} = H_k + \frac{h}{24} [55H'_k - 59H'_{k-1} + 37H'_{k-2} - 9H'_{k-3}] \qquad (A.4e)$$

The values of f''' and H'' at the station k+1 can now be evaluated from A.1 and A.2 using the extrapolated values:

$$\tilde{f}'''_{k+1} = F(\tilde{f}_{k+1}, \tilde{f}'_{k+1}, \tilde{f}''_{k+1}, \tilde{H}_{k+1}, \phi_{1,k+1}) \qquad (A.5a)$$

$$\tilde{H}''_{k+1} = G(\tilde{H}_{k+1}, \tilde{H}'_{k+1}, \tilde{f}_{k+1}, \tilde{f}'_{k+1}, \tilde{f}''_{k+1}, \tilde{f}'''_{k+1}, \phi_{2,k+1}) \qquad (A.5b)$$

The Adams interpolation formulas are now used to determine more accurate values of the unknowns at the station k+1:

$$f''_{k+1} = f''_k + \frac{h}{24} [9\tilde{f}'''_{k+1} + 19f'''_k - 5f'''_{k-1} + f'''_{k-2}] \qquad (A.6a)$$

$$f'_{k+1} = f'_k + \frac{h}{24} [f''_{k+1} + 19f''_k - 5f''_{k-1} + f''_{k-2}] \qquad (A.6b)$$

$$\dot{f}_{k+1} = f_k + hf'_k + \frac{h^2}{360} [38f''_{k+1} + 171f''_k - 36f''_{k-1} + 7f''_{k-2}] \qquad (A.6c)$$

$$H'_{k+1} = H'_k + \frac{h}{24} [9\tilde{H}''_{k+1} + 19H''_k - 5H''_{k-1} + H''_{k-2}] \qquad (A.6d)$$

$$H_{k+1} = H_k + \frac{h}{24} [9H'_{k+1} + 19H'_k - 5H'_{k-1} + H'_{k-2}] \qquad (A.6e)$$

The values of f'''_{k+1} and H''_{k+1} are then calculated from A.1 and A.2. This completes the calculations at the station k+1 and the solution proceeds to the next station.

The errors involved in the formulas (A.4) and (A.6) are of order (h^5) or less. However, the errors in the extrapolation and the interpolation formulas are of opposite signs. Thus, the absolute value of the difference between the predicted and the corrected values provides an upper bound for the error at that particular step. If we define:

$$\varepsilon_k = \max \{ |\tilde{\phi}_k - \phi_k| \; ; \; \phi = f, f', f'', f''', H, H', H'' \} \qquad (A.7)$$

then the error at any point in the solution is bounded by

$$\varepsilon_{max} = \max \{ \varepsilon_k, \; k=1, \, N \} \qquad (A.8)$$

The choice of the step size h is governed by the maximum tolerance allowed on ε_{max}. In all the problems solved by this method, $h = 2^{-6}$ (corresponding to N = 513 for η_e = 8) was found sufficient to bound ε_{max} within 10^{-7}.

To start the solution by the predictor-corrector method described above, solutions at the stations k=1,2,3,4 are required. The values at station k=1 (η=0) are provided by the initial conditions. The solutions at stations 2,3,4 are obtained by a Runge-Kutta method described by Romanelli [54]. Subroutine RKFA solves the initial value problem A.1 using the above algorithm.

APPENDIX B

METHOD OF SOLVING THE LINEARIZED MOMENTUM

AND ENERGY EQUATIONS

In this appendix we describe the finite difference method of solving the linearized problems (3.66,67) and (3.69,70). We use uniform step size in the η-direction and follow the notation of equations (A.2,3).

The following finite difference formulas are used:

Five point symmetric formulas:

$$(\frac{d^3\phi}{d\eta^3})_k = (-\phi_{k-2}+2\phi_{k-1}-2\phi_{k+1}+\phi_{k+2})/2h^3 + 0(h^2) \qquad (B.1a)$$

$$(\frac{d^2\phi}{d\eta^2})_k = (-\phi_{k-2}+16\phi_{k-1}-30\phi_k+16\phi_{k+1}-\phi_{k+2})/12h^2 + 0(h^4) \qquad (B.1b)$$

$$(\frac{d\phi}{d\eta})_k = (\phi_{k-2}-8\phi_{k-1}+8\phi_{k+1}-\phi_{k+2})/12h + 0(h^4) \qquad (B.1c)$$

Five point unsymmetric formulas:

(One forward and three backward points)

$$(\frac{d^3\phi}{d\eta^3})_k = (\phi_{k-3}-6\phi_{k-2}+12\phi_{k-1}-10\phi_k+3\phi_{k+1})/2h^3 + 0(h^2) \qquad (B.2a)$$

$$(\frac{d^2\phi}{d\eta^2})_k = (-\phi_{k-3}+4\phi_{k-2}+6\phi_{k-1}-20\phi_k+11\phi_{k+1})/12h^2 + 0(h^3) \qquad (B.2b)$$

$$\left(\frac{d\phi}{d\eta}\right)_k = (-\phi_{k-3}+6\phi_{k-2}-18\phi_{k-1}+10\phi_k+3\phi_{k+1})/12h + O(h^4) \qquad (B.2c)$$

(Four forward points)

$$\left(\frac{d\phi}{d\eta}\right)_k = (-25\phi_k+48\phi_{k+1}-36\phi_{k+2}+16\phi_{k+3}-3\phi_{k+4})/12h + O(h^4) \qquad (B.3)$$

(Four backward points)

$$\left(\frac{d\phi}{d\eta}\right)_k = (3\phi_{k-4}-16\phi_{k-3}+36\phi_{k-2}-48\phi_{k-1}+25\phi_k)/12h + O(h^4) \qquad (B.4)$$

Three point symmetric formulas:

$$\left(\frac{d^2\phi}{d\eta^2}\right)_k = (\phi_{k-1}-2\phi_k+\phi_{k+1})/h^2 + O(h^2) \qquad (B.5a)$$

$$\left(\frac{d\phi}{d\eta}\right)_k = (-\phi_{k-1}+\phi_{k+1})/2h + O(h^2) \qquad (B.5b)$$

Three point unsymmetric formulas: (Two forward points)

$$\left(\frac{d\phi}{d\eta}\right)_k = (-3\phi_k+4\phi_{k+1}-\phi_{k+2})/2h + O(h^2) \qquad (B.6)$$

The problem given by equations (3.66,67) can be written as:

$$ae''' + b(\eta)e'' + c(\eta)e' + d(\eta)e = f(\eta) \qquad (B.7)$$

$$e(0) = 0 \tag{B.8a}$$

$$e'(0) = 0 \tag{B.8b}$$

$$e'(\eta_e) = 0 \tag{B.8c}$$

where a is a known constant and b,c,d,f are known functions of η.

Replacing e''',e'',e' by the finite difference formulas we obtain the following system of linear algebraic equations for the vector $e_k(k=1,N)$

$$
\begin{bmatrix}
A_1 & B_1 & C_1 & D_1 & E_1 & & & & & \\
A_2 & B_2 & C_2 & D_2 & E_2 & & & & & \\
A_3 & B_3 & C_3 & D_3 & E_3 & & & & & \\
& A_4 & B_4 & C_4 & D_4 & E_4 & & & & \\
& & \cdot & \cdot & \cdot & \cdot & \cdot & & & \\
& & & A_k & B_k & C_k & D_k & E_k & & \\
& & & & \cdot & \cdot & \cdot & \cdot & \cdot & \\
& & & & A_{N-3} & B_{N-3} & C_{N-3} & D_{N-3} & E_{N-3} & \\
& & & & & A_{N-2} & B_{N-2} & C_{N-2} & D_{N-2} & E_{N-2} \\
& & & & & & A_{N-1} & B_{N-1} & C_{N-1} & D_{N-1} & E_{N-1} \\
& & & & & & & A_N & B_N & C_N & D_N & E_N
\end{bmatrix}
\begin{bmatrix}
e_1 \\ e_2 \\ e_3 \\ e_4 \\ \cdot \\ e_k \\ \cdot \\ e_{N-3} \\ e_{N-2} \\ e_{N-1} \\ e_N
\end{bmatrix}
=
\begin{bmatrix}
F_1 \\ F_2 \\ F_3 \\ F_4 \\ \cdot \\ F_k \\ \cdot \\ F_{N-3} \\ F_{N-2} \\ F_{N-1} \\ F_N
\end{bmatrix}
\tag{B.9}
$$

or

$$M \, e = F \tag{B.10}$$

Zero elements of the matrix M are not shown. The elements in each row are normalized so that the magnitude of the largest element equals 1.

The first, second and the last row of (B.9) are obtained from the boundary conditions (B.8) and the finite difference formulas (B.3) and (B.4). Thus we have

$$A_1 = 1 \, , \, B_1 = C_1 = D_1 = E_1 = F_1 = 0 \tag{B.11a}$$

$$A_2 = - \frac{25}{48} \, , \, B_2 = 1 \, , \, C_2 = - \frac{3}{4} \, , \, D_2 = \frac{1}{3} \, , \, E_2 = - \frac{1}{16} \, , \, F_2 = 0 \tag{B.11b}$$

$$A_N = - \frac{1}{16} \, , \, B_N = \frac{1}{3} \, , \, C_N = - \frac{3}{4} \, , \, D_N = 1, \, E_N = - \frac{25}{48} \, , \, F_N = 0 \tag{B.11c}$$

The rows 3 to N-2 are obtained from the differential equation (B.7) using the finite difference formulas (B.1). The elements are given by

$$A_k = (- \frac{a}{2} - \frac{h}{12} b_k + \frac{h^2}{12} c_k)/\alpha \tag{B.12a}$$

$$B_k = (a + \frac{4}{3} hb_k - \frac{2}{3} h^2 c_k)/\alpha \tag{B.12b}$$

$$C_k = (- \frac{5}{2} hb_k + h^3 d_k)/\alpha \tag{B.12c}$$

$$D_k = (-a + \frac{4}{3} hb_k + \frac{2}{3} h^2 c_k)/\alpha \qquad \text{(B.12d)}$$

$$E_k = (\frac{a}{2} - \frac{h}{12} b_k - \frac{h^2}{12} c_k) \, \alpha \qquad \text{(B.12e)}$$

$$F_k = h^3 f_k/\alpha \quad \text{for } k=3,4,\ldots,N-2 \qquad \text{(B.12f)}$$

where α is so chosen that

$$\max \{A_k, B_k, C_k, D_k, E_k\} = 1 \qquad \text{(B.13)}$$

For the (N-1)th row in (B.9) we have used the unsymmetric formulas (B.2). The elements are given by:

$$A_{N-1} = (\frac{a}{2} - \frac{h}{12} b_{N-1} - \frac{h^2}{12} c_{N-1})/\alpha \qquad \text{(B.14a)}$$

$$B_{N-1} = (-3a + \frac{h}{3} b_{N-1} + \frac{h^2}{2} c_{N-1})/\alpha \qquad \text{(B.14b)}$$

$$C_{N-1} = (6a + \frac{h}{2} b_{N-1} - \frac{3}{2} h^2 c_{N-1})/\alpha \qquad \text{(B.14c)}$$

$$D_{N-1} = (-5a - \frac{5}{3} hb_{N-1} + \frac{5}{6} h^2 c_{N-1} + h^3 d_{N-1})/\alpha \qquad \text{(B.14d)}$$

$$E_{N-1} = (\frac{3}{2} a + \frac{11}{12} hb_{N-1} + \frac{h^2}{4} c_{N-1})/\alpha \qquad \text{(B.14e)}$$

$$F_{N-1} = h^2 f_{N-1}/\alpha \qquad \text{(B.14f)}$$

where α is chosen to satisfy (B.13).

The system of equations (B.9) is solved by Gaussian elimination with partial pivoting. (B.10) is first transformed into

$$Ue = \overline{F} \qquad (B.15)$$

where U is a NXN upper triangular matrix. Because of the pentadiagonal form of the matrix M, U is also of band structure with four superdiagonal elements in each row. From (B.15) e is calculated by back substitution.

The procedure outlined above involving initial scaling of the elements and partial pivoting during elimination is recommended by Wilkinson [55], Forsythe and Moler [56] and is known to restrict the growth of round-off errors. The FORTRAN subroutine SLV5 was used to solve the linear system of the form (B.9).

The linearized energy equation leads to the problem (3.69,70) which can be written as

$$ag'' + b(\eta)g' + c(\eta)\, g = d(\eta) \qquad (B.16)$$

$$g'(0) = 0 \quad \text{for insulated surface} \qquad (B.17a)$$

or $\qquad g(0) = 0 \quad$ for constant-temperature surface $\qquad (B.17b)$

and $\qquad\qquad g(\eta_e) = 0 \;. \qquad (B.17c)$

Here a is a known constant and b,c,d are known functions of η.

Since (B.16) is a second degree equation the three point formulas (B.5) are sufficient for truncation errors of $O(h^2)$. The following system of linear algebraic equations is obtained for the vector g_k, (k=1,N)

$$
\begin{bmatrix}
A_1 & B_1 & C_1 \\
A_2 & B_2 & C_2 \\
 & A_3 & B_3 & C_3 \\
 & & \cdot & \cdot & \cdot \\
 & & & A_k & B_k & C_k \\
 & & & & \cdot & \cdot & \cdot \\
 & & & & & A_{N-2} & B_{N-2} & C_{N-2} \\
 & & & & & & A_{N-1} & B_{N-1} & C_{N-1} \\
 & & & & & & & A_N & B_N
\end{bmatrix}
\begin{bmatrix}
g_1 \\ g_2 \\ g_3 \\ \cdot \\ g_k \\ \cdot \\ g_{N-2} \\ g_{N-1} \\ g_N
\end{bmatrix}
=
\begin{bmatrix}
D_1 \\ D_2 \\ D_3 \\ \cdot \\ D_k \\ \cdot \\ D_{N-2} \\ D_{N-1} \\ D_N
\end{bmatrix}
$$

(B.18)

From the boundary conditions (B.17) we have

$$A_1 = -\frac{3}{4} \; , \; B_1 = 1 \; , \; C_1 = -\frac{1}{4} \; , \; D_1 = 0 \tag{B.19a}$$

for insulated surface

or $$A_1 = 1 \; , \; B_1 = 0 \; , \; C = 0 \; , \; D_1 = 0 \tag{B.19b}$$

for constant-temperature surface

and $$A_N = 0 \ , \ B_N = 1 \ , \ D_N = 0 \qquad\qquad \text{(B.19c)}$$

For $k = 2,3,\ldots,N-1$ we have from (B.16) and (B.5)

$$A_k = (a - \frac{h}{2} b_k)/\alpha \qquad\qquad \text{(B.20a)}$$

$$B_k = (-2a + h^2 c_k)/\alpha \qquad\qquad \text{(B.20b)}$$

$$C_k = (a + \frac{h}{2} b_k)/\alpha \qquad\qquad \text{(B.20c)}$$

$$D_k = h^2 d_k/\alpha \qquad\qquad \text{(B.20d)}$$

The scaling factor α is so chosen that

$$\max \ \{A_k \ , \ B_k \ , \ C_k\} = 1 \qquad\qquad \text{(B.21)}$$

The system of equations (B.18) is solved by Gaussian elimination with partial pivoting. The resulting upper triangular matrix is of band structure with two superdiagonal elements. The FORTRAN subroutine SLV3 was used to solve the system (B.18). Also the FORTRAN Subroutine MEEQN was used to solve the momentum and energy equations at any x-station using the method described in Section 3.3a.

APPENDIX C

NUMERICAL METHODS FOR THE INTERACTION PROBLEM

The problem given by equations (3.79,80) can be written as

$$x \frac{d\tau}{dx} + a(x)\tau = b(x) \tag{C.1}$$

$$\tau(x_1) = 0 \tag{C.2}$$

where $a(x)$ and $b(x)$ are known functions of x. Using the arrangement
of x stations described in (3.46), we solve the above problem by a
finite difference method. The following formulas are used:

$$\left(\frac{d\phi}{dx}\right)_j = \frac{1}{\Delta x_j} [c_{11}\phi_j + c_{12}\phi_{j+1} + c_{13}\phi_{j+2} + c_{14}\phi_{j+3} + c_{15}\phi_{j+4}] \tag{C.3a}$$

$$\left(\frac{d\phi}{dx}\right)_j = \frac{1}{\Delta x_j} [c_{21}\phi_{j-1} + c_{22}\phi_j + c_{23}\phi_{j+1} + c_{24}\phi_{j+2} + c_{25}\phi_{j+3}] \tag{C.3b}$$

$$\left(\frac{d\phi}{dx}\right)_j = \frac{1}{\Delta x_j} [c_{31}\phi_{j-2} + c_{32}\phi_{j-1} + c_{33}\phi_j + c_{34}\phi_{j+1} + c_{35}\phi_{j+2}] \tag{C.3c}$$

$$\left(\frac{d\phi}{dx}\right)_j = \frac{1}{\Delta x_j} [c_{41}\phi_{j-3} + c_{42}\phi_{j-2} + c_{43}\phi_{j-1} + c_{44}\phi_j + c_{45}\phi_{j+1}] \tag{C.3d}$$

$$\left(\frac{d\phi}{dx}\right)_j = \frac{1}{\Delta x_j} [c_{51}\phi_{j-4} + c_{52}\phi_{j-3} + c_{53}\phi_{j-2} + c_{54}\phi_{j-1} + c_{55}\phi_j] \tag{C.3e}$$

The coefficients $c_{k\ell}$ $(k,\ell = 1,5)$ are functions of K_x and are given in Table C.1. The truncation errors of the formulas (C.3) are of $O(\Delta x_j^4)$.

Using the formulas (C.3) we obtain from (C.1) the following system of linear equations for $\tau_j, j=1,2,\ldots,J$

$$
\begin{bmatrix}
A_1 & B_1 & C_1 & D_1 & E_1 \\
A_2 & B_2 & C_2 & D_2 & E_2 \\
A_3 & B_3 & C_3 & D_3 & E_3 \\
 & A_4 & B_4 & C_4 & D_4 & E_4 \\
 & & \cdot & \cdot & \cdot & \cdot & \cdot \\
 & & & A_j & B_j & C_j & D_j & E_j \\
 & & & & \cdot & \cdot & \cdot & \cdot & \cdot \\
 & & & & & A_{J-3} & B_{J-3} & C_{J-3} & D_{J-3} & E_{J-3} \\
 & & & & & & A_{J-2} & B_{J-2} & C_{J-2} & D_{J-2} & E_{J-2} \\
 & & & & & & & A_{J-1} & B_{J-1} & C_{J-1} & D_{J-1} & E_{j-1} \\
 & & & & & & & & A_j & B_j & C_j & D_j & E_j
\end{bmatrix}
\begin{bmatrix}
\tau_1 \\ \tau_2 \\ \tau_3 \\ \tau_4 \\ \vdots \\ \tau_j \\ \vdots \\ \tau_{J-3} \\ \tau_{J-2} \\ \tau_{J-1} \\ \tau_J
\end{bmatrix}
=
\begin{bmatrix}
F_1 \\ F_2 \\ F_3 \\ F_4 \\ \vdots \\ F_j \\ \vdots \\ F_{J-3} \\ F_{J-2} \\ F_{J-1} \\ F_J
\end{bmatrix}
$$

$$\text{(C.4)}$$

The elements of the matrix are given by

$$A_1 = 1 \ , \ B_1 = C_1 = D_1 = E_1 = F_1 = 0 \qquad \text{(C.5)}$$

TABLE C.1

The Coefficients $c_{k\ell}$ Appearing in Equations (C.3)

ℓ \ k	1	2	3	4	5
1	$-\dfrac{1+\alpha+\beta+\gamma}{K_x}$	$\dfrac{1}{\gamma K_x^4}$	$-\dfrac{\alpha^2}{\beta\gamma K_x^6}$	$\dfrac{\beta}{\gamma K_x^7}$	$-\dfrac{\gamma}{K_x^7}$
2	$-\gamma K_x^3$	$1 - \dfrac{1+\alpha+\beta}{K_x}$	$\dfrac{\alpha}{\beta K_x^3}$	$-\dfrac{\alpha}{K_x^4}$	$\dfrac{\beta\gamma}{K_x^4}$
3	$\beta\gamma K_x^6$	$-K_x^2\dfrac{\beta}{\alpha}$	$\dfrac{2(K_x-1)}{K_x}$	$\dfrac{\beta}{\alpha K_x^2}$	$-\dfrac{\beta\gamma}{K_x^2}$
4	$-\beta\gamma K_x^8$	αK_x^4	$-\dfrac{\alpha}{\beta} K_x$	$1 - \dfrac{1}{K_x} + \alpha K_x + \beta K_x^2$	$\dfrac{\gamma}{K_x}$
5	γK_x^9	$-\dfrac{\beta K_x^5}{\gamma}$	$\dfrac{\alpha}{\beta\gamma} K_x^2$	$-\dfrac{1}{\gamma}$	$1 + \alpha K_x + \beta K_x^2 + \gamma K_x^3$

$\alpha = 1/(1+K_x)$; $\beta = 1/(1+K_x+K_x^2)$; $\gamma = 1/(1+K_x+K_x^2+K_x^3)$

$$A_2 = c_{21}/\alpha$$

$$B_2 = (c_{22} + \frac{\Delta x_2}{x_2} a_2)/\alpha$$

$$C_2 = c_{23}/\alpha \qquad\qquad (C.6)$$

$$D_2 = c_{24}/\alpha$$

$$E_2 = c_{25}/\alpha$$

$$F_2 = \frac{\Delta x_2}{x_2} b_2/\alpha$$

For $j = 3,4,...J-2$

$$A_j = c_{31}/\alpha$$

$$B_j = c_{32}/\alpha$$

$$C_j = (c_{33} + \frac{\Delta x_j}{x_j} a_j)/\alpha \qquad\qquad (C.7)$$

$$D_j = c_{34}/\alpha$$

$$E_j = c_{35}/\alpha$$

$$F_j = \frac{\Delta x_j}{x_j} b_j/\alpha$$

$$A_{J-1} = c_{41}/\alpha$$

$$B_{J-1} = c_{42}/\alpha$$

$$C_{J-1} = c_{43}/\alpha$$

(C.8)

$$D_{J-1} = (c_{44} + \frac{\Delta x_{J-1}}{x_{J-1}} a_{J-1})/\alpha$$

$$E_{J-1} = c_{45}/\alpha$$

$$F_{J-1} = \frac{\Delta x_{J-1}}{x_{J-1}} b_{J-1}/\alpha$$

$$A_J = c_{51}/\alpha$$

$$B_J = c_{52}/\alpha$$

$$C_J = c_{53}/\alpha$$

(C.9)

$$D_J = c_{54}/\alpha$$

$$E_J = (c_{55} + \frac{\Delta x_J}{x_J} a_J)/\alpha$$

$$F_J = \frac{\Delta x_J}{x_J} b_J/\alpha$$

In equations (C.6-9) the quantities α are so chosen that

$$\max \{A_j, B_j, C_j, D_j, E_j\} = 1 \quad \text{for } j=2,3,\ldots,J \qquad \text{(B.10)}$$

The matrix in the equation (C.4) is of the same form as that in equation (B.9). The linear system (B.9) is solved by the subroutine SLV5. The FORTRAN subroutine PRESS computes the pressure function $\bar{p}$ corresponding to a given $\bar{I}$ distribution by using the method described in Section 3.3b and this Appendix.

APPENDIX D

EVALUATION OF THE INTEGRALS IN CHAPTER V

In this appendix we develop a formula for the numerical evaluation of integrals of the type

$$\int_0^1 x^\omega \phi(x) \, dx \qquad (D.1)$$

using a method similar to the Simpson's rule. The exponent $\omega > -1$ and ϕ_j, $j=1,J$ are specified at a set of points x_j, $j=1,J$ as shown in Figure D.1.
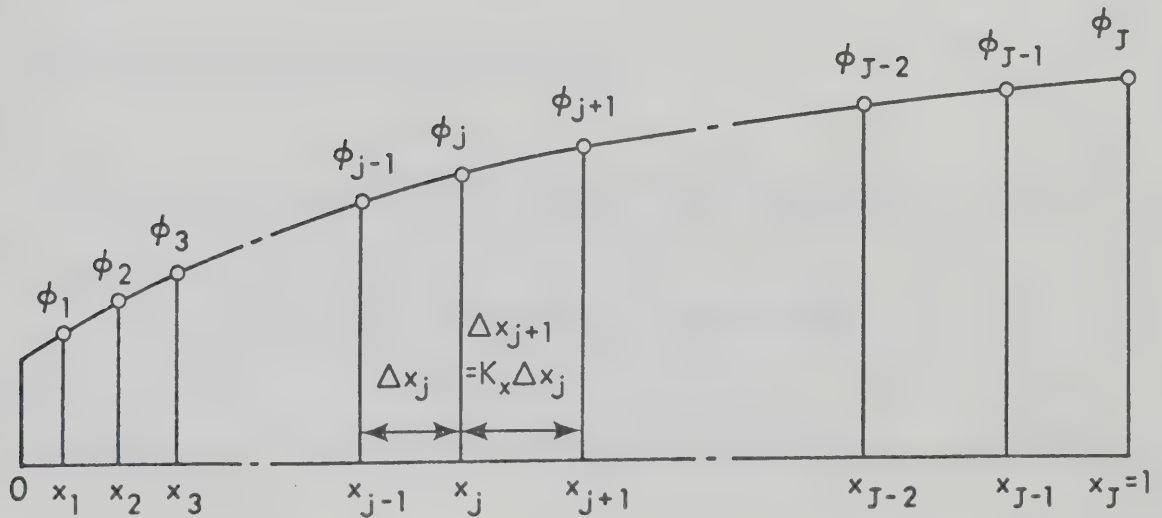

Figure D.1 Set of Points Used to Evaluate Integral (D.1)

For $x_{j-1} \leq x \leq x_{j+1}$ we approximate $\phi(x)$ by a second degree polynomial of the form

$$\phi(x) = ax^2 + bx + c \qquad\qquad (D.2)$$

passing through the points $(x_{j-1}, \phi_{j-1}), (x_j, \phi_j)$ and (x_{j+1}, ϕ_{j+1}). Thus we have

$$\int_{x_{j-1}}^{x_{j+1}} x^\omega \phi(x)\, dx$$

$$= \frac{a}{\omega+3}\, [x_{j+1}^{\omega+3} - x_{j-1}^{\omega+3}] + \frac{b}{\omega+2}\, [x_{j+1}^{\omega+2} - x_{j-1}^{\omega+2}] + \frac{c}{\omega+1}\, [x_{j+1}^{\omega+1} - x_{j-1}^{\omega+1}]$$

$$= x_{j+1}^{\omega+1}\, [A_j\, x_{j+1}^2 + B_j\, x_{j+1} + C_j] - x_{j-1}^{\omega+1}\, [A_j\, x_{j-1}^2 + B_j x_{j-1} + C_j] \quad (D.3)$$

The quantities A_j, B_j, C_j are given by

$$A_j = [\phi_{j+1} - (1+K_x)\phi_j + K_x\phi_{j-1}] / [K_x(K_x+1)\Delta x_j^2(\omega+3)] \qquad (D.4a)$$

$$B_j = [-(x_j+x_{j-1})\phi_{j+1} + (x_{j-1}+x_{j+1})(1+K_x)\phi_j$$

$$- (x_{j+1}+x_j)K_x\phi_{j-1}] / [K_x(K_x+1)\Delta x_j^2(\omega+2)] \qquad (D.4b)$$

$$C_j = [x_j x_{j-1}\phi_{j+1} - x_{j-1}x_{j+1}(1+K_x)\bar{\phi}_j$$

$$+ x_{j+1} x_j K_x \phi_{j-1}] / (K_x(K_x+1) \Delta x_j^2 (\omega+1))] \qquad (D.4c)$$

The error involved in (D.3) is of the order $\Delta x_j^{3+\omega} [\frac{d^3 \phi}{dx^3}]_j$.

If J is odd, then the intervals between x_1 and x_J are grouped two at a time and the formula (D.3) is applied on each group. Thus we have

$$\int_0^1 x^\omega \phi(x) \, dx = x_3^{\omega+1} [(A_2 - A_4) x_3^2 + (B_2 - B_4) x_3 + (C_2 - C_4)]$$

$$+ x_5^{\omega+1} [(A_4 - A_6) x_5^2 + (B_4 - B_6) x_5 + (C_4 - C_6)]$$

$$\cdot \cdot \cdot \cdot \cdot \cdot \cdot \cdot \cdot$$

$$+ x_{J-2}^{\omega+1} [(A_{J-3} - A_{J-1}) x_{J-2}^2 + (B_{J-3} - B_{J-1}) x_{J-2}$$

$$+ (C_{J-3} - C_{J-1})] + A_{J-1} + B_{J-1} + C_{J-1} \qquad (D.5)$$

Here the integral between $x = 0$ and $x = x_1$ has been calculated by using the same second degree curve that passes through the points 1,2,3.

If J is odd, we use the above scheme for the integral up to x_{J-3} and calculate the remaining part by passing a third degree curve through the last four points. This gives the following formula:

$$\int_0^1 x^\omega \phi(x) \, dx = x_3^{\omega+1} [(A_2 - A_4) x_3^2 + (B_2 - B_4) x_3 + (C_2 - C_4)]$$

$$+ x_5^{\omega+1}[(A_4-A_6)x_5^2 + (B_4-B_6)x_5 + (C_4-C_6)]$$

$$\ldots\ldots\ldots\ldots$$

$$+ x_{J-3}^{\omega+1}[-D_0 x_{J-3}^3 + (A_{J-4}-D_1)\, x_{J-3}^2 + (B_{J-4}-D_2)x_{J-3}$$

$$+ (C_{J-4}-D_3)] + D_0 + D_1 + D_2 + D_3 \tag{D.6}$$

The quantities D_0, D_1, D_2, D_3 are given by

$$D_0 = (a_0+a_1+a_2+a_3)/(\omega+4) \tag{D.7a}$$

$$D_1 = - [a_0(x_{J-1}+x_{J-2}+x_{J-3})+a_1(x_{J-2}+x_{J-3}+x_J)$$

$$+ a_2(x_{J-3}+x_J+x_{J-1})+a_3(x_J+x_{J-1}+x_{J-2})]/(\omega+3) \tag{D.7b}$$

$$D_2 = [a_0(x_{J-1}\,x_{J-2}+x_{J-2}\,x_{J-3}+x_{J-3}\,x_{J-1})+ a_1(x_{J-2}\,x_{J-3}+x_{J-3}\,x_J+x_J\,x_{J-2})$$

$$+ a_2(x_{J-3}\,x_J+x_J\,x_{J-1}+x_{J-1}\,x_{J-3})+ a_3(x_J\,x_{J-1}+x_{J-1}\,x_{J-2}+x_{J-2}\,x_J)]/(\omega+2)$$

$$\tag{D.7c}$$

$$D_3 = - [a_0\,x_{J-1}\,x_{J-2}\,x_{J-3}+a_1\,x_{J-2}\,x_{J-3}\,x_J+a_2 x_{J-3}\,x_J\,x_{J-1}$$

$$+ a_3\,x_J\,x_{J-1}\,x_{J-2}]/(\omega+1) \tag{D.7d}$$

where
$$a_0 = \phi_J\, K_x^3/[\Delta x_J^3(K_x+1)(K_x^2+K_x+1)] \tag{D.8a}$$

$$a_1 = - \phi_{J-1}\, K_x^3/[\Delta x_J^3(K_x+1)] \tag{D.8b}$$

$$a_2 = \phi_{J-2} \, K_x^4 / [\Delta x_J^3 (K_x+1)] \qquad\qquad (D.8c)$$

$$a_3 = -\phi_{J-3} K_x^6 / [\Delta x_J^3 (K_x+1)(K_x^2+K_x+1)] \qquad (D.8d)$$

The FORTRAN subroutine INTEG computes the integral (D.1) using this formula.